ornl

ORNL/TM-12374

OAK RIDGE
NATIONAL
LABORATORY

MARTIN MARIETTA

Criticality Safety Studies of Building 3019 Cell 4 and In-Line Storage Wells

R. T. Primm, III

MANAGED BY
MARTIN MARIETTA ENERGY SYSTEMS, INC.
FOR THE UNITED STATES
DEPARTMENT OF ENERGY

DISTRIBUTION OF THIS DOCUMENT IS UNLIMITED

This report has been reproduced directly from the best available copy.

Available to DOE and DOE contractors from the Office of Scientific and Technical Information, P.O. Box 62, Oak Ridge, TN 37831; prices available from (615) 576-8401, FTS 626-8401.

Available to the public from the National Technical Information Service, U.S. Department of Commerce, 5285 Port Royal Rd., Springfield, VA 22161.

This report was prepared as an account of work sponsored by an agency of the United States Government. Neither the United States Government nor any agency thereof, nor any of their employees, makes any warranty, express or implied, or assumes any legal liability or responsibility for the accuracy, completeness, or usefulness of any information, apparatus, product, or process disclosed, or represents that its use would not infringe privately owned rights. Reference herein to any specific commercial product, process, or service by trade name, trademark, manufacturer, or otherwise, does not necessarily constitute or imply its endorsement, recommendation, or favoring by the United States Government or any agency thereof. The views and opinions of authors expressed herein do not necessarily state or reflect those of the United States Government or any agency thereof.

DISCLAIMER

Portions of this document may be illegible electronic image products. Images are produced from the best available original document.

ORNL/TM-12374

Engineering Physics and Mathematics Division

CRITICALITY SAFETY STUDIES OF BUILDING 3019 CELL 4 AND IN-LINE STORAGE WELLS

R. T. Primm, III

DATE PUBLISHED — November 1993

Research sponsored by the
Defense Programs
U.S. Department of Energy

Prepared by the
OAK RIDGE NATIONAL LABORATORY
Oak Ridge, Tennessee 37831
managed by
MARTIN MARIETTA ENERGY SYSTEMS, INC.
for the
U.S. DEPARTMENT OF ENERGY
under contract DE-AC05-840R21400

MASTER

DISTRIBUTION OF THIS DOCUMENT IS UNLIMITED

TABLE OF CONTENTS

ABSTRACT ix

ACKNOWLEDGEMENTS x

1. CRITICALITY SAFETY STUDIES OF BUILDING 3019 CELL 4 AND IN-LINE STORAGE WELLS 1
1.1 INTRODUCTION 1

2. FACILITY DESCRIPTION 1
2.1 NOMINAL FISSILE MATERIAL INVENTORY 10
2.2 CREDIBLE ABNORMAL CONDITIONS 11
2.2.1 Fissile Loading 11
2.2.2 Fissile Isotopics 12
2.2.4 Double-Batching of Fissile Material 13
2.2.5 Other Materials Present in Canisters Containing Fissile Material 13
2.2.6 Water Ingress to Storage Wells 14
2.2.7 Structural Integrity of Storage Facilities 14

3. CALCULATIONAL METHODS 14
3.1 SOFTWARE REQUIREMENTS - PROGRAMS AND CROSS SECTIONS 14
3.2 ACCREDITATION 14
3.3 VALIDATION 15
3.3.1 Data Sources 15
3.3.2 Validation Philosophy 15
3.4 VERIFICATION OF SOFTWARE 16
3.5 COMPUTATIONAL MODELS 17
3.5.1 In-line Storage Well Model 18
3.5.2 Cell 4 Array Model 18
3.5.3 Combined Cell 4 and In-line Model 18

4. DESIGN SCOPING CALCULATIONS 18
4.1 IN-LINE STORAGE WELL CALCULATIONS 20
4.1.1 Comments on Statistical Methods 24
4.1.2 Special Limits for Application to Sample Storage—Unrestricted Moderation . . . 25
4.2 CELL 4 STORAGE WELL CALCULATIONS 25
4.2.1 Comparisons to Previous Studies 25
4.2.2 Area of Applicability for Nominal Conditions 27
4.2.3 Cell 4 Calculations with CEUSP Material Explicitly Modeled 27
4.3 COMBINED CELL 4 AND IN-LINE WELL CALCULATIONS 33
4.3.1 Modification to In-Line Portion of the Model 33
4.3.2 Flooding of Storage Wells 33
4.3.3 Double-Batching of Fuel 36
4.3.4 Summary of Assumptions Relevant to Model Validity 37
4.4.1 Mixing Fuel Types Within a Storage Array 39
4.4.1.1 Neutron Moderation in Concrete 40
4.4.1.2 Adjacent Wells with Differing Fissile Materials 40
4.4.1.3 Intermixing Fissile Materials Within a Well 40
4.4.1.4 Relationship of Derived Safety Limits to ANSI Standards 44
4.4.2 Effect of Fixed Poisons in Cell 4 Materials 44
4.4.3 Acceptability of Linear Loading as a Parameter for Judging Subcriticality 45

5. COMPUTED SUBCRITICAL LIMITS 46

6. COMMENTS 47

7. CONCLUSIONS 47

8. REFERENCES 47

Appendix A. DETERMINATION OF ATOM DENSITIES FOR CELL 4 ARRAY CONCRETE A-1

Appendix B. ASSUMPTIONS FOR CREDIBLE ABNORMAL CONDITION B-1

Appendix C. VALIDATION OF COMPUTER CODES AND CROSS SECTION LIBRARY FOR URANIUM-233 SYSTEMS C-2
C.1 INTRODUCTION C-2
C.2 EXPERIMENTAL AND CALCULATED NEUTRONICS PARAMETERS C-2
C.2.1 Metal Spheres C-6
C.2.2 Single Units filled with Aqueous Solutions C-7
C.2.3 Uranyl Nitrate Experiments Conducted in Arrays and Simple Geometries C-13
C.2.4 Large, Unreflected Spheres Filled with Dilute Uranyl Nitrate C-21
C.2.5 Arrays of Bottles of ^{233}U Nitrate Solution C-23
C.3 SUBCRITICAL LIMIT FOR ^{233}U SYSTEMS C-24
C.3.1 Fissile Isotope Density Variation C-25
C.3.3 Array of Storage Wells Instead of a Single Unit C-25
C.3.4 Concrete Reflection C-25
C.3.5 Interstitial Moderation C-25
C.3.6 Degree of Moderation in the Fissile Material C-26
C.3.7 Determination of the Safely Subcritical Limit for ^{233}U Systems C-26
C.3 REFERENCES C-26

Appendix D. VALIDATION OF COMPUTER CODES AND CROSS SECTION LIBRARY FOR URANIUM-235 SYSTEMS D-1
D.1 INTRODUCTION D-2
D.2 CALCULATED NEUTRONICS PARAMETERS D-6
D.3 DERIVATION OF SUBCRITICAL LIMIT D-8
D.3.1 Density of Fissile Isotope D-8
D.3.2 Physical Form of Fissile Material D-8
D.3.3 Array of Cylinders Versus Single Element D-8
D.3.4 Concrete Reflection D-8
D.3.5 Interstitial Array Moderation D-9
D.3.6 Variation in Degree of Moderation within Fissile Material D-9
D.3.7 Determination of Subcritical Limit D-9
D.4 REFERENCES D-12

Appendix E. VALIDATION OF COMPUTER CODES AND CROSS SECTION LIBRARY FOR PLUTONIUM SYSTEMS E-1
E.1 INTRODUCTION E-2
E.2 CALCULATED NEUTRONICS PARAMETERS E-2
E.3 DETERMINATION OF SUBCRITICAL LIMIT E-3

E.3.1 Plutonium-240 Content E-3
E.3.2 Density of Fissile Isotope E-4
E.3.3 Physical Form of Fissile Material E-4
E.3.4 Array Geometry versus Single Element E-4
E.3.5 Concrete Reflection E-4
E.3.6 Interstitial Moderation E-4
E.3.7 Variation in Degree of Moderation of Fissile Material E-4
E.3.8 Derivation of Subcritical Limit E-4
E.4 REFERENCES E-8

Appendix F. VALIDATION OF COMPUTER CODES AND CROSS SECTION LIBRARY FOR MIXED U-233, U-235 SYSTEMS F-1
F.1 INTRODUCTION F-2
F.2 CALCULATED NEUTRONICS PARAMETERS F-2
F.3 REFERENCES F-2

Appendix G. AUTONOMOUS, IN-LINE ARRAY MODEL G-1

Appendix H. AUTONOMOUS, CELL 4 MODELS H-1
H.1 MODEL FOR COMPARISON TO REF. 1 STUDIES H-2
H.2 MODEL OF CELL 4 WITH EXPLICIT CEUSP AND U4 REPRESENTATION H-7

Appendix I. COMBINED CELL 4 AND IN-LINE STORAGE ARRAY MODELS I-1
I.1. INCLUSION OF HEMISPHERES INTO REFERENCE MODEL I-7
I.2. FINAL, COMBINED MODEL CONTAINING TWO WATER-FLOODED COLUMNS I-8

LIST OF TABLES

Table 1. Atom densities for cell wall concrete 7
Table 2. Atom densities for Cell 4 array concrete 10
Table 3. Assumed credible abnormal storage well inventories as derived from expected current maximum well loadings 11
Table 4. Fissile/total uranium ratios for selected Cell 4 locations 12
Table 5. Isotopic content of uranium in CEUSP fuel 13
Table 6. Comparison of discrete ordinates and Monte Carlo k-effectives 17
Table 7. K-effectives for various ^{233}U, in-line configurations 21
Table 8. K-effectives for various ^{235}U, in-line configurations 22
Table 9. K-effectives for various ^{239}Pu, in-line configurations 23
Table 10. Subcritical limits for autonomous, dry, in-line storage 24
Table 11. Percentage decreases in Table 10 limits from Ref. 1 limits 24
Table 12. Determination of unrestricted moderation concentration for in-line wells 25
Table 13. Initial, uniformly fueled Cell 4 studies 27
Table 14. ^{233}U configurations in the autonomous, Cell 4 model 28
Table 15. ^{235}U configurations in the autonomous, Cell 4 model 29
Table 16. ^{239}Pu configurations in the autonomous, Cell 4 model 30
Table 17. Fissile load limits based on autonomous, unflooded Cell 4 model 31
Table 18. Reactivity effect of combining storage array models 33
Table 19. Calculated parameters for two flooded wells in Cell 4 35
Table 20. Flooded well load limits and possible fissile material densities 36
Table 21. Double-batching in selected Cell 4 37
Table 22. Examination of mixed material array configuration 40
Table 23. Examination of axial variation of materials within a well 43
Table 24. Safe fissile material linear mass loadings for Building 3019 Penthouse Storage Well 46
Table A.1. Average of silo 5 & 6 analyses of Type I Portland cement dated 4/17/78 & 4/24/78 . . . . . A-2
Table A.2. Representative limestone manufactured sand and 7 lb stone A-2
Table A.3. Definition of concrete mix A-2
Table A.4. Summary of Cell 4 storage well concrete at 150 lb/cu ft (2.403 g/cc) A-3
Table C.1. Uranium-233 benchmarks C-2
Table C.2. Characteristics of U-233 critical experiments C-4
Table C.3. Calculated parameters for 1727 ^{233}U metal experiments C-7
Table C.4. Impact of experimental uncertainties C-7
Table C.5. Single unit aqueous solution experiments C-8
Table C.6. Nitrate molarity in some aqueous experiments C-9
Table C.7. Fluoride molarity in some aqueous experiments C-10
Table C.8. Isotopic composition of uranium in solutions C-10
Table C.9. Calculated parameters for single unit aqueous experiments C-11
Table C.10. Correlation of Koponen I.D. 111 experimental parameters to calculated k-effective C-12
Table C.11. Variation in k-effectives for Koponen I.D. 111 experiments due to experimental conditions C-13
Table C.12. Critical parameters for cubic arrays of uranyl nitrate solution C-14
Table C.13. Calculated parameters for arrays of aqueous solutions C-14
Table C.14. Experimental and calculated parameters for uranyl nitrate solutions in simple geometries C-15
Table C.15. Correlation of 1211 experimental parameters to calculated k-effectives C-16

Table C.16. Variation in k-effectives for 1211 experiments due to experimental conditions C-21
Table C.17. Calculational results for large, dilute systems C-22
Table C.18. Calculational results for 114 experiments using ENDF/B-V cross sections C-22
Table C.19. Data for Koponen I.D. 1250 experiments C-24
Table C.20. Calculated neutronics parameters for Koponen I.D. 1250 experiments C-24
Table D.1. Uranium-235 benchmarks D-2
Table D.2. Calculated results for ^{235}U experiments D-6
Table D.3. Correlation of k-effective value to physical form of U-235 bearing material D-8
Table D.4. Correlation of k-effective and reflection condition D-9
Table E.1. Plutonium benchmarks E-3
Table E.2. Characteristics of critical experiments E-5
Table E.3. Calculated results for Pu experiments E-7
Table F.1. Spherical ^{233}U, ^{235}U reflected critical experiments F-2
Table H.1. Definition of KENO materials input H-5
Table H.2. Definition of KENO geometry input H-5
Table H.3. Definition of materials in Fig. H.3 . . . . . H-11
Table H.4. Definition of geometric zones in Fig. H.3 . . . . . H-11
Table H.5. Computed Dancoff Factors for Cell 4 materials H-13
Table I.1. Box type definition for combined model I-2

LIST OF FIGURES

Fig. 1. Cross-sectional view of Building 3019. 2
Fig. 2. Layout of shielded hot cells. 3
Fig. 3. Cross section of eastern end of Building 3019. 4
Fig. 4. Cell IV storage facility (isometric). 5
Fig. 5. Identification pattern for Cell 4 storage wells. 6
Fig. 6. Vertical inter-cells solid storage. 8
Fig. 7. Building 3019 ^{233}U storage wells, Cells II—III. 9
Fig. 8. Available locations (shaded circles) for storing material in the Cell 4 array. 19
Fig. 9. Comparison of infinite lattice spectra 40
Fig. 10. Fuel loading for examining impact of mixing materials in available Cell 4 wells. 41
Fig. 11. Model for examining intermixing of fissile materials in storage wells. 42
Fig. C.1. Horizontal view of experiment 1211-1 array produced by KENO-Va. C-17
Fig. C.2. Vertical view of 1211-1 experiment as produced by the KENO-Va program. C-18
Fig. C.3. Horizontal view through array in experiment 1211-2. . . . . C-19
Fig. C.4. Axial view through array in experiment. C-20
Fig. C.5. ^{233}U validation studies. C-27
Fig. C.6. ^{233}U validation studies (thermal range). C-28
Fig. C.7. Comparison of groupwise fissions for ^{233}U systems. C-29
Fig. D.1. ^{235}U validation studies (KENO-Va, Hansen-Roach). D-10
Fig. D.2. Comparison of groupwise fissions for ^{235}U systems. D-11
Fig. E.1. Pu validation studies (KENO-Va, Hansen-Roach). E-6
Fig. G.1. Representative KENO input for in-line calculations G-3
Fig. G.2. Cross-sectional KENO plot of in-line array. G-4
Fig. H.1. Representative KENO input for initial Cell 4 model. H-4
Fig. H.2. KENO plot from Fig. H.1 input. H-6
Fig. H.3. Representative KENO-Va input for Cell 4 model with explicitly modeled CEUSP and U4 material. H-10
Fig. H.4. KENO plot produced from input in Fig. H.3. . . . . H-12
Fig. I.1. Portion of KENO Va input describing geometry of Cell 4, in-line 3 & 4 model. I-3
Fig. I.2. KENO plot produced from data in Fig. I.1. . . . . I-4
Fig. I.3. Portion to KENO Va input describing geometry of Cell 4, in-line 4 & 5 model. I-5
Fig. I.4. KENO plot produced from data in Fig. I.3 . . . . . I-6
Fig. I.5. Explicitly modeled hemisphere in well M I-7

ABSTRACT

New fissile material load limits for storage facilities located in Building 3019 are derived in a manner consistent with currently applicable Martin Marietta Energy Systems requirements. The limits for ^{233}U loading are 2.00, 1.80, 1.45, and 0.19 kg/ft for hydrogen-to-^{233}U atoms ratios of 3, 5, 10, and unrestricted, respectively. Limits were also found for ^{235}U and ^{239}Pu systems. The KENO-Va Monte Carlo program and Hansen-Roach cross sections were used to derive these limits.

ACKNOWLEDGEMENTS

The author would like to thank A. M. Krichinsky for his support of this work. C. M. Hopper and E. C. Crume, Jr. and D. E. Mueller provided valuable technical advice and reviews of this work. Ruth D. Lawson supervised publication of this report.

1. CRITICALITY SAFETY STUDIES OF BUILDING 3019 CELL 4 AND IN-LINE STORAGE WELLS

1.1 INTRODUCTION

This report supplies the technical documentation needed to support a nuclear criticality safety analysis and approval for the Cell 4 and in-line fissile material storage wells in the Radiochemical Processing Plant (Building 3019) at Oak Ridge National Laboratory. The report provides only the criticality safety analyses and derived, operational, fissile material storage limits. While described in this report, formal documentation of facility configuration and storage well content and preparation of fissile material handling procedures are the responsibility of other individuals/organizations. A procedure incorporating the results from this report is available (Proc. No. RDF-OP-024).

A considerable amount of work was performed prior to this study and documented in the form of an internal communication (Ref. 1) and a technical memorandum (Ref. 2). Lack of computer code validation and inadequate specification of building structural materials necessitated performance of the current studies. While the validation studies documented in this memo were made to support the current work, they also serve to validate some of the previous studies. Where appropriate, that earlier work is presented here.

2. FACILITY DESCRIPTION

Reference 3 provides the following description of Building 3019 and the fissile material storage wells.

> Plan views of the shielded hot cells in Building 3019 are shown in Figs. 1, 2, and 3. Cell 1 has nominal floor dimensions of ~10 × ~20 ft, whereas each of Cells 2-7 has floor dimensions of ~20 × ~20 ft; all of the cells have floor-to-ceiling heights of ~27 ft. Cells 6 and 7 are interconnected and are separated only by a partial wall.
>
> All cell walls are built of poured, reinforced concrete. The outer walls on the north, east, and west sides have a thickness of 5 ft, and those on the south side and the top have a thickness of 4 ft. The interior walls separating the cells have a thickness of 5 ft.
>
> Each cell has a 9 × 9 ft hatch in the southwestern corner of the cell roof; this hatch is used primarily as an equipment portal. However, in Cell 4, the equipment hatch and the cell space beneath it have been displaced by the installation of a group of storage wells, for solid forms of uranium and/or other radionuclides.
>
> An array of 68 wells, illustrated in Fig. 4, was installed in the southwestern corner of Cell 4, beneath the 9-ft × 9-ft equipment hatch, primarily to store the Consolidated Edison Uranium Solidification Project (CEUSP) material. The identification pattern for the 68 wells is shown in Fig. 5. These wells are arranged in a triangular (pitch with 12.75 inch center-to-center spacing). Each consists of a (mild) steel tank which is encased in a hexagonal concrete structure. The structure extends from the cell floor to ~ 1 ft above the (equipment) hatch (into an area known as the Penthouse)...; thus, each tank is (32) ft long. The tanks (for) 45 of the wells are constructed from 4-in-diam, schedule 40 pipe (inside radius is 5.08 cm, outside radius is 5.682 cm based on thickness data from Marks' Standard Handbook for Mechanical Engineers, 8th ed, pp 8-163).... The tanks inside the other 23 wells are constructed from 5-in-diam (outside), 0.25-in-thick tubing. Each tank is vented through a manifold to the Vessel Off-Gas (VOG) System, and the area immediately above each tank is shielded with a 2-ft-thick removable shielding plug.

This page intentionally left blank

PUBLICATION ERROR

Pages 3, 4, and 5 should be numbered 2, 3, and 4

ORNL DWG 84-7010

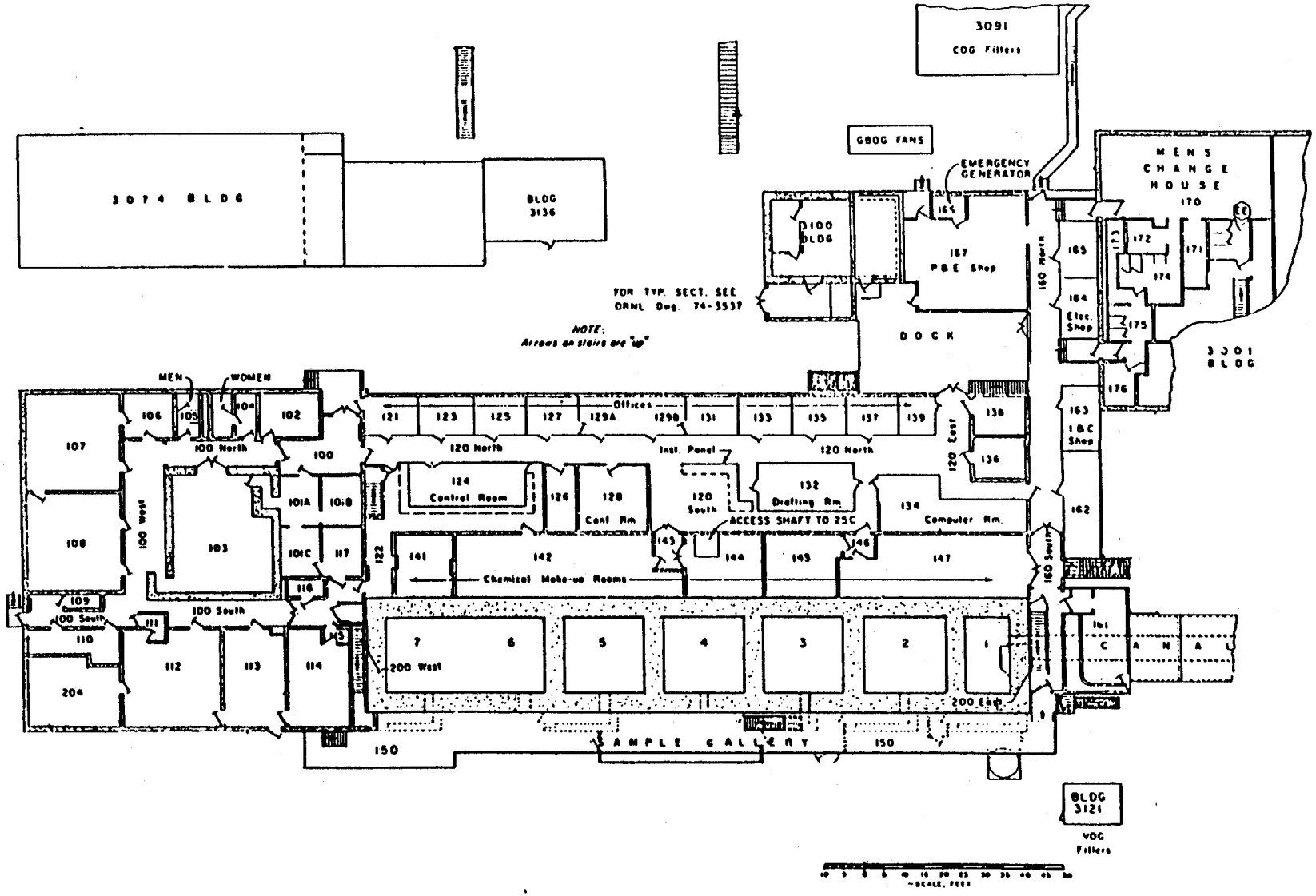

Fig. 1. Cross-sectional view of Building 3019.

ORNL DWG 84-7017R

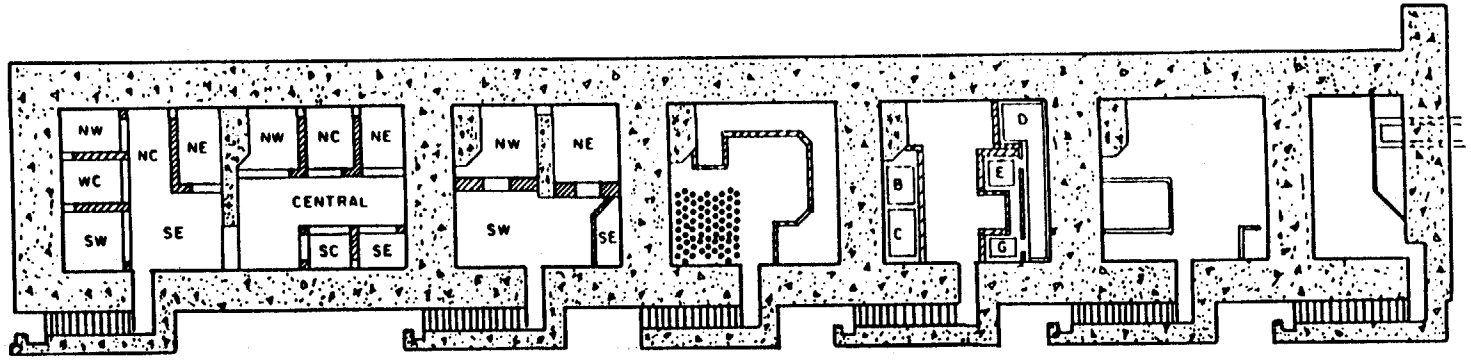

1st. FLOOR PLAN EL. 830.3

N

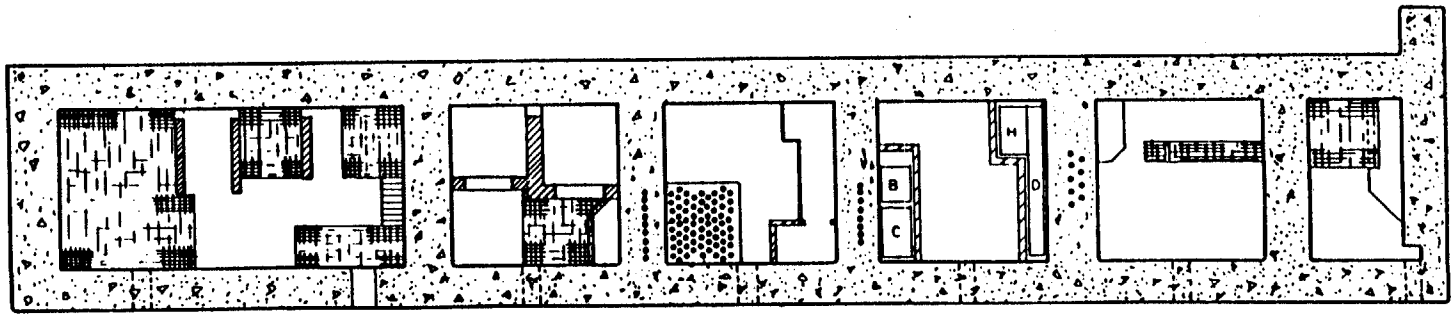

2nd. FLOOR PLAN EL. 845.3

Fig. 2. Layout of shielded hot cells.

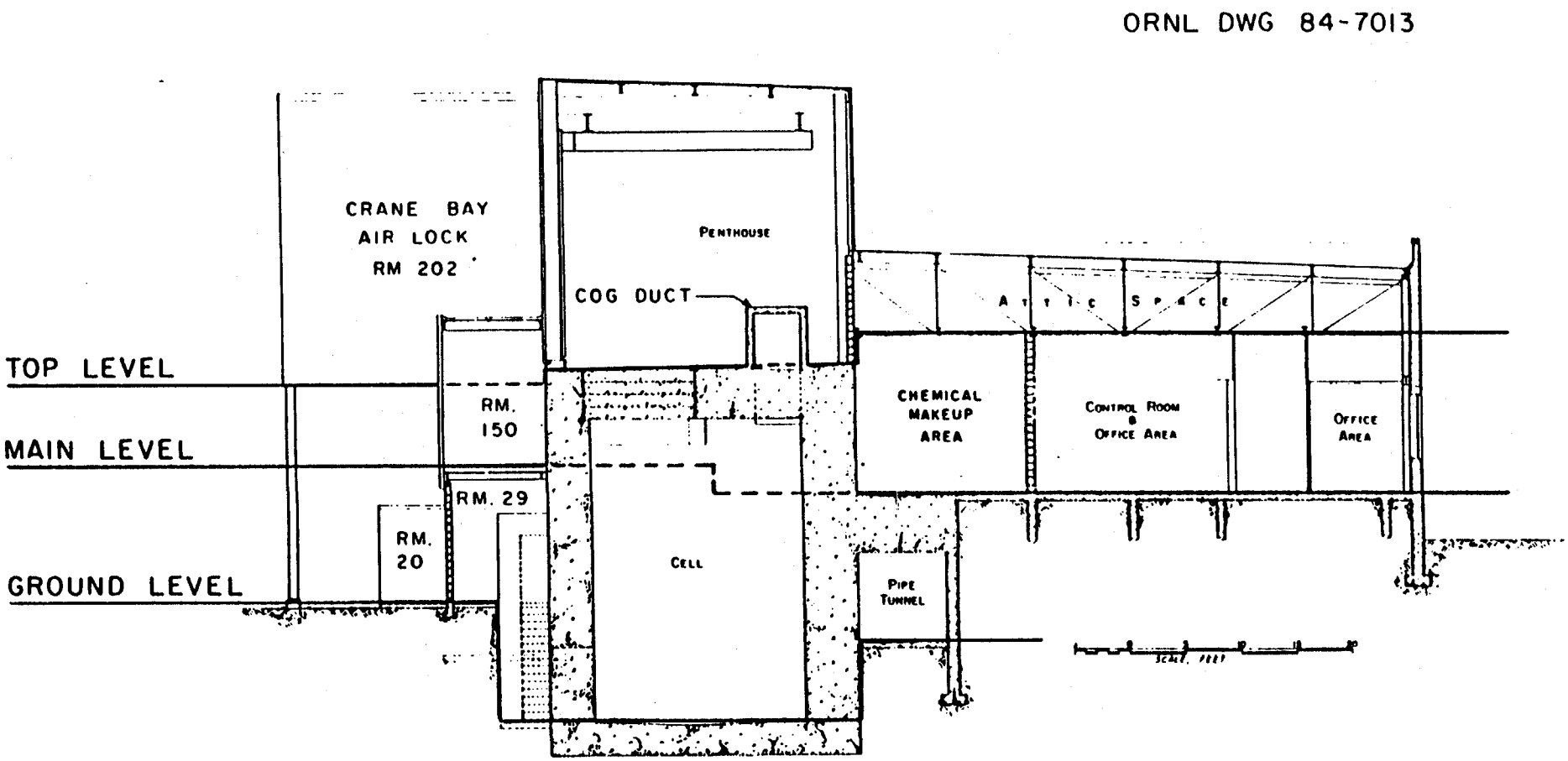

Fig. 3. Cross section of eastern end of Building 3019.

This page intentionally left blank

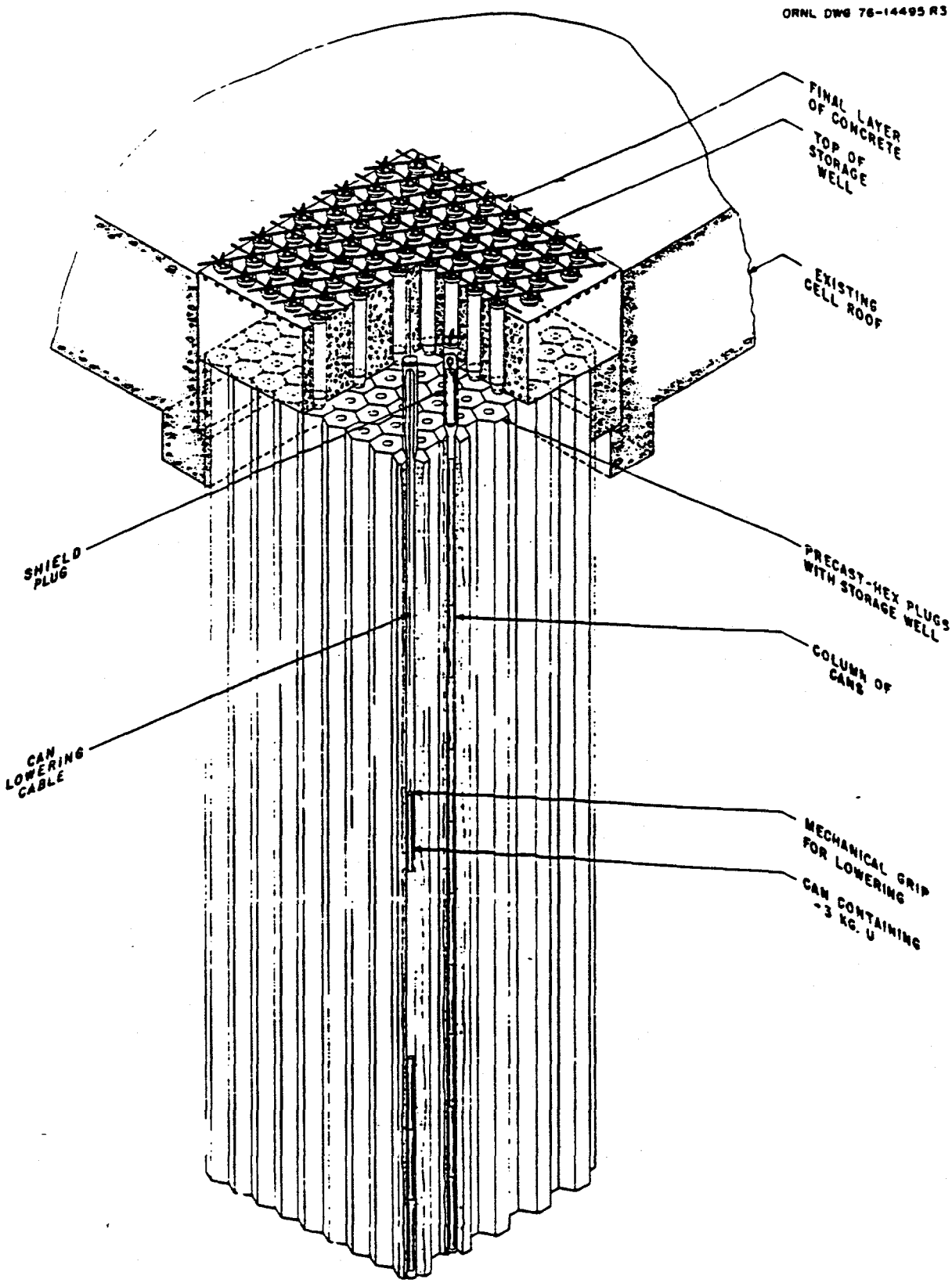

Fig. 4. Cell IV storage facility (isometric).

ORNL-DWG 93M-4773

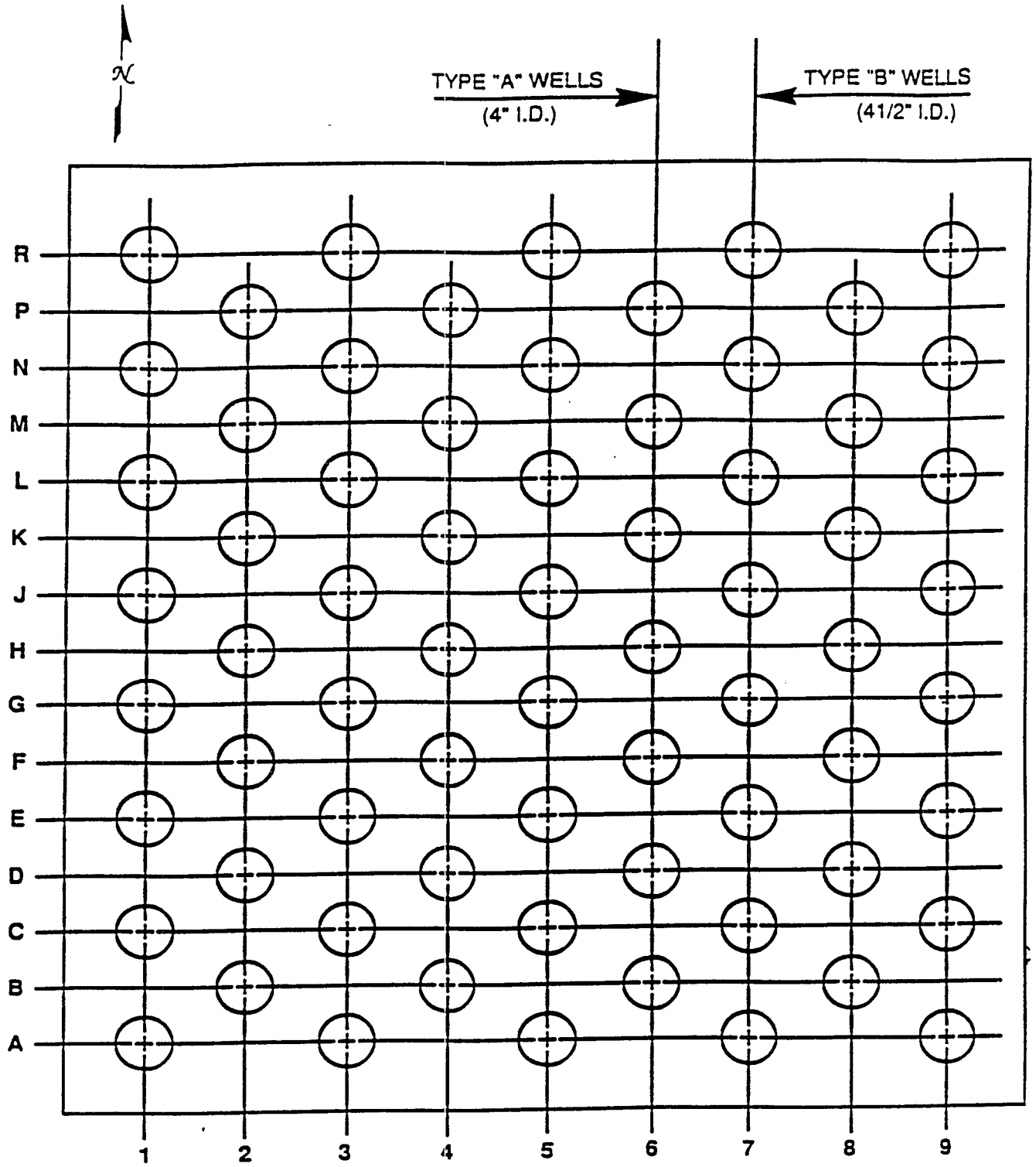

Fig. 5. Identification pattern for Cell 4 storage wells.

Three sets of inter-cell storage wells (a total of 26 wells) are located (in the walls) between Cells 2 and 3, Cells 3 and 4, and Cells 4 and 5, and are also accessible from the Penthouse. The layout, dimensions, and typical construction are illustrated in Figs. 6 and 7. (The in-line wells are located on a 12 inch pitch.) Within each hole, a 4-in-diam, schedule 40, stainless steel tank serves as the storage well. Each of these tanks is also vented through a manifold to the VOG system, and the top of each is (closed) with a...removable (cap). The top of each well is shielded with an 8-in-thick removable plug. Since the wells between Cells 2 and 3 are (arranged) in a triangular pattern (two rows), they...have (less) concrete shielding than the other sets of intercell wells which are configured in a single row centered along the length of the wall). Larger holes were drilled and lead shielding was added to these wells.

Storage of mixed oxide waste in Intercell 2 & 3 wells has been evaluated previously (Ref. 2).

The cell wall concrete composition was analyzed and the results are reported in Ref. 2. The derived atom densities at maximum water content are given in Table 1. Because the chemical analysis provided only an upper limit for hydrogen concentration, a second set of atom densities was generated with the hydrogen contents set to zero in all of the three samples sent for chemical analysis. For the no hydrogen case, the atom density of oxygen increases from that shown in Table 1 to $2.78196(10^{-2})$ - the H atom density, of course, goes to zero. *Unless specified otherwise, all calculations in which the Table 1 concrete was used were based on zero hydrogen content.* The concrete was assumed to contain no steel rebar even though Ref. 3 states that rebar is present.

Table 1. Atom densities for cell wall concrete[a]

Element	Atom density[b] (atoms/(barn*cm))
C	3.82155e-4
H	4.54991e-3
S	2.52827e-5
Na	9.58077e-5
Mg	1.18155e-4
Al	7.68645e-4
Si	1.24659e-2
K	2.15730e-4
Ca	1.71935e-3
Fe	2.29130e-4
Zn	9.36739e-6
O	2.75330e-2

[a] Unless otherwise specified, all calculations performed with zero hydrogen content.
[b] e-x = * 10^{-x}

ORNL Dwg 81-4465

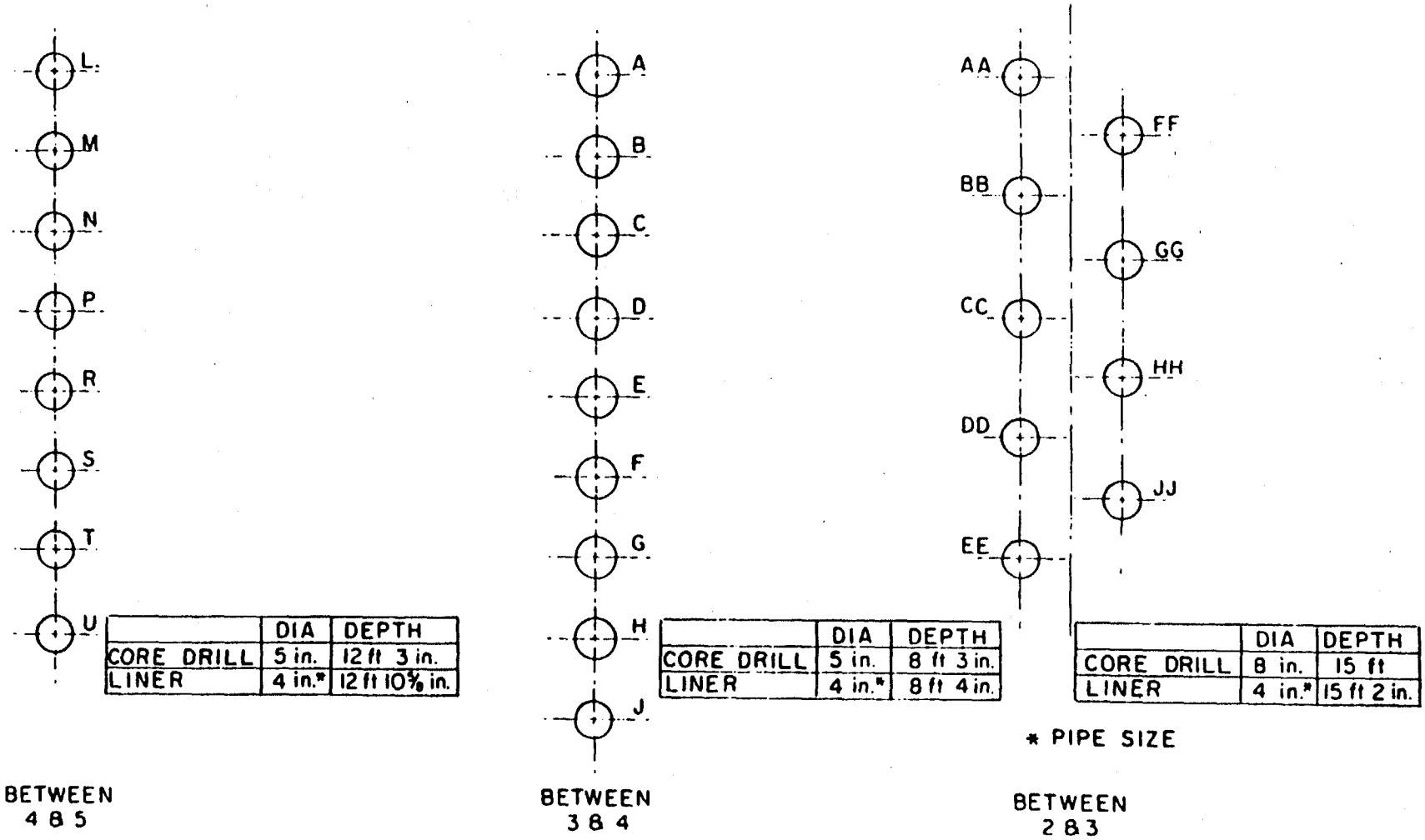

	DIA	DEPTH
CORE DRILL	5 in.	12 ft 3 in.
LINER	4 in.*	12 ft 10⅝ in.

	DIA	DEPTH
CORE DRILL	5 in.	8 ft 3 in.
LINER	4 in.*	8 ft 4 in.

	DIA	DEPTH
CORE DRILL	8 in.	15 ft
LINER	4 in.*	15 ft 2 in.

Fig. 6. Vertical inter-cells solid storage.

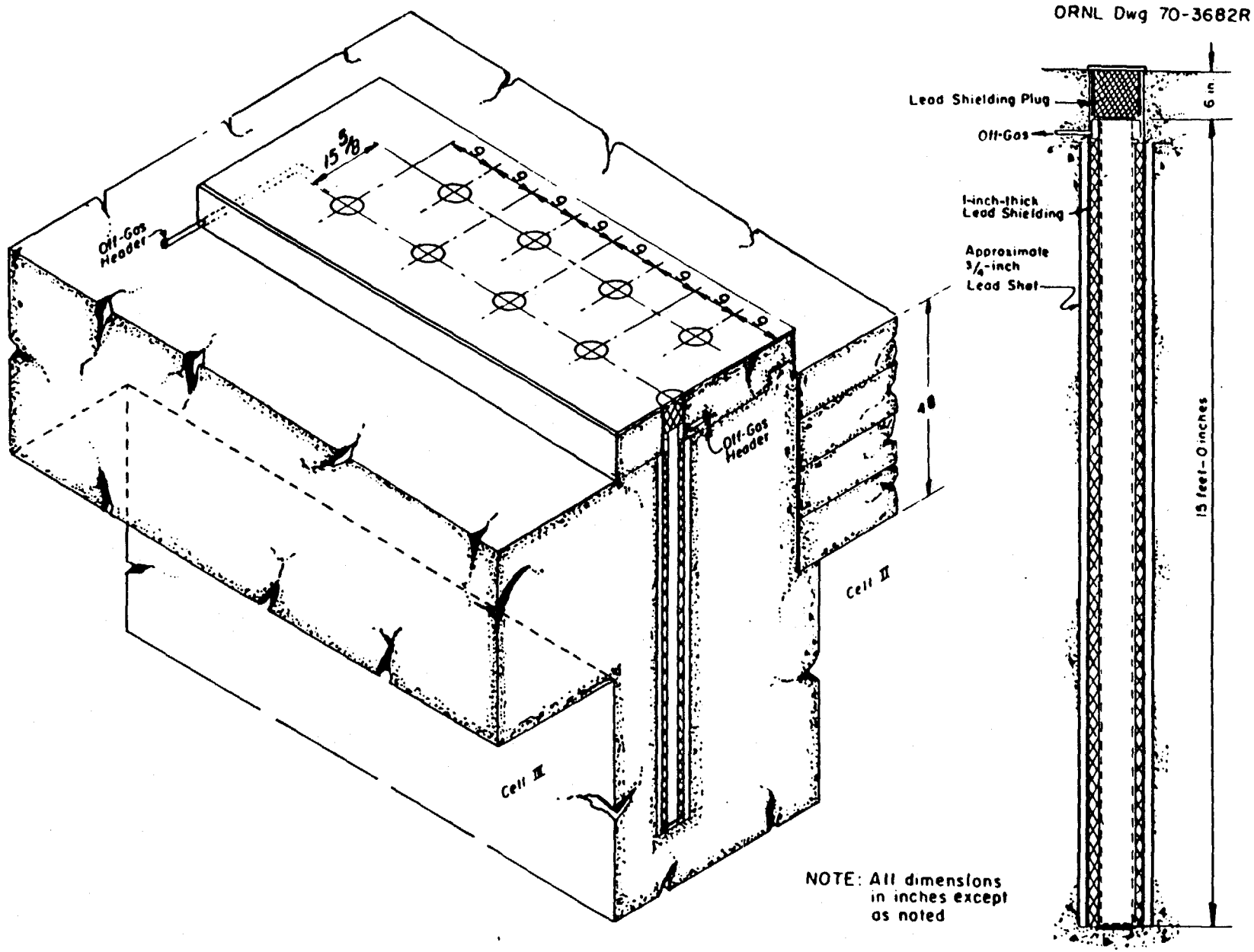

Fig. 7. Building 3019 ^{233}U storage wells, Cells II—III.

The concrete interstitial material of the Cell 4 array has a different composition from the cell wall concrete. Chemical analyses of the concrete constituents from the supplier are contained in Appendix A. The derivation of the atom densities for the concrete is also contained in Appendix A. The values are presented in Table 2.

Table 2. Atom densities for Cell 4 array concrete

Element	Atom density[1] (atoms/(barn*cm))
H	9.46197e-3[2]
C	1.05173e-2
O	4.60778e-2[3]
Na	1.28310e-5
Mg	5.09498e-3
Al	4.16956e-4
Si	2.67500e-3
S	9.61505e-5
K	1.27795e-5
Ca	8.76440e-3
Fe	1.39779e-4
Zn	1.11783e-5

[1] e-x = * 10^{-x}

[2] If assume only bound water in concrete, H atom density is 7.25655e-3.

[3] If assume only bound water in concrete, O atom density is 4.49751e-2.

2.1 NOMINAL FISSILE MATERIAL INVENTORY

A computer database maintained by the staff of Building 3019 provides array inventory information. Fissile loadings and container height are specified. Intercell 2 & 3 storage wells are currently empty but are expected to be filled during 1993 and 1994 with material received from Nuclear Fuel Services (see Ref. 2). For safeguards and security considerations and also because studies showed that credible abnormal conditions (defined in Section 2.2) lead to more reactive configurations, a detailed accounting of the current fissile material inventory is not provided.

Documentation of the fissile material configurations inside the containers is not readily available. Documentation of the container specifications is also not readily available but communication from C. M. Hopper, ORNL, indicates that the fissile material containers are made of steel (composition unspecified). According to A. M. Krichinsky, ORNL, the inside diameter of these canisters is 8.255 cm (3.25 inches) and the outside diameter is 8.5725 cm (3.375 inches). Canister heights vary from 7.54 cm to 61 cm (2.97 inches to 2 feet).

2.2 CREDIBLE ABNORMAL CONDITIONS

2.2.1 Fissile Loading

Based on a review of the computer database, the maximum ^{233}U (or sometimes total U) loading in each storage well was identified. Each storage well containing material was assumed to be filled completely (although several are only partially loaded) with the maximum fissile content material in that well. The identified inventory is given in Table 3 (current as of April, 1993).

Table 3. Assumed credible abnormal storage well inventories as derived from expected current maximum well loadings

Storage array	Well Location	Designation	Loading (kg U/ft)
Cell 4	1A	^{233}U	1.28
	1C	^{233}U	1.36
	1E	Jezebel[a]	1.85
	1G	^{233}U	1.38
	1J to 1R	empty	0.0
	2B	empty	0.0
	2D to 2P	CEUSP	0.96 - 1.58
	3C to 3R	CEUSP	"
	4D to 4P	CEUSP	"
	5C to 5R	CEUSP	"
	6D to 6P	CEUSP	"
	7L, 7R	CEUSP	"
	3A, 4B	empty	0.0
	5A, 6B	empty	0.0
	7A	^{233}U	1.57
	7C	^{233}U	1.35
	7E	^{233}U	0.93
	7G	^{233}U	1.00
	7J	^{233}U	0.37
	7N	U4[b]	1.34
	8D, 8H	U4[b]	1.32, 1.14
	8B, 8F	empty	0.0
	8K, 8M	empty	0.0
	8P	^{233}U	1.89
	9A	^{233}U	0.12
	9C to 9G	empty	0.0
	9J	^{233}U	0.62
	9L	^{233}U	0.75

Table 3. Assumed credible abnormal storage well inventories as derived from expected current maximum well loadings

Storage array	Well Location	Designation	Loading (kg U/ft)
	9N	^{233}U	0.75
	9R	^{233}U	0.78
2 & 3	all	empty	0.0
3 & 4	A	^{233}U	0.81
	B-G	^{233}U	0.83-0.84
	H-J	^{233}U	0.74,0.75
4 & 5	L	^{233}U	0.93
	M	^{233}U	2.13[c]
	N	^{233}U	1.94
	P	empty	0.0
	R	^{233}U	0.97
	S, T	empty	0.0
	U	^{233}U	0.92

[a] Jezebel is a disassembled ^{233}U metal sphere.
[b] U4 material is neutronically similar to CEUSP material.
[c] Peak loading is due to three metal hemispheres which have center-to-center separation of 17 inches.

For well N in intercell 4 & 5, there is a 1.5 inch segment in which the loading is 7.1 kg/ft. The average value considering the material loaded on either side of the segment is less than the maximum listed in Table 3.

2.2.2 Fissile Isotopics

For the intercell wells, the ^{233}U content is greater that 95 wt % of the total uranium present. For Cell 4, ^{233}U material, the wt % may be as low as 60. The isotopics of the material stored in the Cell 4 wells with some of the highest U loading per foot (excluding CEUSP and U4 materials) are given in Table 4. Because of fast fission effects, discussed in Ref. 2, it is appropriately conservative to regard all of the uranium inventory listed in Table 3 as ^{233}U (except for the CEUSP material) when comparing to the subcritical limits which are derived in Section 5.

Table 4. Fissile/total uranium ratios for selected Cell 4 locations

Cell 4 Well Location	kg Total U/ft	Fissile/Total U ratio
1A	1.28	0.98
1C	1.36	0.98
7A	1.57	0.978 - 0.981
7C	1.35	0.969 - 0.984
8P	1.89	0.867

The isotopics of the CEUSP material are given in Table 5 (from Ref. 1). These values were used in all criticality calculations.

Table 5. Isotopic content of uranium in CEUSP fuel

Isotope	Weight %
^{233}U	9.7
^{234}U	1.4
^{235}U	76.5
^{236}U	5.6
^{238}U	6.8

All of the U4 material was assumed to be ^{233}U. Likewise the metal hemispheres located in in-line well M were assumed to be 100% ^{233}U (19.05 g/cm^3, atom density = $4.92368*10^{-2}$).

2.2.3 Fuel Form

All Cell 4 fissile material is present as either metal or oxide. Approximately 3 kg of ^{233}U fluoride is stored in intercell 4 & 5 wells, the remainder of the material stored in intercell wells is either metal or oxide.

No information is available regarding the integrity of the fluoride material. Based on a brief, in-place inspection of containers in the well by A. M. Krichinsky, the containers appeared intact. Behavior of the material under flooding conditions is not known. It is assumed that the material would not escape from its storage containers.

2.2.4 Double-Batching of Fissile Material

Double batching of fuel inside a given storage container is possible for some of the fuel stored in the arrays. To account for double batching in existing loadings (double batching in future loadings is treated in the evaluation for the derivation of subcritical), it is assumed that the entire column is filled with the highest density present anywhere in the array of that column's material designation (CEUSP, ^{233}U, etc.). For instance, all CEUSP material in the array would be assumed to have a linear loading of 1.58 kg U/ft. In fact, the CEUSP material in the computational model was assumed to have a linear loading of 1.55 kg/ft. This value was believed to be the maximum at the start of these studies. The reactivity effect of the single canister which has a loading of 1.58 kg/ft is judged to be insignificant.

Double-batching as related to deriving subcritical limits is addressed by doubling the fissile concentration along a three-foot length in any given well This abnormal condition will be further described in Section 4.

2.2.5 Other Materials Present in Canisters Containing Fissile Material

In addition to the fissile material specified in Tables 3 and 5, each CEUSP canister contains 800 grams of Cd, present as CdO, and 100 grams Gd, present as Gd_2O_3 (These values are from Part B of Permit for Hazardous Material Storage. There is some variation among canisters and the values quoted are averages). The volume of each canister is 3.13 liters (inside radius = 4.04 cm) yielding a Cd atom density of $1.36928*10^{-3}$ atoms/(bn*cm) and a Gd atom density of $1.22353*10^{-4}$ atoms/(bn*cm). Except where noted, neither the Gd nor Cd was included in the criticality calculations.

The water content of the materials listed in Table 3 is specified in Appendix B. Note that the linear loading limit specified in Appendix B conflicts with values in Table 3 and was found to be in error.

2.2.6 Water Ingress to Storage Wells

Also found in Appendix B is the specification that flooding of any two wells simultaneously is possible. However procedural requirements for loading and unloading fissile material in 3019 storage wells specify that the open wells must be non-adjacent. (This is contrary to the statement made in Appendix B but at the time that memorandum was issued it was the desire of facility operators to remove the non-adjacent restriction. Subsequent studies showed this was not possible.) It is possible that during a flooding event, such as activation of the overhead water sprinklers, water could enter the wells and the containers inside the wells. The configuration of the fissile material inside a flooded canister was treated as an unknown and was subsequently defined via computational studies reported in Section 4.0.

Subsequent to the completion of these studies, fissile material handling procedures were revised and incorporated into Procedure RDF-OP-024. This procedure specified that "fire sprinklers serving the well access area must be valved out and relieved of its residual line pressure before accessing any wells (Section 9.5.7)" and "up to four available wells may be opened at the same time."

2.2.7 Structural Integrity of Storage Facilities

It is assumed that the structural integrity of the containers in the wells is unaffected over time. It is also assumed that the steel liners and lead shielding in the wells do not degrade over time. These assumptions have not been verified.

The Safety Analysis Report (Ref. 2) states that all fuel storage facilities are safe from disruption by a design basis earthquake or other natural hazards. Therefore, the assumed computational models are predicated upon design and operational parameters specified herein.

3. CALCULATIONAL METHODS

All evaluations are based on Monte Carlo calculational techniques. Confidence in their accuracy is gained by comparison to previous calculations by Hopper and Turner, by the validation calculations reported in Appendices C, D, E, and F and by verification studies reported in Ref. 4 and in this document. This work was performed to fulfill the requirements of Martin Marietta Energy Systems, Inc. Standard number ESS-CS-103, "Nuclear Criticality Safety Calculations."

3.1 SOFTWARE REQUIREMENTS - PROGRAMS AND CROSS SECTIONS

The nuclear criticality safety calculations were performed using the multigroup Monte Carlo criticality program KENO-Va as called from the CSAS25 module of the SCALE[5] system. All calculations were performed with the 16-energy-group cross sections identified as HANSEN-ROACH within the SCALE system. The versions of KENO-Va, SCALE, and the cross section library were those contained in the Martin Marietta Nuclear Criticality Safety Software (NCSS, Ref. 6) procedure on the IBM-3090 during June 1992 through August 1993. The same programs/libraries were used for the safety analyses as were validated with the critical experiments.

3.2 ACCREDITATION

While the KENO-Va program is a state-of-the-art analysis program, some of the data in the Hansen-Roach library dates to the early 1960s. This aging cross section library is selected to maintain continuity with previous work[1,3] and because it is the library recommended by the Oak Ridge National Laboratory

Criticality Safety Review committee. While the current document is peer reviewed, the comparison to this independently conducted, previous study,[1] the use of Safety Review committee recommendations for data library selection, and prior publications by the author[2,7,8,9] add to the assurance that trained, technically competent personnel performed the calculations and reviews.

3.3 VALIDATION

3.3.1 Data Sources

The principal reference for critical experiments for validation was B. L. Koponen's compilation (Ref. 6). However other sources provided valuable tabulations of data (^{233}U in Ref. 10, ^{235}U in Ref. 11, and Pu in Ref. 12). Jordan's datasets from Ref. 11 provided a starting point for modeling ^{235}U systems. The datasets documented in Ref. 12 are contained in the CESAR library program which is a part of the SCALE system. These datasets were the starting point for the plutonium calculations. Some modifications to both the ^{235}U and Pu datasets were needed to accommodate changes in the SCALE system since the datasets were created.

All critical experiment datasets prepared for this report were contributed to the CESAR(SCALE) system. All of the computer-generated output was recorded on microfiche and provided to the Nuclear Criticality Safety Group of the Facility Safety Section of the Office of Operational Readiness and Facility Safety, Oak Ridge National Laboratory.

Validation studies for uranium-233 bearing experiments are contained in Appendix C. Studies for ^{235}U systems are in Appendix D; plutonium experiments are analyzed in Appendix E. Two critical experiments performed with both ^{233}U and highly enriched ^{235}U are analyzed in Appendix F. All data were analyzed according to the statistical method presented in Ref. 13. The appendices provide brief descriptions of the critical experiments and references to more detailed descriptions. Comparisons of the similarities and differences between the critical experiments and the calculations used to derive the safety limits are also included in these appendices.

3.3.2 Validation Philosophy

The ideal validation would be one which is performed with experiments which exactly resemble the configuration to be certified as safe. Of course, if these experiments existed, there would be no need to perform calculations as the configuration of interest would have already been shown to be safely subcritical. Consequently, whenever calculations are required for evaluating subcriticality, it is to be expected that the critical experiment database will always be lacking desired data to some degree.

To compensate for an incomplete database, a philosophy of "separation of variables" is used. K-effective is assumed to be a function of all of the physical variables in the problem. If all of the data, including the cross section data, are measured accurately then k-effective should equal a constant, 1.0 (assuming the computational model and program are accurate). However it is assumed that, due to incomplete or inaccurate data, trends and/or biases in k-effective due to variations in the physical parameters exist. By the assumption of separation of variables, it is assumed that the bias or trend due to one physical variable is independent of the bias or trend due to another.

The function which represents k-effective is determined by a stepwise procedure. The physical conditions of the configuration under evaluation are identified. Those experiments which are the closest match to these physical conditions are selected, k-effectives are calculated, any trends or biases are identified, and appropriate tolerance or confidence limits are applied.

To account for those physical conditions which exist in the configuration under study but which do not exist in the set of critical experiments previously identified, pairs or pairs of sets of critical experiments are sought. In these pairs, only a single physical parameter, present in the configuration undergoing a safety evaluation, is allowed to vary. By examining calculated k-effectives for a pair (or a pair of sets) of critical experiments, the effect of the physical variable on calculated k-effective can be determined. The neutron spectra in the pairs should be the same as in the initial set of critical experiments (and as in the configuration under study). If it is different, then reaction rates and the point or groupwise nuclear data must be examined to determine if the results from the paired experiments are relevant to the configuration under study.

If paired experiments cannot be found, then the nuclear data libraries must be examined to determine if the nuclear data which cause the physical phenomena could have a significant impact on calculated k-effective. If not, the phenomena is ignored. If so, or if no nuclear data exist or if the uncertainties in the data are so large that one cannot confidently assess the impact of the data on the calculation, then additional experiments (either critical or cross section measurement or both) must be performed. If the critical experiments in the initial group contain physical parameters which are not present in the configuration under study, then pairs of experiments should be sought which assess the impact on k-effective of the presence of those parameters. If paired experiments cannot be found then the same procedure as described previously should be followed.

For this study, six physical variables were identified. These included: fissile isotope present, density of fissile isotope, physical form of fissile isotope-bearing-material (oxide, metal), degree of hydrogenous moderation, array of cylinders geometry, concrete moderation and reflection. Separate validation studies were performed for each of the three fissile isotopes considered in this study. Thus each instance of the first variable was considered separately. The next three variables - density, form, and degree of moderation - were treated by examining the large databases available for each nuclide. The final two were assessed by examining pairs of experiments (see Appendices C, D, and E).

The separation of variables procedure is believed to be a good approach provided the neutron spectra for the critical experiments is a close match to that believed to exist in the configuration under study. However, in the pairwise correction terms, if the fissile material in the paired experiments differs from that in the configuration under study, the calculated reactivity worth due to the physical variable being studied may or may not be a conservative estimate. This is due to variation in fission/absorption cross section ratios among fissile nuclides. Nevertheless, the estimate from pairwise comparisons is believed to be the best available.

3.4 VERIFICATION OF SOFTWARE

As noted previously, Ref. 4 provides a verification plan for the NCSS system. Verification is the confirmation that the coded algorithms solve correctly the equations which describe the behavior of the system. One method of verification, consistent with Ref. 4, is to calculate the same configuration with two different programs. The simple geometries present in several of the critical experiments provide additional, easy-to-model verification of the KENO-Va program.

Experiments conducted in spherical geometry can be modeled exactly with one-dimensional discrete ordinates theory. Table 6 provides a comparison of k-effectives calculated with CSAS1X - using a 1D discrete ordinates program, XSDRNPM - with those from the CSAS25 (KENO-Va) module. Experiments were taken from the uranium-233, mixed ^{233}U and ^{235}U, and plutonium validation studies. Agreement is excellent.

It is sometimes argued that the comparisons in Table 6 only verify the KENO-Va program for spherical geometries. This argument seems too restrictive and it is proposed instead that routines common to all geometry types in KENO-Va are verified. These include random number generation, ray-tracing and border crossing determination algorithms, macroscopic cross-section generation and others.

Table 6. Comparison of discrete ordinates and Monte Carlo k-effectives

Koponen Citation I.D.	k-effective		One standard deviation for CSAS25 calcs.
	CSAS1X	CSAS25	
2110-1	1.01308	1.01399	0.00121
2110-2	1.00313	1.00061	0.00418
2110-3	1.00230	1.00177	0.00335
2110-4	1.00324	1.00310	0.00568
2110-7	1.00553	1.00217	0.00350
2110-30	1.00896	1.01325	0.00483
2110-32	1.00513	1.00497	0.00489
1727-1	1.00589	1.00931	0.00411
1727-2	0.99935	0.98943	0.00327
1727-3	1.00528	1.01044	0.00323
1727-4	1.00602	1.00165	0.00373
1727-5	0.98553	0.99146	0.00365
1727-6	0.99203	0.98712	0.00370
1727-7	1.02217	1.01410	0.00358
1727-8	1.01560	1.00771	0.00366
1727-09	0.99490	0.99885	0.00393
1727-10	1.00209	1.00486	0.00356
1727-14	1.00557	1.00574	0.00369
1727-15	1.00667	1.00367	0.00349

3.5 COMPUTATIONAL MODELS

Initially, each set of storage wells was to have its own set of loading limits. Consequently, several computational models were developed to establish these limits. During the course of study, it was determined that, under certain assumptions, the Cell 4 array interacted neutronically with the in-line 4&5 storage wells. Consequently, the Cell 4 model was joined with the in-line 4&5 well model and a single set of fissile loading limits was established for both storage arrays. To avoid confusion of facility operators, the same set of limits were applied to Intercell 3&4.

Though not used to determine the fissile load limits, the results which were calculated for each array independently are presented. These data aid in understanding the sensitivity of the calculated k-effectives to the physical parameters. They might also be useful for extending the allowable fissile loadings to higher values should certain assumptions be proved in the future to be unnecessarily conservative.

3.5.1 In-line Storage Well Model

In-line storage wells (Intercell 3 & 4 and 4 & 5) were represented by a single computational model. Nine storage wells were assumed (as in 3 & 4), each with a depth of 12 feet, 3 inches (as in 4 & 5). The wells were placed on a 12 inch pitch with array placement relative to cell walls being like that of 4 & 5 wells.

The fissile material was assumed to fill the entire region inside the pipe liner. Previous studies (Ref. 2) have shown that, regardless of fissile material, at a given degree of moderation, k-effective decreases as fissile material diameter decreases (linear fissile loading remaining the same). No canisters were included in the model but the pipe liner was included. The cell wall concrete was that specified in Table 1 but with no water. (This assumption is very conservative and could be relaxed with better concrete analyses). Detailed specifications of this model are given in Appendix G.

3.5.2 Cell 4 Array Model

The Cell 4 array was modeled as shown in Fig. 8. Several Cell 4 models were developed and all are documented in Appendix H. In the final model, the CESUP and U4 materials were placed in the positions noted in Table 3. The remaining positions, shown in Fig. 8, were assumed to be empty and available for filling with new material. The subcritical limits described in the next section apply to ONLY the empty wells shown in Fig. 8. Limits for the other wells are the maximum values shown in Table 3.

As for the in-line model, in Cell 4, the fissile material was assumed to fill the entire region inside the pipe liner. No canisters were included in the model but the pipe liner was included. The Cell 4 concrete array was assumed to contain only bound water. The Cell 4 walls were assumed to contain no water.

The Cell 4 walls, floor, and ceiling were modeled as shown in Figs. 2 and 3 with one exception. The two cell walls immediately adjacent to the Cell 4 array were 2 feet thick instead of 4 feet. This was a propagation of a model description taken from Ref. 1 studies. The anomaly was discovered when the combined Cell 4 and in-line model was created. Scoping calculations which are reported in Section 4 revealed that this difference between model and reality did not significantly impact calculated k-effectives. Detailed specifications of this model are given in Appendix H.

3.5.3 Combined Cell 4 and In-line Model

This model was used to generate the safely subcritical limits which are presented in Section 5.0. The model was created by forming a two-unit array. The in-line model described in Section 3.5.1 was the first unit of the array. The Cell 4 model (Section 3.5.2), with corrected concrete wall thicknesses, was the second unit of the array. The in-line model was modified so that the hemispheres in well M were modeled explicitly. The hemispheres were assumed to be located at/around the vertical mid-point of the well. Detailed specifications of this model are given in Appendix I.

4. DESIGN SCOPING CALCULATIONS

The calculations presented in this section were not used to derive subcritical limits but nevertheless meet the requirements imposed by Martin-Marietta standard ESS-CS-103. All calculations reported in this section were performed with the verified, validated methods discussed in Section 3. The results of these studies enabled the proper model for establishing subcritical loading limits to be developed (Section 5.0). Additionally, with some changes which are noted in Section 6.0, these calculations could serve at the basis for revised, higher loading limits.

All input datasets for these cases are stored on the floppy disk which is attached to the inside back cover of this report. All output datasets were microfiched and are the responsibility of the Criticality Safety Group of the Office of Operational Readiness and Facility Safety of Oak Ridge National Laboratory.

ORNL-DWG 93M-4773R

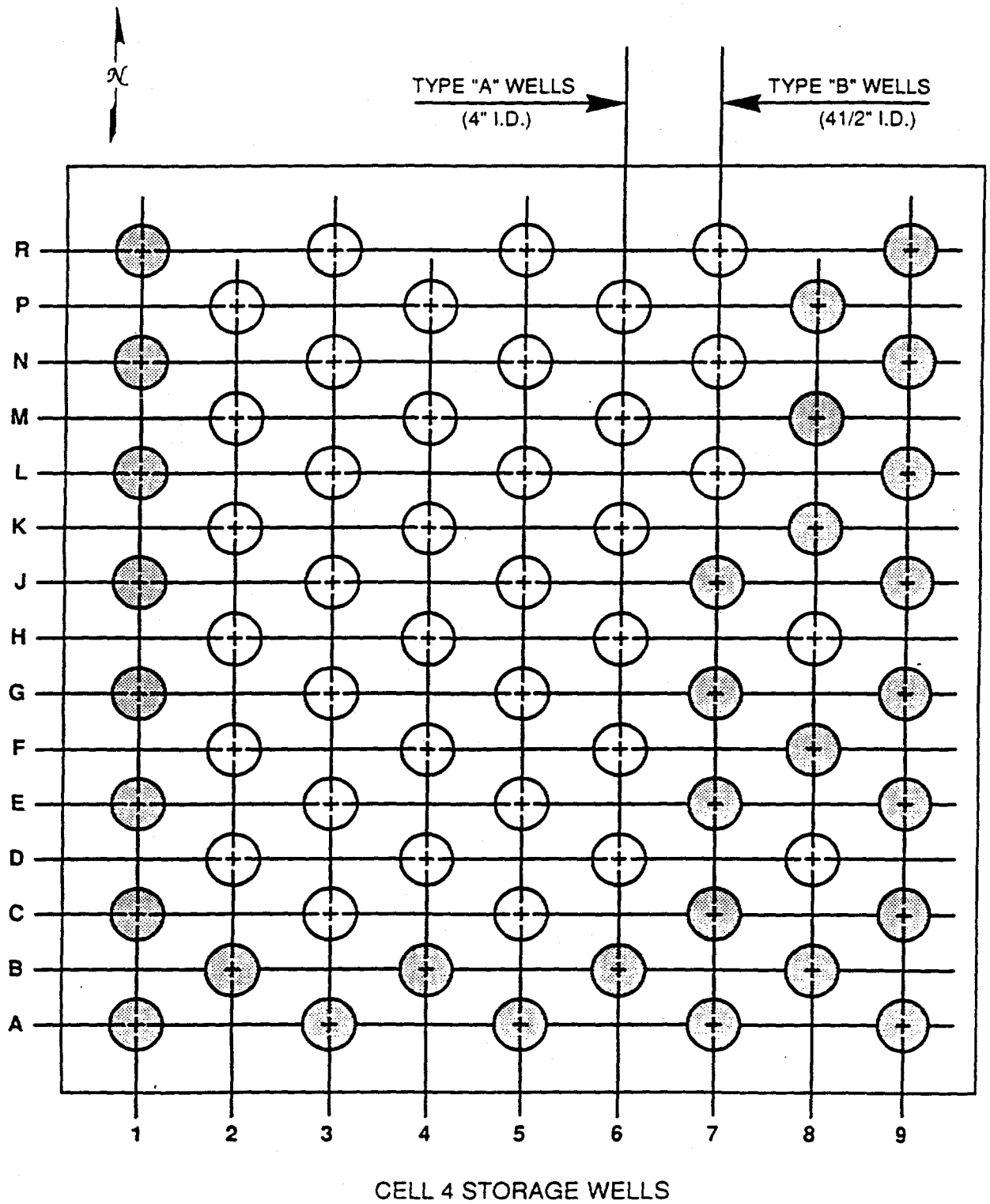

Fig. 8. Available locations (shaded circles) for storing material in the Cell 4 array.

4.1 IN-LINE STORAGE WELL CALCULATIONS

At the beginning of these studies, the in-line wells were treated separately from the Cell 4 storage wells. A single KENO model for the in-line wells - intercell 3 & 4 and 4 & 5 shown in Fig. 6 - was created by assuming the most reactive features of each storage array. An array of 9 storage wells was created, as in intercell 3 & 4, each having a depth of 373.38 cm (12 ft, 3 in), as in intercell 4 & 5. Reference 3 provides the following information regarding cell wall construction.

> All cell walls are built of poured, reinforced concrete. The outer walls on the north, east, and west sides have a thickness of 5 ft, and those on the south side and the top have a thickness of 4 ft. The interior walls separating the cells have a thickness of 5 ft.

The in-line wells have a 30.48 cm (12 in) pitch.

A KENO model of this "generic" in-line array is documented in Appendix H. The model contains one unit repeated nine times. The unit has 3 concentric cylinders, fissile material with a radius of 5.08 cm, steel well liner with radius of 5.68198 cm, and void with a radius of 6.35 cm. These cylinders are surrounded by a cuboid of concrete 152.4 cm thick (through the wall from cell to cell), 30.48 cm wide (well pitch), and height of 373.38 cm. The array of nine wells was then reflected by cell wall concrete according to dimensions given in Section 2.0 of this report.

Three sets of calculations were performed to determine the subcritical limits for ^{233}U, ^{235}U and Pu-239. These studies, which are searches for "target" k-effective values, are reported in Tables 7, 8, and 9. The target values of k-effective which were defined to be subcritical are based on the limits defined in Appendices C, D, and E. Assuming a one standard deviation value of 0.00350, the target k-effectives were 0.913 for ^{233}U, 0.929 for ^{235}U and 0.943 for ^{239}Pu (subcritical limit from appropriate appendix minus two standard deviations). All of the datasets for Tables 7, 8, and 9 are stored on the floppy disk attached to the back cover of this report. The datasets are in directory /section4.0/4.1/x where x is table7.u233, table8.u235, or table9.pu239.

The results of the three studies are shown in Table 10. If it were impossible to flood the in-line wells and if the in-line wells could be shown to be neutronicly isolated from the Cell 4 wells (for instance, by reanalyzing the cell wall concrete to accurately determine the hydrogen content) then these limits could be applicable to fissile material storage. The values are significantly higher than the currently proposed values.

Table 7. K-effectives for various ^{233}U, in-line configurations

Case Number (i3_4u3XX where XX is shown here)	H/^{233}U	kg ^{233}U/ft	k-effective	One standard deviation for k-effective
1	0	8.7	1.03684	0.00362
2	1	6.0	0.94663	0.00370
3	3	4.7	0.95566	0.00355
4	5	4.0	0.97753	0.00364
5	10	2.6	0.96344	0.00377
6	0	6.0	0.89271	0.00370
7	1	5.0	0.87963	0.00330
8	3	4.0	0.89328	0.00353
9	5	3.0	0.86367	0.00340
10	0	6.5	0.91976	0.00349
11	1	5.4	0.90292	0.00301
12	3	4.25	0.92173	0.00363
13	5	3.4	0.90651	0.00346
14	10	2.3	0.91940	0.00357
15	0	6.4	0.91196	0.00360
16	1	5.6	0.91815	0.00332
17	3	4.15	0.89856	0.00327
18	5	3.5	0.92415	0.00364
19	10	2.2	0.89472	0.00340
20	1	5.5	0.91536	0.00327
21	3	4.2	0.91160	0.00361
22	20	1.0	0.76945	0.00342
23	20	1.7	1.00545	0.00392
24	20	1.4	0.91970	0.00398
25	20	1.3	0.88153	0.00369

Table 8. K-effectives for various ^{235}U, in-line configurations

Case Number (i3_4u5XX where XX is given here)	$H/^{235}U$	kg ^{235}U/ft	k-effective	One standard deviation for k-effective
1	0	17.1	1.06575	0.00334
2	1	13.11	1.06218	0.00337
3	3	9.68	1.05849	0.00321
4	5	8.5	1.11376	0.00363
5	5	7.5	1.06641	0.00333
6	10	4.87	1.06676	0.00344
7	1	10.4	0.97243	0.00284
8	3	7.3	0.96376	0.00342
9	5	5.9	0.97532	0.00307
10	10	3.7	0.95475	0.00316
11	0	11.7	0.92526	0.00330
12	1	9.1	0.92414	0.00315
13	3	6.5	0.91806	0.00338
14	5	5.1	0.91402	0.00362
15	10	3.4	0.92065	0.00343
16	0	11.9	0.92672	0.00319
17	1	9.3	0.93219	0.00311
18	3	6.75	0.93174	0.00307
19	5	5.4	0.93135	0.00341
20	10	3.5	0.92731	0.00326
21	0	12.1	0.93006	0.00309
22	3	6.6	0.92136	0.00324
23	5	5.3	0.93184	0.00323
24	20	1.5	0.79396	0.00334
25	20	2.3	0.97739	0.00376
26	20	2.1	0.93978	0.00369
27	20	2.0	0.92068	0.00360

Table 9. K-effectives for various ^{239}Pu, in-line configurations

Case Number (i3_4XX where XX is given here)	H/^{239}Pu	kg ^{239}Pu/ft	k-effective	One standard deviation for k-effective
1	0	7.73	0.93932	0.00367
2	1	8.42	1.06203	0.00339
3	3	6.77	1.07283	0.00350
4	10	4.01	1.07248	0.00376
5	5	6.0	1.10320	0.00353
6	5	5.5	1.06478	0.00351
7	1	6.0	0.90155	0.00329
8	1	5.0	0.82592	0.00310
9	3	4.0	0.83502	0.00331
10	3	3.0	0.71440	0.00299
11	5	3.0	0.78421	0.00338
12	5	2.0	0.63124	0.00287
13	10	2.5	0.86193	0.00375
14	10	1.5	0.64490	0.00320
15	10	3.1	0.95122	0.00371
16	5	4.5	0.97155	0.00348
17	3	5.2	0.94810	0.00345
18	1	6.5	0.94101	0.00343
19	3	5.0	0.92939	0.00306
20	3	5.1	0.94146	0.00349
21	5	4.2	0.93586	0.00373
22	10	2.9	0.92542	0.00361
23	10	3.0	0.93941	0.00336
24	20	2.0	0.95884	0.00338
25	20	1.8	0.90348	0.00347
26	20	1.9	0.94065	0.00329

Table 10. Subcritical limits for autonomous, dry, in-line storage

H/fissile atom	^{233}U (kg/ft)	^{235}U (kg/ft)	^{239}Pu (kg/ft)
0	6.4	12.1	7.7
1	5.5	9.3	6.5
3	4.2	6.7	5.1
5	3.4	5.4	4.2
10	2.2	3.5	3.0
20	1.3	2.0	1.9

The values in Table 10 are, in every case, a reduction from previously accepted values as documented in Ref. 1. The percentage decrease is noted in Table 11. The reductions are believed due to: (1) differing assumptions regarding the water content of cell wall concrete; and (2) the safely subcritical value of k-effective for ^{233}U and ^{235}U is lower in the current work than in Ref. 1.

Table 11. Percentage decreases in Table 10 limits from Ref. 1 limits

H/fissile atom	^{233}U	^{235}U	^{239}Pu
0	27	29	0
1	28	29	23
3	34	31	24
10	36	28	25
20	36	31	27

The Table 10 limits could be applicable for intermixing fissile types and degrees of moderation within the storage array. Studies presented in Section 4.3 support this conclusion.

4.1.1 Comments on Statistical Methods

Considerable effort is devoted in Ref. 1 to fitting equations to data such as that shown in Tables 7-9. The resulting equations are then used to predict the load limit which corresponds to a particular value of k-effective. It is acknowledged that this procedure uses all the information determined during the search rather than simply finding a single calculation which closely matches the target k-effective (the procedure used in the current work) and therefore should be more accurate. However, the procedure as stated in Ref. 1 does not include consideration of the uncertainties on the coefficients for the fitted equations. Just as a given calculation from the current study must be two standard deviations below the derived safety limit, some degree of uncertainty, possibly also two standard deviations, must also be applied to the fitted coefficients. The statistical theory underlying the selection of a single case for examination as compared to the subcritical limit is well-developed and has been published. The use of a fitted line, while intuitively superior, needs further statistical analysis before being utilized.

4.1.2 Special Limits for Application to Sample Storage—Unrestricted Moderation

Though maximum inventory is noted in Table 3, some locations are filled with samples enclosed in several plastic bags. The quantity of each of these samples is small - less than 200 grams of fissile material. Since the weight of the packaging material is comparable to the sample, the H/fissile atom ratio can easily be greater than 20. As a result, there are no defined limits in Table 10 for this material.

A study was conducted in which all in-line wells were assumed to be filled with water. The concentration of fissile species was then gradually increased until the previously identified safely subcritical limits were achieved. A 1% reduction in water density due to the presence of the fissile species was not taken into account but is believed to be statistically insignificant. The KENO model used was the same as documented in Appendix H. All calculations are reported in Table 12. The derived, unrestricted moderation limits for in-line wells were 0.235 kg ^{233}U/ft (at H/^{233}U = 269), 0.408 kg ^{235}U/ft (at H/^{235}U = 155) and 0.272 kg ^{239}Pu/ft (at H/^{239}Pu = 238).

Table 12. Determination of unrestricted moderation concentration for in-line wells

Fissile Material	Concentration (g/L)	k-effective	One standard deviation for k-effective
^{233}U	59	0.77730	0.00313
"	125	0.98423	0.00375
"	100	0.92524	0.00387
"	95	0.90215	0.00338
^{235}U	80	0.77871	0.00329
"	170	0.93516	0.00360
"	160	0.91337	0.00364
"	165	0.92101	0.00319
^{239}Pu	49	0.80851	0.00334
"	98	0.92519	0.00364
"	105	0.93117	0.00348
"	115	0.94514	0.00361
"	110	0.93090	0.00344

4.2 CELL 4 STORAGE WELL CALCULATIONS

As noted in Section 4.1, at the beginning of these studies, the Cell 4 facility was to be treated separately from the other storage arrays. Consequently studies similar to those presented in Section 4.1 were performed for the Cell 4 array. Several KENO-Va models, based on the description presented in Section 2.0 and described in Appendix H, were used to determine subcritical fissile load limits.

4.2.1 Comparisons to Previous Studies

The goal of the first set of Cell 4 studies was to replicate earlier results from Ref. 1 (see similar studies in Ref. 2). All locations in the new Cell 4 array model were assumed to be filled with the same type of

fuel and same moderator-to-fissile-atom ratio when determining k-effective. This procedure was followed in Ref. 1 in determining the original array limits.

At the time that the calculations in Ref. 1 were performed, neither the composition of the cell wall concrete (Table 1) nor the composition of the Cell 4 array concrete (Table 2) were known. Consequently the material ORCONCRETE from the SCALE standard composition library was used. However, studies conducted subsequent to the writing of Ref. 1 had supposedly shown that substitution of Cell 4 atom densities into the KENO model had no significant effect.

In the current studies, the Table 2 atom densities are used (Table 1 data were not yet available) but the remainder of the KENO model is intended to duplicate the earlier, Ref. 1 studies. Studies are conducted to determine if, by varying the water content of the Cell 4 concrete (the actual value being somewhere between the poured and bound values), the results from Ref. 1 could be reproduced. These initial studies along with two calculations from Ref. 1 are contained in Table 13. Datasets corresponding to the case I.D. values can be found on the floppy disk attached to the back cover of this report. They are stored in the directory /section4.0/4.2/4.2.1 .

Good agreement is obtained between the two values from the earlier work and the current model with H atom density equal to the poured concrete value. The hydrogen atom density in "poured " concrete ($9.46197*10^{-3}$) is 11.3% larger than the value for ORCONCRETE ($8.50018*10^{-3}$) but the value for bound water ($7.25655*10^{-3}$) is 14.6% lower. Presumably the differences observed are due to the differing concentrations of other concrete constituents.

Several aspects of this Cell 4 model differed from later models described in subsequent sections. These include:

(1) All wells were taken to be 11.43 cm (4.5 inches) in diameter. Later models (Section 4.2.3) included the differing diameters seen in Fig. 8.

(2) The hexagonal cross section concrete logs (see Fig. 4), separated by air gaps, were modelled as cylinders with equal center to center spacings and nearly equal air gaps between surfaces, Later models (Section 4.2.3) had Cell 4 concrete with bound water hydrogen spread uniformly throughout the hexagonal pitch array.

(3) The boundaries of the model were taken to include 60.96 cm (24 inch) thick concrete walls, a 91.44 cm (3 feet) thick concrete ceiling and a 60.96 cm (24 inch) thick concrete floor. Later models (Section 4.3) were based on the wall thicknesses provided in Ref. 3.

Besides establishing continuity with earlier work, these studies document the high degree of sensitivity of k-effective to the assumed water content in the Cell 4 concrete. The assumed bound value is defensible (based on Appendix A) and conservative (based on Table 12). It is likely that the fissile load limits documented in the next section could be increased if more accurate data regarding the water content of Cell 4 array concrete could be determined.

Table 13. Initial, uniformly fueled Cell 4 studies

Case I.D.	$H/^{235}U$	Water content of Cell 4 concrete[a]	k-effective	One standard deviation for k-effective	Average energy group for fissions
cell4_1[b]	1	bound	1.00335	.00258	11.64
cell4_2[b]	1	int	0.97966	.00208	11.75
cell4_3[b]	1	poured	0.95201	.00245	11.83
Ref. 1[b]	1	oak ridge	0.95813	.00426	-
cell4_4	5	bound	1.03074	.00243	12.27
cell4_5	5	int	0.99661	.00243	12.35
cell4_6	5	poured	0.96609	.00240	12.39
cell4_7[c]	20	bound	1.00522	.00268	13.74
cell4_8[c]	20	int	0.97500	.00248	13.77
cell4_9[c]	20	poured	0.94879	.00250	13.80
Ref. 1[c]	20	oak ridge	0.95737	.00480	-

[a] See Appendix A. Data are provided for water content of the concrete as poured ("poured"), chemically bound water ("bound") and an intermediate value ("int", average of poured and bound values). The term "oak ridge" refers to the SCALE standard composition designated ORCONCRETE.

[b] Problem definition taken from Ref. 1, Table 3, pg. 13, ^{235}U density = 1.3007 g/cm^3, radius of fuel mixture = 5.715 cm.

[c] Problem definition taken from Ref. 1, Table 3, ^{235}U density = 0.4644 g/cm^3, radius of fuel mixture = 5.715 cm.

4.2.2 Area of Applicability for Nominal Conditions

Another important item from Table 13 is the range of the average energy group for fission (AFG) values. Appendix B notes that the maximum value expected for $H/^{235}U$ in the array is 3 which means the AFG value under nominal conditions should range between 11.6 and 12.4. As documented in Appendix C, there are no critical experiments in this range of AFG values. It will be seen later that consideration of credible abnormal conditions will determine the load limit and that in those cases, the AFG values are also not within the range of values determined for critical experiments.

4.2.3 Cell 4 Calculations with CEUSP Material Explicitly Modeled

The verification of the Ref. 1 calculations was both gratifying and troublesome. The compatibility in calculated k-effectives meant that the subcritical limits derived from Ref. 1 calculations could be validated by the studies documented in Appendices C, D, E, and F. However, using the Ref. 13 techniques, subcritical limits derived for ^{233}U and ^{235}U were lower than the 0.95 value assumed in the Ref. 1 study. This meant that all fissile load limits for building 3019 arrays would have to be lowered by some to-be-determined amount. A review of the inventory data in Table 3 showed that *any* reduction in fissile load limits would cause the facility to be in violation of its operating procedures.

Because the evaluation of Ref. 1. could not demonstrate subcriticality for assumed operating conditions of Appendix B and concrete constituents, it was necessary to develop a realistic computational model for evaluations of subcriticality. Reference 1 had established an acceptable load limit for CEUSP (Consolidated Edison Uranium Solidification Project) material of 3.71 kg fissile material/foot. The

current *maximum* loading in the Cell 4 array is 1.58 kg U/foot. Clearly the reactivity worth of the CEUSP material must be far below that which would yield a k-effective of 0.95 (assuming the array full of CEUSP material). Consequently the decision was made to explicitly model the CEUSP material in the well locations noted in Table 3. Since the U4 material was stipulated to be neutronicly similar to the CEUSP material, the U4 locations were also explicitly modeled.

As a result of using the new Cell 4 model, only the locations shown in Fig. 8 are now available for storage of additional fissile material. Likewise any material currently stored in those positions is subject to limits derived from calculations based on explicitly modeling CEUSP and U4 materials.

The Cell-4-with-CEUSP (C4WC) model is documented in Appendix H. The changes noted in Section 4.2.1 are incorporated as well as explicitly including the CEUSP and U4 materials. In all calculations, the fissile material assigned to a given well fills that well.

Calculations to determine a subcritical load limit for ^{233}U are reported in Table 14. These calculations reflect the limits which would be achievable under nominal conditions. That is, under the assumption that no flooding of the storage wells was possible. At the time these studies were performed, the assumptions regarding water ingress to the storage containers had not been defined. Subsequent assumptions and studies revealed that the water-flooded case was the constraining condition. Nevertheless, the data in Table 14 are important should the facility someday be modified to preclude water ingress.

Table 14. ^{233}U configurations in the autonomous, Cell 4 model

Case I.D.[a]	H/^{233}U	kg ^{233}U/ft	k-effective	One standard deviation for k-effective
c4_u31	0	6.5	1.05264	0.00315
c4_u32	0	4.61	0.99534	0.00318
c4_u33	0	4.40	0.98082	0.00332
c4_u34	1	2.0	0.89141	0.00311
c4_u35	1	2.25	0.90511	0.00313
c4_u36	1	2.75	0.92709	0.00310
c4_u37	3	2.0	0.90052	0.00338
c4_u38	3	2.3	0.92620	0.00307
c4_u39	3	2.6	0.94270	0.00356
c4_u310	5	1.5	0.88535	0.00307
c4_u311	5	1.8	0.91393	0.00308
c4_u312	5	2.2	0.93968	0.00343
c4_u313	10	1.3	0.90129	0.00320
c4_u314	10	1.5	0.91572	0.00335
c4_u315	10	1.7	0.94149	0.00360
c4_u316	0	2.2	0.88720	0.00332
c4_u317	0	2.8	0.91666	0.00301
c4_u318	1	2.4	0.90420	0.00314

Table 14. ^{233}U configurations in the autonomous, Cell 4 model

Case I.D.[a]	H/^{233}U	kg ^{233}U/ft	k-effective	One standard deviation for k-effective
c4_u319	3	2.15	0.91943	0.00326
c4_u320	10	1.45	0.90862	0.00344
c4_u321	0	2.75	0.91832	0.00327
c4_u322	1	2.45	0.91059	0.00313
c4_u323	3	2.10	0.91833	0.00315
c4_u324	0	2.65	0.91919	0.00307
c4_u325	3	2.00	0.90390	0.00368
c4_u326	0	2.50	0.90466	0.00323
c4_u327*	0	2.50	0.91311	0.00323
c4_u328*	1	2.45	0.91252	0.00325
c4_u329*	3	2.00	0.90768	0.00357
c4_u330*	5	1.80	0.90390	0.00315
c4_u331*	10	1.45	0.91326	0.00368
c4_u332*	20	1.00	0.90776	0.00310

[a] Cases marked with an * had slightly different cross-section processing treatment than others (5.08 cm radius for well assumed). See Appendix H.

Calculations for ^{235}U and ^{239}Pu are shown in Tables 15 and 16, respectively. The safely subcritical limits noted in Appendices C, D, and E and in Section 4.1 where used in conjunction with the data from Tables 14-16 to determine fissile load limits. These are reported in Table 17.

Table 15. ^{235}U configurations in the autonomous, Cell 4 model

Case I. D.[a]	H/^{235}U	kg ^{235}U/ft	k-effective	One standard deviation for k-effective
c4_u51	0	8.52	0.95868	0.00275
c4_u52	0	9.5	0.97944	0.00294
c4_u53	0	10.5	1.00082	0.00302
c4_u54	1	3.77	0.86141	0.00300
c4_u55	1	5.0	0.90367	0.00311
c4_u56	1	6.0	0.92132	0.00262
c4_u57	3	3.19	0.86520	0.00316
c4_u58	3	4.0	0.89734	0.00293
c4_u59	3	5.0	0.94579	0.00328
c4_u510	5	2.5	0.85201	0.00300

Table 15. ^{235}U configurations in the autonomous, Cell 4 model

Case I. D.[a]	H/^{235}U	kg ^{235}U/ft	k-effective	One standard deviation for k-effective
c4_u511	5	3.5	0.91253	0.00324
c4_u512	5	4.0	0.93643	0.00294
c4_u513	10	2.02	0.86598	0.00299
c4_u514	10	2.75	0.92960	0.00317
c4_u515	10	3.0	0.95141	0.00348
c4_u516	0	7.4	0.93664	0.00272
c4_u517	1	6.4	0.93489	0.00292
c4_u518	3	4.75	0.93308	0.00324
c4_u519	5	3.95	0.93035	0.00304
c4_u520	10	2.85	0.93963	0.00290
c4_u521	0	7.2	0.92913	0.00294
c4_u522	10	2.80	0.92990	0.00295
c4_u523	3	4.6	0.92563	0.00320
c4_u524	1	6.2	0.93274	0.00293
hx0*	0	7.2	0.92541	0.00299
hx1*	1	6.2	0.93274	0.00293
hx3*	3	4.6	0.92563	0.00320
hx10*	10	2.75	0.93241	0.00295
c4_u525*	5	3.8	0.92449	0.00306
c4_u526*	20	1.9	0.95357	0.00353
c4_u527*	20	1.7	0.91980	0.00324

[a] Cases marked with an * had slightly different cross-section processing treatment than others (5.08 cm radius for well assumed). See Appendix H.

Table 16. ^{239}Pu configurations in the autonomous, Cell 4 model

Case I.D.[a]	H/^{233}U ratio	kg ^{233}U/ft	k-effective	One standard deviation for k-effective
c4_pu1	0	3.5	0.87606	0.00320
c4_pu2	0	4.57	0.92478	0.00343
c4_pu3	0	5.5	0.95699	0.00317
c4_pu4	1	2.78	0.85833	0.00279
c4_pu5	1	3.50	0.89958	0.00287
c4_pu6	1	4.50	0.94420	0.00290
c4_pu7	3	2.30	0.84756	0.00313

Table 16. ^{239}Pu configurations in the autonomous, Cell 4 model

Case I.D.[a]	H/^{233}U ratio	kg ^{233}U/ft	k-effective	One standard deviation for k-effective
c4_pu8	3	3.00	0.89862	0.00289
c4_pu9	3	4.00	0.95567	0.00321
c4_pu10	5	2.00	0.84890	0.00278
c4_pu11	5	3.50	0.95067	0.00342
c4_pu12	5	3.00	0.92744	0.00294
c4_pu13	10	1.70	0.86504	0.00298
c4_pu14	10	2.50	0.94462	0.00340
c4_pu15	10	3.50	1.03837	0.00316
c4_pu16	0	5.20	0.94699	0.00314
c4_pu17	3	3.70	0.93271	0.00302
c4_pu18	5	3.30	0.93807	0.00290
c4_pu19	0	5.10	0.94699	0.00303
c4_pu20	3	3.80	0.94141	0.00310
c4_pu21	0	4.95	0.93696	0.00329
c4_pu22	0	5.0	0.94618	0.00320
hx0*	0	4.95	0.93655	0.00300
hx1*	1	4.50	0.93570	0.00316
hx3*	3	3.80	0.94056	0.00312
hx5*	5	3.30	0.93827	0.00317
c4_pu23*	10	2.50	0.94332	0.00332
c4_pu24*	20	1.40	0.89783	0.00306
c4_pu25*	20	1.80	0.95674	0.00309
c4_pu26*	20	1.70	0.94689	0.00335
c4_pu27*	20	1.60	0.93052	0.00320

[a] Cases marked with an * had slightly different cross-section processing treatment than others (5.08 cm radius for well assumed). See Appendix H.

Table 17. Fissile load limits based on autonomous, unflooded Cell 4 model[a]

Material	H/X ratio	Maximum linear well loading (kg fissile/ft)
^{233}U	0	2.50
"	1	2.45
"	3	2.00
"	5	1.80
"	10	1.45

Table 17. Fissile load limits based on autonomous, unflooded Cell 4 model[a]

Material	H/X ratio	Maximum linear well loading (kg fissile/ft)
"	20	1.00
"	unrestricted	0.19
^{235}U	0	7.20
"	1	6.20
"	3	4.60
"	5	3.95
"	10	2.75
"	20	1.70
"	unrestricted	0.25
^{239}Pu	0	4.95
"	1	4.50
"	3	3.80
"	5	3.30
"	10	2.50
"	20	1.40
"	unrestricted	0.15
CEUSP	-	1.58
U4	-	1.34

[a] These limits ONLY apply to the following Cell 4 well locations, 1A through 1R, 2B, 3A, 4B, 5A, 6B, 7A through 7J, 8A, 8F, 8K through 8P, and 9A through 9R. All other locations in Cell 4 are subject to either CEUSP or U4 limit, according to material stored in a given well. These limits apply to all in-line, intercell wells. If fissile materials are mixed within a given well, the minimum of the fissile load limits for any given linear foot applies to all materials within that linear foot of the well.

AGF values for the cases in Table 17 ranged from 11.2 to 13.3. Experiments in the plutonium validation study span this range. For the ^{233}U and ^{235}U studies, there are no critical experiments in this range.

Table 17 also contains values for unrestricted moderation fissile load limits. The definition and need for these values are the same as was discussed in Section 4.1.2. The datasets used to calculate the unrestricted moderation limits were much simpler than the previously discussed Cell 4 models. A one-dimensional discrete ordinates calculation was performed using the CSAS1X module from the SCALE system. The cross section processing treatment was the same as discussed previously. The limits thus calculated are slightly conservative as the one-dimensional model represents an infinite lattice whereas previous KENO models accounted for leakage. One-dimensional calculations are much cheaper and any differences in derived limits is likely to be masked by the uncertainty in Monte Carlo calculations had that computational route been chosen. The datasets for the unrestricted moderation cases are in the floppy disk directory /section4.0/4.2/4.2.3/table17.unrestricted.

4.3 COMBINED CELL 4 AND IN-LINE WELL CALCULATIONS

It had been expected, due to the thickness of the cell wall containing the in-line 4 & 5 array, that there would be no interaction between the in-line array and the Cell 4 array. To confirm this lack of interaction, two "combined" models were prepared. Cell 4 and in-line 3&4 arrays were incorporated into a single KENO model. Cell 4 and in-line 4 & 5 arrays were modeled in a second, combined model. A detailed description of these two models is given in Appendix I.

Table 18 shows a comparison among three cases. Case c4_u327 is from Table 17 and represents the reference case whereby only the Cell 4 array is present in the KENO model. The ^{233}U loading is 2.5 kg/ft with an $H/^{233}U$ ratio of 0.0. Case cell_4_3_4 is the first combined model with Cell 4 and in-line 3 & 4 arrays. Case cell_4_4_5 is the second combined model, discussed previously. In the in-line portions of the combined models, the ^{233}U loading was 6.4 kg/ft at an $H/^{233}U$ value of 0.0. Thus both arrays contained maximum loadings of the systems with the fastest energy spectra. This configuration is believed to maximize prospects for neutron interaction. The combined models are stored under the appendix.i directory on the floppy disk accompanying this report.

Table 18. Reactivity effect of combining storage array models

Case I.D.	k-effective	One standard deviation for k-effective
c4_u327	0.91311	0.00323
cell_4_3_4	0.91492	0.00331
cell_4_4_5	0.94724	0.00340

The increase in k-effective due to including the in-line 4 & 5 array in the KENO model is statistically significant. It is felt that this coupling is due to the assumption of zero hydrogen content in the cell wall concrete.

Even though in-line 3 & 4 array was shown to be neutronicly isolated, the calculations in Table 18 led to the decision to treat all storage wells in building 3019 as a single facility with a single set of limits applied. Consequently, Cell 4 limits were applied to the in-line wells. The possibility that some intermediate value between the Cell 4 and previously discussed in-line limits could be successfully applied to the in-line wells was not investigated.

4.3.1 Modification to In-Line Portion of the Model

Cell inventories (Table 3) were being continuously revised during the course of these studies. As the combined models were being prepared, the existence of three hemispheres in well M were brought to the author's attention. As the linear loading due to these hemispheres exceeded the currently derived ^{233}U load limits, these hemispheres were explicitly included in the KENO model. A detailed description of this modification is contained in Appendix I.

4.3.2 Flooding of Storage Wells

Early and undocumented studies of well flooding had been based on the assumption that any canister within a well was water-tight. Based on this assumption, flooding of wells did not lead to a reactivity increase and, in fact, in some cases led to a reactivity decrease.

Further discussions with facility personnel, documented in Appendix B, led to the removal of the previous assumption and instead, mandated the consideration that fissile material and water could be intimately mixed. In spite of the statement made in Appendix B, the two wells which may be open at any given time must be non-adjacent.

The final series of calculations to determine fissile load limits was based on having two flooded columns in the Cell 4 storage array. Upon examining the effect of flooding, problems occurred when the fissile material was assumed to be uniformly dispersed inside a fully flooded can. Allowable load limits would have been far below the values shown in Table 3.

Appendix B notes that the fissile material would not dissolve in the water entering the canister containing the fissile material. It was further assumed that the fissile material would not be in suspension in the water. Since in-leakage to a canister would be slow, if at all - Appendix B specifies that the canister would retain structural integrity - this assumption seems quite plausible.

As a result of this assumption, a minimum fuel density of 1.5 g/cm^3 was specified (Source: E. C. Crume, Jr, Oak Ridge National Laboratory). Even under water-flooded conditions, all fissile material is assumed to attain at least this density as it is initially loaded into the canister.

In the flooded wells, uranium was assumed to exist in the form of UO_3, the least dense oxide form. In all other wells, it was assumed in the computational model to exist in the form of UO_2. Plutonium was assumed to exist in the form PuO_2 regardless of location in the array.

Due to time constraints and since Appendix B specifies that the material currently stored in Cell 4 can have an H/X value as large as 3, no values lower than this were considered. There is no reason that the higher load limits available at the low H/X values could not be used. However additional flooded calculations would have to be performed and the canisters would have to be certified as leak-tight.

A final modification to the combined model was to reduce the diameter of the fissile region to 8.5725 cm (3 and 3/8 inches) for the fissile material which is in the flooded wells. For the fissile material which is in the dry wells, the outside diameter of the fissile material was the same as the inside diameter of the well liner. As noted in Refs. 1 and 2, limiting the fissile material diameter to some value less than the well diameter reduces the reactivity of the system. Current operating procedures restrict inside can diameter to 3.375 inches so this assumption is in accordance with practice.

A rigorous evaluation of the location of the most reactive, two, non-adjacent, flooded, Cell 4 storage wells was not performed. However, by examining the cases in Tables 14, 15, and 16, it is obvious that the most reactive dry locations are among the available locations shown in Fig. 8. The wells along the edges of the Cell 4 array are high leakage locations and are unlikely to significantly impact the multiplication factor of the array. Interior wells which are subject to a higher neutron flux than edge wells and should produce the largest impact on k-effective when flooded. Wells 7G and 8K were selected as the two locations to be flooded.

Since a rigorous study of the most reactive flooded location was not performed and since the diameter of the fissile material in the flooded columns was restricted to 8.5725 cm, a *de facto* requirement on inside diameter of a fissile material canister was established. Until additional calculations are performed, all canisters in the available wells (identified in Fig. 8) and in the in-line wells must have an inside diameter no greater than 8.5725 cm. Note that if incorporated into the computational model, allowable load limits would be increased above the values reported subsequently.

Table 19 contains the results of the water flooded studies. Several of the limits in Table 17 required modification due to examining water flooding scenarios. If one were willing to accept a higher, but still

subcritical calculated value of k-effective than that derived in Appendices C and E, i.e., reduce the margin of subcriticality, the limits in Table 17 would likely be acceptable. Of course, if that philosophy were adopted, then the other limits could be increased beyond the values derived from Table 19. The author chose to maintain the same degree of confidence of subcriticality for all possible configurations regardless of their being nominal or credible abnormal.

Table 19. Calculated parameters for two flooded wells in Cell 4

Case I.D.	Fissile material	H/fissile atom ratio	kg fissile material/ft	Density of fissile material in flooded well (g/cm^3)	k-effective	One standard deviation in k-effective	Average energy group for fission[b]
fl1	^{233}U	5	1.80	2.00	0.8949	0.0033	12.54
fl2	^{233}U	3	2.00	1.50	0.9673	0.0040	12.59
fl3	^{233}U	3	2.00	2.00	0.9128	0.0040	12.40
fl4	^{233}U	3	2.00	2.50	0.8889	0.0033	12.41
fl5	^{233}U	3	2.00	3.50	0.8756	0.0036	12.45
fl6	^{233}U	10	1.45	1.50	0.8988	0.0036	12.77
fl7	^{233}U	5	1.80	1.50	0.9329	0.0039	12.69
fl8	^{233}U	5	1.70	1.50	0.9069	0.0048	12.58
ufl1	^{235}U	5	3.95	3.05	0.9170	0.0029	12.03
ufl2	^{235}U	10	2.50	2.00	0.8993	0.0031	12.82
ufl3	^{235}U	5	3.00	2.50	0.8824	0.0030	12.49
ufl4	^{235}U	3	3.50	2.50	0.8775	0.0027	12.32
ufl5	^{235}U	3	4.60, 3.50[a]	2.50	0.9286	0.0033	11.87
ufl6	^{235}U	3	4.60	3.50	0.9219	0.0033	11.73
ufl7	^{235}U	5	3.95	2.71	0.9308	0.0036	11.98
pufl1	^{239}Pu	10	2.20	1.50	0.9235	0.0031	12.82
pufl2	^{239}Pu	10	2.20	2.00	0.9038	0.0033	12.62
pufl3	^{239}Pu	5	3.00	2.00	0.9442	0.0034	12.29
pufl4	^{239}Pu	3	3.40	2.50	0.9364	0.0033	12.09
pufl5	^{239}Pu	3	3.30	2.50	0.9325	0.0035	12.12
pufl6	^{239}Pu	3	3.80	2.50	0.9613	0.0030	11.84

[a] Dry wells have a loading of 4.60 kg ^{235}U/ft, flooded wells have a loading of 3.50 kg/ft as that is the maximum which can be loaded at a density of 2.5 g $^{235}U/cm^3$

[b] HANSEN-ROACH cross sections used. One standard deviation ≡ 0.05.

It was mentioned earlier but is stressed again that flooding scenarios in which a significant amount of water, containing no fissile material, exists at regular intervals along a flooded column will be no more reactive than an array full of "dry" wells. Ten to 15 cm of water between fissile material bearing regions will effectively isolate those regions from each other and consequently reduce reactivity. The engineering parameter of importance to the safety analysis of credible abnormal flooding conditions is the density of the fissile material in the flooded wells. For a given linear loading, there will be a unique fissile material density at which the fissile material will fill all the available volume in the flooded well (water also being present with the oxide). As the density increases from this minimal value, the linear loading being kept constant, a zone of pure water (no fissile material entrained) will form between the fissile regions. The existence of this water zone does not guarantee a lower multiplication factor (the higher density oxide may have a more optimal H/fissile atom ratio than the minimum density value), but the constant fuel loading does (see Section 4.4.3). However, once the water zone height approaches 15 cm, a reactivity

decrease (for a fixed linear load limit) will always result since the fissile regions are neutronically isolated.

Table 20 shows the linear load limits derived from Table 19. The range of fissile material density values corresponding to zero and 15 cm of water between fissile material regions are also shown. The final column provides a summary of the density values (from Table 19) at which calculations were performed. No calculations were performed at less than 1.50 g fissile material/cm^3 as that was the minimal value judged to be credible.

Table 20. Flooded well load limits and possible fissile material densities

Fissile material	H/fissile atom ratio	Fissile load limit (kg/ft)	Minimum possible oxide density (g/cm^3)[a]	Maximum considered oxide density (g/cm^3)[b]	Calculated oxide densities (g/cm^3, from Table 19)
^{233}U	3	2.00	1.37	2.70	1.50, 2.00, 2.50, 3.50
^{233}U	5	1.80	1.23	2.43	1.50, 2.00
^{233}U	10	1.45	0.99	1.96	1.50
^{235}U	3	4.60	3.15	6.20	2.50[c], 3.50
^{235}U	5	3.95	2.70	5.32	2.71, 3.05
^{235}U	10	2.50	1.71	3.37	2.00
^{239}Pu	3	3.40	2.19	4.31	2.50
^{239}Pu	5	3.00	1.93	3.81	2.00
^{239}Pu	10	2.20	1.42	2.79	1.50, 2.00

[a] Density corresponding to flooded well containing uniform mixture of fissile material and water given the constraints of H/fissile atom ratio and fissile load limit.
[b] Density corresponding to 15 cm of water between fissile material zones inside a flooded well.
[c] Linear loading in flooded wells was 3.50 kg ^{235}U/ft

In all instances in which multiple calculated densities for a given fissile material/load limit were considered, k-effective monitonically decreased as the fissile oxide density in the flooded column increased. Consequently, those cases at the minimum possible density or 1.50 g/cm^3, whichever is higher, are the ones which establish the fissile load limit. By observing Table 20, it is seen that all minimum or near minimum values were evaluated.

The values of k-effective for minimum densities for ^{233}U at H/^{233}U values of 3 and 5 exceeds the subcritical limit derived in Appendix C. If the minimum oxide density is raised to 2.00 g/cm^3, then the calculated values of k-effective are acceptable. Consequently, for those wells in which the stored ^{233}U has an H/^{233}U ratio less than or equal to 5, the minimum oxide density must be greater than or equal 2.0 g/cm^3 to satisfy the desired, subcritical limit of k-effective.

4.3.3 Double-Batching of Fuel

Previously, it was noted that double-loading (double-batching) of CEUSP or U4 had been examined by assuming that the maximum linear fuel loading over all the array for CEUSP or U4 exists in each CEUSP or U4 location, as appropriate. However it was still necessary to examine double-loading of new material which might be added in an available well.

Two double-loading scenarios were examined. Both were based on the Cell 4 model described in Appendix G. The reference fissile material was ^{233}U at a linear loading of 2.0 kg/ft and having an $H/^{233}U$ ratio of 3 (case c4_u37 from Table 14). In both models, the central region of ^{233}U (100 cm in length centered about the axial midplane of the well) was replaced with material having twice the fissile loading and twice the hydrogen loading (constant $H/^{233}U$ ratio). The 100 cm length is approximately six times the nominal height of fissile material containers to be used for future storage of mixed oxide waste (see Ref. 2). Having more than this number of containers containing doubly-loaded material was deemed incredible.

Calculated k-effectives (datasets are stored on floppy disk) for all three cases are reported in Table 21. Case hx3_db was a Cell 4 model in which the doubly-loaded fuel was placed in well 7J (as near as possible to the center of the array). Case hx3_db2 was for a Cell 4 model with the doubly-loaded fuel placed in position 7A (concrete reflection along one side of the storage well). The differences among calculated k-effectives are statistically insignificant. The fission density profiles in the KENO output show that a significant number of neutrons encountered the well containing doubly-loaded fuel.

Table 21. Double-batching in selected Cell 4

Case I.D.	k-effective	One standard deviation for k-effective	Average energy group for fissions
c4_u37	0.90052	0.00338	12.40
hx3_db	0.89883	0.00365	12.60
hx3_db2	0.90392	0.00383	12.63

All existing containers and all plans for future containers limit the height of the fissile material container to less than 61 cm. In many instances, the heights are less than 20 cm. The small size of individual containers limits the possible hazard from doubly loading a particular or even a group of containers.

4.3.4 Summary of Assumptions Relevant to Model Validity

During the discussion of calculations performed for Cell 4, it has been noted that additional studies or analyses could lead to increased fissile load limits. Because these studies may be conducted later, it seemed prudent to collect in one place the assumptions underlying the combined model which significantly impact calculated k-effective. The assumptions are simply itemized since quantification of impact has either already been stated or is unknown.

(1) The impact of water flooding is limited to two non-adjacent storage wells (modification to Appendix B).

(2) The cans containing fissile material are not water-tight and would fill with water should the wells become flooded. The fissile material would mix with the water but would not be in suspension; it would settle to the bottom of the can.

(3) The fuel inside the flooded cans would have a packing density no less than 1.5 g/cc.

(4) The entire well is filled with material of the same density as the highest local density anywhere within that individual well.

(5) The nominal H/fissionable atom ratio is 3 and the only credible method of increasing this ratio is by flooding the column.

(6) The Cell 4 wells and the in-line 4 & 5 wells are assumed to interact even though this was verified only for an H/fissionable atom ratio of 0 and for zero hydrogen content in the cell wall concrete.

(7) All fertile material in a well is to be treated as fissile material.

(8) Any fixed poisons (Cd and Gd) are to be ignored.

(9) Only bound water is to be included in modeling the Cell 4 concrete.

(10) The building cell wall concrete contains no water.

(11) The fuel cans are ignored in the KENO models, but are assumed to retain structural integrity under *all* normal and credible abnormal conditions (Section 4.4.3).

(12) In the non-flooded wells, the can diameter equals the inside diameter of the pipe liner in the well. However in the flooded wells, the can inside diameter is required to be no larger than 8.5725 cm (3.375 inches). Since there is no way to determine which column may flood, by default, all fissile material storage cans are required to have an inside diameter no larger than 8.5725 cm. In all dry wells in the KENO model, the fissile material fills the interior of the pipe liner.

(13) The CEUSP and U4 materials will remain in place or be replaced by material of equal or less reactivity worth.

(14) The U4 material is neutronicly the same as CEUSP.

(15) Even though the in-line 3 & 4 array was shown to be neutronicly isolated, the more restrictive Cell 4 limits were applied to this array. The possibility that some intermediate value between the Cell 4 and previously discussed in-line limits could be successfully applied to all of the in-line wells was not investigated.

(16) For those wells containing ^{233}U with H/^{233}U less than or equal to 5, the density of the ^{233}U oxide must be at least 2.0 g/cm^3 (^{233}U density of 1.66 g/cm^3).

(17) When considering double-batching of new fissile material to be stored in an available well, no more than 100 cm of well height can be loaded with the doubly-loaded material and only one well in the array contains the doubly-loaded material.

While not relevant to these analyses, it is noted that procedure RDF-OP-024 requires that the U+Pu loading in any canister not exceed 3 kg.

4.4 PROOF-OF-PRINCIPLE STUDIES

4.4.1 Mixing Fuel Types Within a Storage Array

The subcritical limits in Table 17 are based on the assumption that all *available* locations in a given storage facility would be filled with a single type of material. However the facility operators are permitted to intermix fissile materials (including differing moderation ratios) within a given facility. It is necessary that limits derived on the basis of a single type of waste in a storage array could be applied to the mixed waste configuration.

4.4.1.1 Neutron Moderation in Concrete

Computational studies revealed that, for each of the storage facilities, the well pitch was sufficiently large such that any neutron leakage spectra from a storage well would be well-moderated before the neutrons reentered fissile material. A particular instance is shown in Fig. 9. Spectra at two locations for the unrestricted moderation case discussed in Section 4.2.3 are compared to two spectra from a case with little moderation. The "well centerline" values are at the center of the fissile material. The reflector midpoint (ref. midpoint) values are at a radius of 16.9 cm from the well centerline (triangular pitch is 32.385 cm). Four bars, representing the two locations for two cases, are displayed for each energy group - group 1 being the highest energy. The spectra in the fissile material is quite different for the two cases, the solution system having a sizable thermal component (energy group 16) and the dry system having many more neutrons in groups 2—5.

At the reflector midpoint, most differences in spectra have been removed. The unrestricted moderation case still has a higher fraction of thermal neutrons. However this location is at the center of the reflector. As neutrons continue to travel towards another storage well, further equalization in the fast groups will reduce or eliminate the thermal imbalance. Thus the spectra inside a given well is dependent only on the material in that well (the concrete reflector/moderator constituents being the same on all cases.). All wells should receive the same background spectra due to the other wells in the array. Consequently, it is possible to show that a storage limit derived for a particular type of fissile material is applicable even though different materials are stored in the same array.

4.4.1.2 Adjacent Wells with Differing Fissile Materials

A study was conducted to demonstrate that intermingling of fissile material types (but with each well containing a single type of material) had inconsequential reactivity effects. Materials from cases c4_u37 (Table 14), c4_u55 (Table 15), and c4_pu5 (Table 16) were loaded into the Cell 4 array in the pattern shown in Fig. 10. The calculated k-effective together with the three previously calculated values are shown in Table 22. Note that no statistically significant change in k-effective is seen. The program output was examined to verify that a significant number of fissions was occurring in the "mixed" portion of the array. The dataset corresponding to Fig. 10 is stored on the accompanying floppy disk.

Table 22. Examination of mixed material array configuration

Case I.D.	Fissile material in available wells	Fissile loading (kg/ft)	H/fissile atom ratio	k-effective	One standard deviation for k-effective
c4_u37	^{233}U	2.0	3	0.90052	0.00338
c4_u55	^{235}U	5.0	1	0.90367	0.00311
c4_pu5	^{239}Pu	3.5	1	0.89958	0.00287
Fig. 10	^{233}U, ^{235}U, and ^{239}Pu	varied	varied	0.90234	0.00302

4.4.1.3 Intermixing Fissile Materials Within a Well

Facility operators may mix fissile materials within a given column provided the limits specified in Table 20 are not exceeded but there remains some question as to placing highly moderated material adjacent (vertically) to dry material. While the calculation in Section 4.4.1.2 proved the beneficial impact of concrete moderation between wells, changes in moderation within a well might lead to an increase in

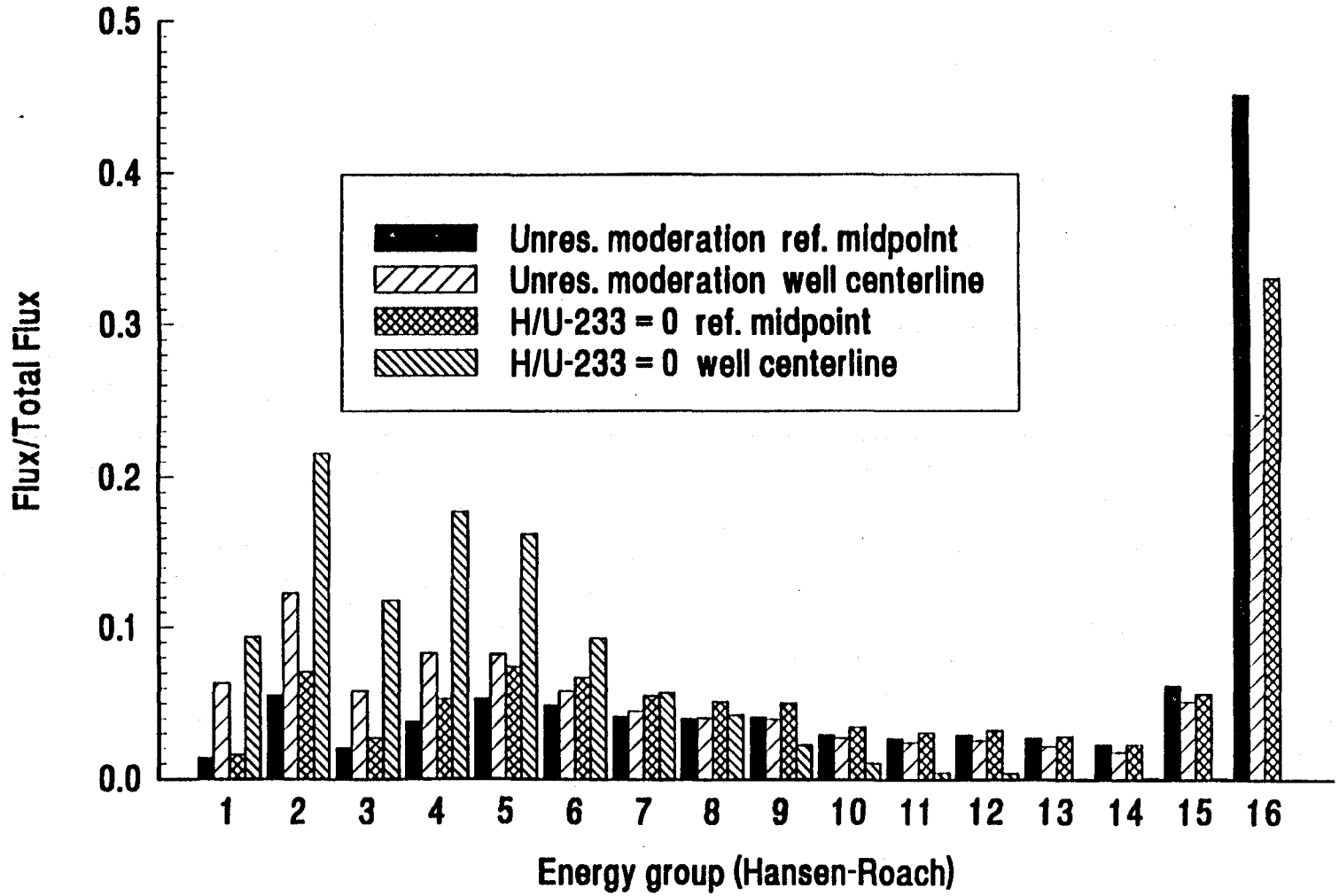

Fig. 9. Comparison of infinite lattice spectra
(All cases are U-233 fueled)

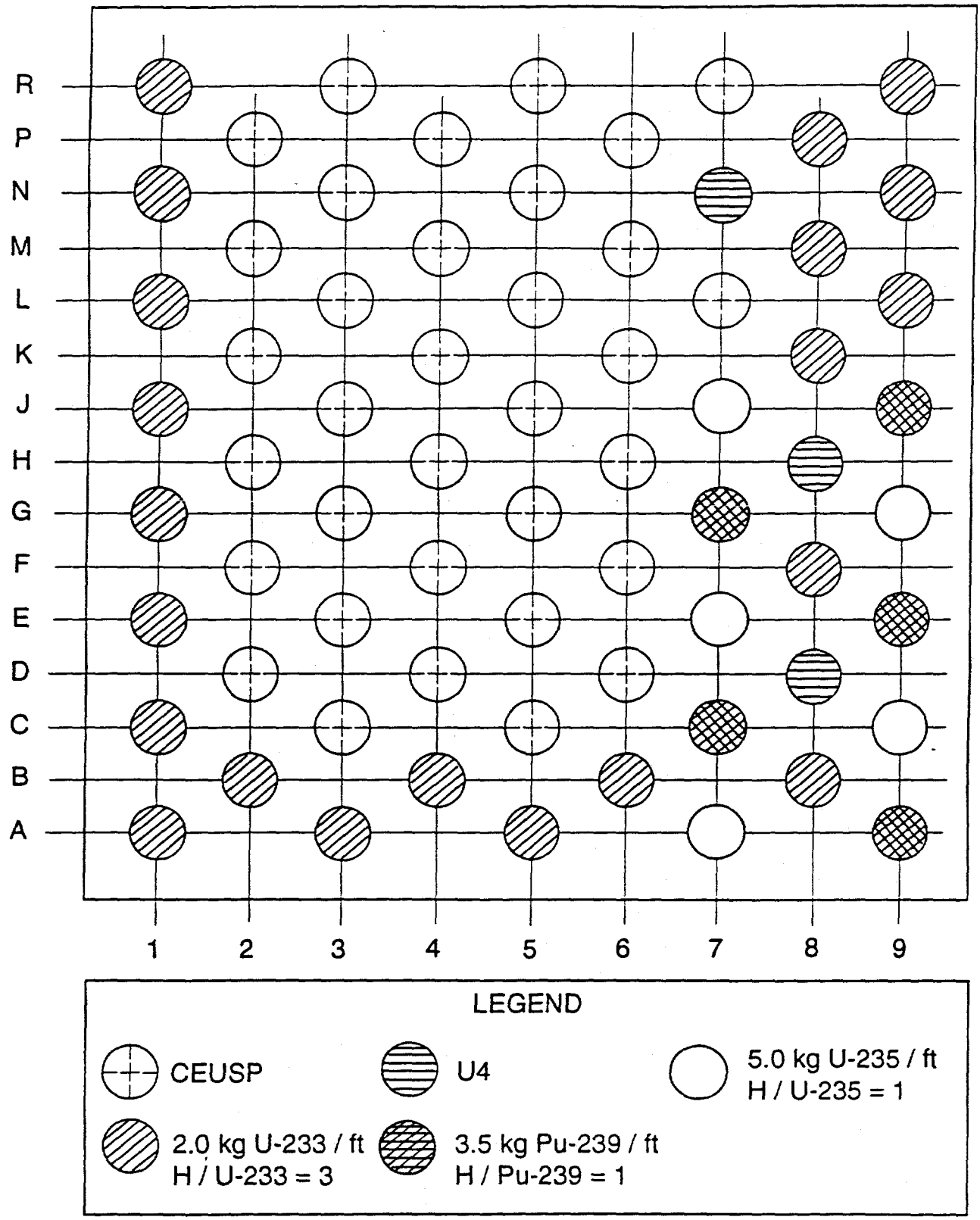

Fig. 10. Fuel loading for examining impact of mixing materials in available Cell 4 wells.

ORNL-DWG 93M-9915

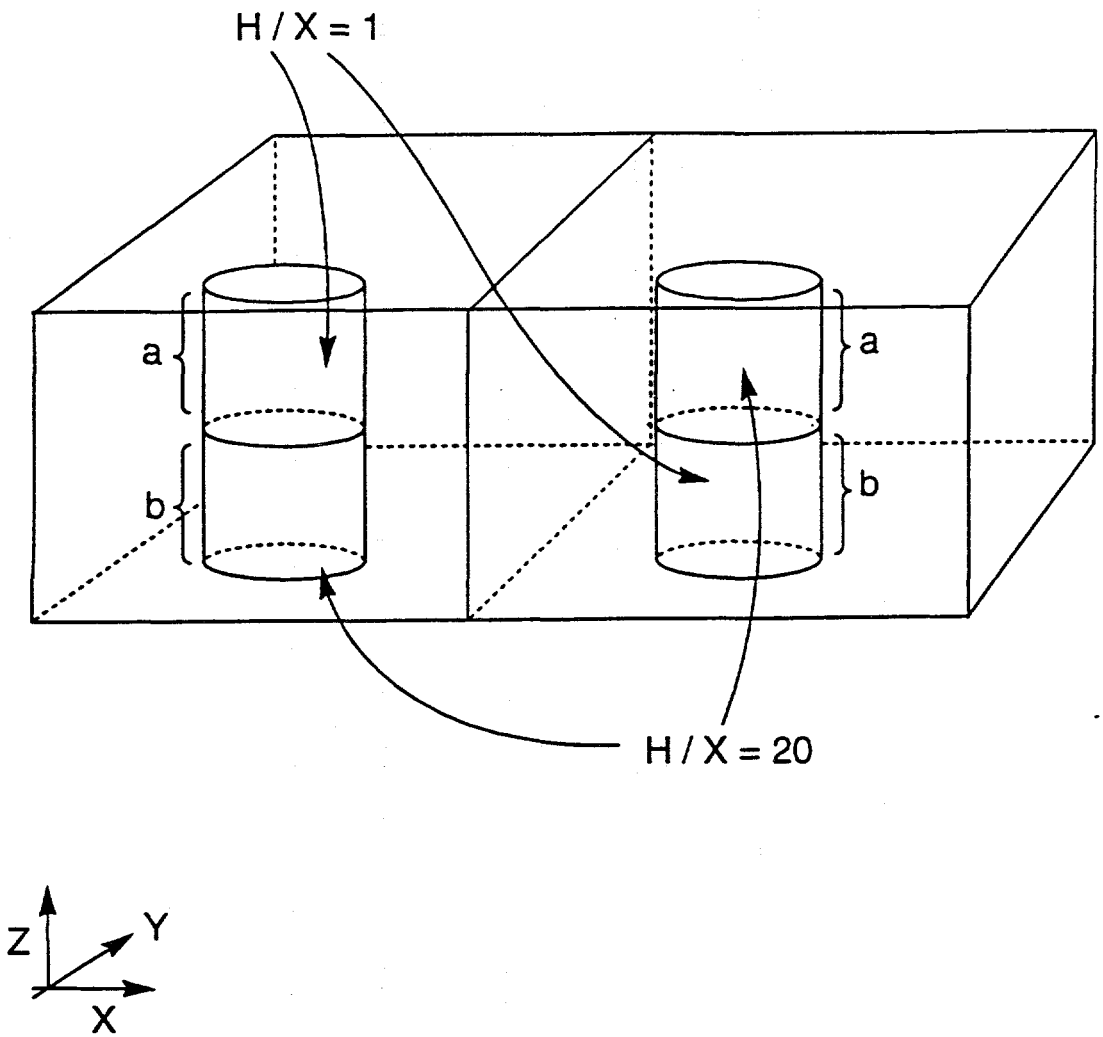

Fig. 11. Model for examining intermixing of fissile materials in storage wells.

k-effective. The model shown in Fig. 11 was created to examine the reactivity effect of axial variation of fissile material within a well. This two-unit KENO problem had periodic reflection in the z-direction and specular reflection in the x and y directions. The cylinders were filled with fissile material and the remainder of each cube was filled with Cell 4 concrete. The radii and pitch of the fissile bearing regions corresponded to values for the large wells in the Cell 4 array.

Four cases were considered. In the first, the H/X = 20 material was replaced with the H/X = 1 material. That is all columns were filled with 1.85 kg ^{233}U/ft. In the second case, all columns were filled with well moderated material (H/X = 20), the loading being 1.0 kg ^{233}U/ft. The third case was Fig. 11 as shown with a = 15.24 cm (6 inches) and b = 30.48 cm (12 inches). The fourth case was the same as the third but with a = b = 15.24 cm. The results of the calculations are given in Table 23. The datasets are stored on the accompanying floppy disk.

Table 23. Examination of axial variation of materials within a well

Case number	Description	k-effective	One standard deviation for k-effective
1	All dry material (H/X = 1)	1.06002	0.00327
2	All damp material (H/X = 20)	1.06017	0.00351
3	Fig. 11, a = 15.24 cm, b = 30.48 cm	1.05693	0.00345
4	Fig. 11, a = b = 15.24 cm	1.06573	0.00318

The lack of significant variation in k-effective shows that the axial interaction is insignificant. Note that case 4 would not have been allowed under the Table 20 limits as the applicable limit would have been the H/X = 20 limit due to evaluating the loading on a linear foot basis.

Near the end of these studies, facility operators for Building 3019 reported that the canister height of some of the cans stored in the wells was 7.544 cm (2.97 inches). Previously, the minimum height had been identified as 15 cm. Concern was raised as to whether the limits identified under the assumption that canister height was at least 15 cm are still valid when the canister height is only half of that value. While some confirmatory calculations were performed, the acceptance of the fissile load limits for smaller height canisters is based on the method by which linear loading is calculated within a storage well.

In deriving limits, it was assumed that facility operators would be required to know the fissile loading and associated H/fissile atom ratio in *any* given axial foot along the storage well. The allowed fissile loading is then based on the derived, average H/fissile atom ratio which will exist *after* material is loaded to a given position in a well. Since the limit for fissile loading at any given position depends on the characteristics of the material in the neighboring positions in the storage well, the *only* configuration in which the limits noted in Table 20 can be obtained uniformly throughout a single well would be for all canisters in the well to have the same H/fissile atom ratio. Consequently, if one is to closely approach or reach the fissile load limits, the canister height is irrelevant as all of the fissile material must have the same H/fissile atom ratio.

If canisters with differing H/fissile atom ratios are mixed within a storage well, then the linear averaging process to determine effective H/fissile atom ratio per foot would result in the requirement that canisters with the lower H/fissile atom ratios must have fissile loadings significantly lower than the values reported

in Table 20. In fact, the allowed value for the lowest H/fissile atom ratio material would be no greater than that tabulated for the next higher H/fissile atom ratio given in Table 20 for a particular fissile material. This is due to the requirement that the Table 20 limits be applied in a stepwise fashion rather than interpolating between values. Note that the result of this procedure is that a particular canister might be acceptably stored in one position of the storage array but would be unacceptable if placed in a different position in the array. This consideration would be quite important should someone choose to retrieve a particular canister from the storage array.

A high H/fissile atom ratio canister could only be inserted among low H/fissile atom ratio canisters *only* if the low ratio canisters are significantly below the Table 20 limits and therefore the multiplication factor of the system will be significantly less than the allowable subcritical limit. A low H/fissile atom ratio canister could only be inserted among high H/fissile atom ratio canisters if its fissile loading is essentially the same as the high ratio canisters. Thus, the height of the fissile material canisters is not a safety concern due to the averaging process used to determine the effective H/fissile atom ratio and due to applying Table 20 values in a stepwise fashion.

The averaging procedure as defined in procedure RDF-OP-024 differs from that discussed in the previous paragraphs. However, the height of the canisters is not believed to be a safety concern due to a similar argument as that which has been presented.

4.4.1.4 Relationship of Derived Safety Limits to ANSI Standards

Given that more than one type of fuel may be in a storage array, the term "subcritical margin of the array" is difficult to evaluate. Careful examination of the validation studies presented here reveals that each fissile material has a different value of subcritical margin (defined as the difference between the tolerance limit and the estimated, critical k-effective). Presumably the margin of the array would be the minimum of the margins of each of the fuel types. Yet this could create confusion if it is reported that the subcritical margin of a facility was less than the prescribed margin for one of the types of fuel stored in the array.

A similar difficulty arose with calculating k-effective for an array with mixed materials. Since each fissile material has a different estimated critical k-effective, it was conceivable that a subcritical array could have a calculated k-effective which would exceed the estimated critical k-effective for one of the fissile materials contained in the array. The relationship of calculated k-effective, using this analysis procedure, to degree of subcritical margin was ambiguous.

The proper manner in which to access mixed fissile arrays is to examine the margin of confidence of subcriticality rather than the subcritical margin. All of the tolerance limits presented in the appendices have the same margin of confidence of subcriticality (95.0% confidence on 99.9% of the data). Therefore any combination of the limiting values of the fissile types in the storage array will also have the same margin. For non-limiting concentrations, the margin of confidence of subcriticality is the minimum of the values of each of the types of fissile material. While literally different from the content of the ANSI/ANS 8.1 standard, the intent of establishing a subcritical configuration with a high degree of certainty is achieved through the use of this measure and the measure is unambiguous.

4.4.2 Effect of Fixed Poisons in Cell 4 Materials

As noted in Section 2.2.5, the CEUSP material also contains gadolinium and cadmium mixed with the fissile material. No credit is taken for the neutron poisoning effect of these two elements because to do so would require that periodic inspection of the presence and condition of the fixed poisons be conducted. Hence, these neutron absorbers provide some unaccounted, additional margin of subcriticality.

To provide an estimate of this unaccounted margin, the atom densities for Gd and Cd noted in section 2.2.5 were added to the CEUSP material description. Case fl6 from Table 19 was reexecuted with the fixed poisons added to the CEUSP material. The fl6 case had a ^{233}U loading of 1.45 kg/ft, an H/U-233 ratio of 10, and a packing density for the uranium oxide in the flooded wells of 1.50 g/cm^3.

The calculated k-effective is 0.8770 $\pm$ 0.0037. The value for case fl6 from Table 19 (the unpoisoned case) is 0.8988 $\pm$ 0.0036. The small decrease in k-effective appears due to the system being driven from the available well locations. The CEUSP material is acting as a neutron-multiplying reflector. Thus, the effect of the fixed poison is reduced and is similar to placing a neutron absorber in a reflector of a near critical configuration rather than the effect seen when the poison is intimately mixed with the fissile material.

The value of the average energy group for fissions for the case with fixed poisons is 12.4726 $\pm$ 0.05. The value for case fl6 is 12.7671 $\pm$ 0.04. The small difference between the two values provides further indication that the fixed poisons exhibit a noticeable but small perturbation on the neutron population.

4.4.3 Acceptability of Linear Loading as a Parameter for Judging Subcriticality

Using the parameter, kg/ft, to specify criticality safety limits has been presented without justification. The choice was suggested by facility operators as it was a convenient unit to use when documenting the inventory stored in an array. An examination of existing calculations and some intuitive insight can provide justification in terms of reactor physics principles.

In Ref. 1, studies are presented which show that the most reactive configuration for a given fissile loading is for the material to be homogeneously distributed radially throughout the storage well. Reducing the radial dimension of the fissile-bearing region reduces k-effective. Consequently, only variations in the axial height of the fissile-bearing region (achievable by treating the storage wells as containing canisters each of which may not be fully filled with fissile-bearing material) need be considered.

The flooded wells studies presented in Table 19 show the impact of axial fuel variation. As the axial height of the fissile-bearing region in each canister (each foot of the storage well is assumed to be a separate canister) decreases, the value of k-effective decreases even though the fissile material loading is held constant. In these cases, the reduction in k-effective is likely due to hydrogen absorption in water which fills the volume between the fissile material regions. Since all limits derived previously are for certain fixed H/fissile atom ratios, fissile material densities which are so high that the H (water) is "squeezed" from the material would therefore have a lower value of k-effective than for homogeneous systems.

For systems which have a homogeneous mixture of fissile material and hydrogen, an increase in fissile material density from the value at which the fissile material fills the available volume can be shown to reduce reactivity. Reference 14 provides data for subcritical mass limits for individual spheres of ^{235}U, ^{233}U, and ^{239}Pu. In all cases, for a fixed mass, as the concentration of fissile material increases, the value of k-effective decreases. If each canister in an array is treated as an individual unit, then as the fissile material in that canister is compressed (but to less than or equal to theoretical density values), the reactivity worth of the isolated canister will decrease. Since a storage well can be treated as an array of canisters and since the k-effective of an array is equal to the k-effective of the most reactive unit within the array, k-effective of a storage well will either decrease or remain unchanged as fissile material distributions within canisters are allowed to vary from the fully filled concentration value. Hence, it is appropriate to average over a linear foot. However, the integrity of each of the canisters must remain intact, otherwise the assumption regarding the most reactive unit in an array is no longer valid as the units of the array have not been maintained.

As long as the integrity of the canisters is maintained, the actual fissile material concentration, for a given H/fissile atom ratio, inside a given canister is of no consequence. The volume-averaged value, however, must be no greater than the kg/ft limits which are specified in Table 20.

5. COMPUTED SUBCRITICAL LIMITS

The models, programs, libraries, and acceptably subcritical values of k-effective were used to determine the maximum limits for loading fissile materials into the in-line and Cell 4 arrays. The future loading to Intercell 2 & 3 array has been addressed in another document (Ref. 2). The fissile loading limit as a function of degree of moderation from Table 20 is shown in Table 24. These values reflect k-effectives + 2 standard deviations being less than or equal to the appropriate tolerance limit as identified in Appendices C, D, or E.

Table 24. Safe fissile material linear mass loadings for Building 3019 Penthouse Storage Well[a]

Material	H/X	Selected Cell 4 wells and all in-line wells[b] (kg/ft)
^{233}U	3	2.00
	5	1.80
	10	1.45
	unrestricted	0.19
^{235}U	3	4.60
	5	3.95
	10	2.50
	unrestricted	0.25
^{239}Pu	3	3.4
	5	3.0
	10	2.2
	unrestricted	0.15
	All CEUSP wells have actinide limit of 1.58 kg/ft. All U4 wells have actinide limit of 1.34 kg/ft.	

[a] The safety of all loadings relies on assuring that the linear loadings are not exceeded.

[b] These limits ONLY apply to the following Cell 4 well locations, 1A through 1R, 2B, 3A, 4B, 5A, 6B, 7A through 7J, 8B, 8F, 8K through 8P, and 9A through 9R. All other locations in Cell 4 are subject to either CEUSP or U4 limit, according to material stored in a given well. These limits apply to all in-line, intercell wells. If fissile materials are mixed within a given well, the minimum of the fissile load limits for any given linear foot applies to all materials within that linear foot of the well. For wells in which the stored ^{233}U has an H/^{233}U ratio less than or equal to 5, the minimum oxide density must be greater than or equal 2.0 g/cm^3. If deuterium or beryllium are present with the fissile material, these limits must be reevaluated. In the absence of additional studies, all actinides should be considered to be the fissile material in the fuel mixture which has the most restrictive limit.

6. COMMENTS

From the studies presented in Section 4, significant increases in the in-line load limits could be obtained if the water content of the cell wall concrete could be more accurately estimated. Additional analysis of this parameter is recommended.

It is crucially important to note that the safety of the Cell 4 storage array relies on a particular configuration of CEUSP and U4 material. ANY proposed change to the storage configuration MUST be reviewed. Existing CEUSP or U4 material can be replaced ONLY with material of the same or lesser fissile loading AND the new material MUST have the same relative abundances of fissile elements and isotopes.

The lack of critical experiments conducted with mixtures of ^{233}U and ^{235}U at the AGF values expected in the 3019 storage arrays is troublesome. The values reported in Table 24 certify Cell 4 wells to operate with neutronic conditions, i.e., fissile material content and moderator-to-fuel ratio, for which no critical experiment data exist. Only the fact that the existing configuration is subcritical and that the cross-section data are believed to be well-known permits one to state that storage operations in Building 3019 are within the area of applicability of the validation studies.

Formal documentation of fissile inventory in Building 3019 should be readily available. Inspection of the condition of some of the stored material should be performed on no-less-than a five year basis. Results of the inspection should be documented. Documentation of the credible abnormal conditions expected to exist in the storage wells should be formalized.

7. CONCLUSIONS

New fissile loading limits exist for both Cell 4 and in-line storage wells. The derivation of these limits is in a manner consistent with currently applicable Martin-Marietta Energy Systems requirements. All of the material in Building 3019 storage wells is stored in a safely subcritical condition. All locations in Cell 4 currently containing CEUSP or U4 material are limited to containing only those materials and at no greater actinide concentration than the currently identified maxima. Future storage of new materials is subject to the new limits derived herein. New analyses of the water content of the cell walls should be conducted, for improved storage capacity. The results of these studies have been incorporated into a new procedure (RDF-OP-024).

8. REFERENCES

1. C. M. Hopper, unpublished memorandum, *Nuclear Criticality Safety Assessment of Storage Wells within Building 3019* (circa 1985).

2. R. T. Primm, III, C. M. Hopper, and G. R. Smolen, "Criticality Safety Studies for the Storage of Waste from Nuclear Fuel Services in Intercell Storage Wells 2 and 3 of Building 3019," ORNL/TM-12152 (November 1992).

3. *Final Safety Analysis Report for the Radiochemical Processing Plant (RPP),* ORNL/CF-81/37, Draft version, cover letter from R. S. Wiltshire to J. A. Lenhard (August 30, 1984).

4. N. F. Landers, L. M. Petrie and J. C. Turner, "Martin Marietta Energy Systems Nuclear Criticality Safety Software Verification Plan SRR_0," December 31, 1991, contained in *Martin Marietta Energy Systems Nuclear Criticality Safety Software Configuration Control Plan,* K/ESH-3, December 18, 1991.

8. REFERENCES (cont'd)

5. *SCALE - A Modular Code System for Performing Standardized Computer Analyses for Licensing Evaluation,* NUREG/CR-0200, Rev. 4 (ORNL/NUREG/CSD-2/R4), Vols. I, II, and III (draft February 1990). Available from Radiation Shielding Information Center, Oak Ridge National Laboratory, as CCC-545.

6. B. L. Koponen, et. al., *Nuclear Criticality Experiments from 1943 to 1978, An Annotated Bibliography,* UCRL-52769 (April 1979).

7. J. A. Bucholz, J. F. Mincey, R. T. Primm, III, and F. E. Weber, "Criticality Safety Studies of a Continuous, Rotary Dissolver," ORNL/TM-9020 (May 1984).

8. R. T. Primm, III, "Validation Studies for KENO-IV with Mixed Plutonium-Uranium Critical Experiments," ORNL/TM-9668 (November 1985).

9. R. T. Primm, III, "Critical Experiments With Mixed Plutonium-Uranium Nitrate Solutions Having Pu:(Pu+U) Ratios Greater than 0.5," ORNL-6161 (April 1986).

10. S. R. McNeany and J. D. Jenkins, "An Evaluation of ENDF/B-IV and Hansen-Roach Uranium-233 Cross Sections for Use in Criticality Calculations," *Nuclear Science and Engineering,* Vol. 65, pp. 441-453 (1978).

11. W. C. Jordan, N. F. Landers, and L. M. Petrie, *Validation of KENO-V.a, Comparison with Critical Experiments,* ORNL/CSD/TM-238 (December 1986).

12. M. E. Easter and R. T. Primm, III, *Validation of the SCALE Code System and Two Cross-Section Libraries for Plutonium Benchmark Experiments,* ORNL/TM-9402 (January 1985).

13. H. R. Dyer, W. C. Jordan, and V. R. Cain, "A Technique for Code Validation for Criticality Safety Calculations," *Trans. Am. Nuc. Soc.,* Vol. 63, pp. 238-239 (June 1991).

14. J. T. Thomas (Ed.), *Nuclear Safety Guide,* TID-7016, *Revision* 2, NUREG/CR-0095, ORNL/NUREG/CSD-6, June 1978.

Appendix A

DETERMINATION OF ATOM DENSITIES FOR CELL 4 ARRAY CONCRETE

Appendix A

DETERMINATION OF ATOM DENSITIES FOR CELL 4 ARRAY CONCRETE

Documentation from the supplier of Cell 4 array concrete is included in this appendix. Atom densities were derived by C. M. Hopper using a procedure summarized in Tables A.1 through A.4.

Table A.1. Average of silo 5 & 6 analyses of Type I Portland cement dated 4/17/78 & 4/24/78

Actual weight percent	Adjusted weight percents
21 w/o SiO_2	21.415 w/o SiO_2
5.3 w/o Al_2O_3	5.405 w/o Al_2O_3
2.45 w/o Fe_2O_3	2.498 w/o Fe_2O_3
64 w/o CaO	65.268 w/o CaO
2.5 w/o MgO	2.549 w/o MgO
2.45 w/o SO_3	2.498 w/o SO_3
0.217 w/o K_2O	0.221 w/o K_2O
0.143 w/o Na_2O	0.146 w/o Na_2O
TOTAL 98.06 w/o	**TOTAL** 100% w/o

Table A.2. Representative limestone manufactured sand and 7 lb stone

w/o	Material
51.4	$CaCO_3$
38.1	$MgCO_3$
9.4	SiO_2
0.4	Fe_2O_3
0.6	Al_2O_3
0.1	ZnS
Total 100	

Table A.3. Definition of concrete mix[a]

As mixed	Equivalent weight
3.75 gal/100 lb cement (31.3 lb)	14,795 g H_2O
100 lb Type I Portland cement	45,360 g cement
400 lb Limestone sand and stone	181,440 g limestone

[a]Yields 3.542 cu ft concrete (100,298.283 cm^3).

Table A.4. Summary of Cell 4 storage well concrete at 150 lb/cu ft (2.403 g/cc)

Element	Atom Density (atoms/barn-cm)[a]			
	H_2O[b]	Cement[c]	Limestone[d]	Total[e]
H	9.46197-3			9.46197-3
C			1.05173-2	1.05173-2
O	4.73098-3	6.11209-3	3.52347-2	4.60778-2
Na		1.28310-5		1.28310-5
Mg		1.72242-4	4.92274-3	5.09498-3
Al		2.88744-4	1.28212-4	4.16956-4
Si		9.70688-4	1.70431-3	2.67500-3
S		8.49722-5	1.11783-5	9.61505-5
K		1.27795-5		1.27795-5
Ca		3.16982-3	5.59458-3	8.76440-3
Fe		8.52043-5	5.45744-5	1.39779-4
Zn			1.11783-5	1.11783-5

[a]Read a-x as $a*10^{-x}$.
[b]Density = 0.14153 g/cm^3.
[c]Density = 0.45225 g/cm^3.
[d]Density = 1.80900 g/cm^3.
[e]Density = 2.40278 g/cm^3.

American Limestone Company

AGRICULTURAL LIMESTONE
CRUSHED STONE
MANUFACTURED SAND

P.O. BOX 2389
KNOXVILLE, TENNESSEE 37901
PHONE (615) 573-4501

SAND GRAV
CONCRETE

SOUTHERN CAST STONE CO. KNOXVILLE, TENNESSEE
RECEIVED MAY 22 1978

May 17, 1978

Mr. Bill Ayres
Southern Cast Stone Company
2100 Sutherland Ave.
Knoxville, TN 37919

Re: Gradations American Limestone
Mascot Plant

Dear Bill:

The limestone aggregates which we are presently furnishing to Southern Cast Stone from our Mascot plant are checked daily under our quality control program at this plant. The #7 stone and the manufactured limestone sand are checked for gradation to meet A.S.T.M. C33 standards for #7 stone and concrete sand. If you need any further information on these gradations we will be glad to supply them.

We appreciate the business Southern Cast Stone has given us, and I can assure you we will be working to keep our high quality control standards which we know you require on a daily basis at our plant.

Representative analyses 5/13/85 from Sid Cameron of Am. Limestone Co. says Kingsport dolomite region

Very truly yours,

W. Hoyl Gill
Vice President-Sales

$CaCO_3$	51.40%
$MgCO_3$	38.10%
SiO_2	9.40%
Fe_2O_3, Al_2O_3 →	1.00%
ZnS	.1 %

WHG:pm

See attached sheets for elemental constituents

A Division of ASARCO

Southern Cast Stone
Concrete Products

BLOCK PLANT 2100 SUTHERLAND AVE. 524-3351
PRECAST PLANT 2000 SUTHERLAND AVE. 524-3615

P. O. BOX 1669 KNOXVILLE, TENNESSEE 37901

May 16, 1978

Mr. H. H. Sigmon
Union Carbide Corporation
P. O. Box M, Cheyenne Hall
Oak Ridge, Tennessee 37830

RE: ORDER #21X-80629
X-10 PLANT

Dear Mr. Sigmon,

The mix design we propose to use for casting the precast material on the referenced order is proportioned as follows:

100# Type 1 Portland Cement
150# Manufactured Limestone Sand
250# #7 Mascot Rock
4 oz. PDA Liquid 25XL
½ oz. Protex Concentrate Air Entraining Solution
Slump 2" to 4"

The manufacturer's certification for the cement, sand, aggregate and admixture are enclosed.

Sincerely,

SOUTHERN CAST STONE COMPANY, INC.

W. A. Ayres

William A. Ayres, General Manager
Precast Division

WAA/bs

enclosures

PRESTRESSED CONCRETE INSTITUTE PCI

78
Sou 4141
4136
319281
319258
94200
C of G 1493

7941

SILO No. 5
General Portland Cement Company Signal Mountain Division

LABORATORY MILL TEST

Date 4-17-78

We certify that the following analysis is representative for our Type I Cement and that it complies with A.S.T.M. C-150, A.A.S.H.O. M-85, or A.S.T.M. C-91.

CHEMICAL ANALYSIS

SiO_2	21.1 %	C_3S	55.8 %
Al_2O_3	5.3 %	C_2S	18.5 %
Fe_2O_3	2.4 %	C_3A	10.0 %
CaO	64.5 %	C_4AF	7.3 %
MgO	2.5 %	Total alkali Na_2O Equiv.	0.35 %
SO_3	2.5 %	Insol. Res.	0.26 %
Ig. Loss	1.2 %		

PHYSICAL TESTS

Setting Time: Gillmore

Initial: 2 Hrs. 30 Min.

Final: 3 Hrs. 30 Min.

Fineness - cm^2/gm

Blaine 3745

Wagner

Entrained Air 8.4

Water Retention

325 mesh 92.0

Setting Time: Vicat

Initial: 1 Hrs. 55 Min.

Final: 3 Hrs. 30 Min.

False Set 90.0 %

% Exp. 0.12 %

COMPRESSIVE STRENGTH

1 Day 1480 psi

3 Days 3280 psi

7 Days 4510 psi

28 Days psi

A-6

QUALITY CONTROL MANAGER

Air Rel # 3565

P-41

4-21-78 Silo No. 6

General Portland Cement Company Signal Mountain Division

Sou 93929

LABORATORY MILL TEST

Date: 4-24-78

We certify that the following analysis is representative for our Type I Cement and that it complies with A.S.T.M. C-150, A.A.S.H.O. M-85, or A.S.T.M. C-91.

CHEMICAL ANALYSIS

SiO_2	20.9 %	C_3S	53.3 %
Al_2O_3	5.3 %	C_2S	19.8 %
Fe_2O_3	2.5 %	C_3A	9.8 %
CaO	63.5 %	C_4AF	7.6 %
MgO	2.5 %	Total alkali Na_2O Equiv.	0.37 %
SO_3	2.4 %	Insol. Res.	0.30 %
Ig. Loss	1.3 %		

PHYSICAL TESTS

Setting Time: Gillmore

Initial: 2 Hrs. 35 Min.

Final: 3 Hrs. 30 Min.

Fineness - cm^2/gm

Blaine 3723

Wagner

Entrained Air 8.5

Water Retention

325 mesh 92.0

Setting Time: Vicat

Initial: 2 Hrs. 10 Min.

Final: 3 Hrs. 20 Min.

False Set 88.1 %

% Exp. 0.13 %

COMPRESSIVE STRENGTH

1 Day 1570 psi

3 Days 3160 psi

7 Days 4480 psi

28 Days psi

A-7

QUALITY CONTROL MANAGER

4-21-78 Silo No. 6

General Portland Cement Company — Signal Mountain Division

Sou 93929

LABORATORY MILL TEST

Date 4-24-78

We certify that the following analysis is representative for our Type I Cement and that it complies with A.S.T.M. C-150, A.A.S.H.O. M-85, or A.S.T.M. C-91.

CHEMICAL ANALYSIS

SiO_2	20.9 %	C_3S	53.3 %
Al_2O_3	5.3 %	C_2S	19.8 %
Fe_2O_3	2.5 %	C_3A	9.8 %
CaO	63.5 %	C_4AF	7.6 %
MgO	2.5 %	Total alkali Na_2O Equiv.	0.37 %
SO_3	2.4 %	Insol. Res.	0.30 %
Ig. Loss	1.3 %		

PHYSICAL TESTS

Setting Time: Gillmore

Initial: 2 Hrs. 35 Min.

Final: 3 Hrs. 30 Min.

Fineness - cm^2/gm

Blaine 3723

Wagner

Entrained Air 8.5

Water Retention

325 mesh 92.0

Setting Time: Vicat

Initial: 2 Hrs. 10 Min.

Final: 3 Hrs. 20 Min.

False Set 88.1 %

% Exp. 0.13 %

COMPRESSIVE STRENGTH

1 Day 1570 psi

3 Days 3160 psi

7 Days 4480 psi

28 Days psi

A-8

QUALITY CONTROL MANAGER

PROTEX INDUSTRIES INC.
1331 West Evans Avenue—Denver, Colorado 80223
Telephone: 303/935-3508 Cable: Protex

February 3, 1975

MANUFACTURER'S
CERTIFICATION

Southern Cast Stone
PO Box [illegible]
Knoxville, Tennessee 37901

Attn: Mr. Bill Ayres

Re: Protex PDA Liquid 25XL

Gentlemen:

This is to certify that PDA Liquid 25XL conforms to the requirements of A.S.T.M. C-494-71, A.A.S.H.O. M-194-70, and C.R.D. C-87-70, Type A Admixture, when used at the rate of four fluid ounces per 100 lbs. of cement.

PDA Liquid 25XL is manufactured from a lignosulfonate which has been purified and desugared and does not contain any form of calcium chloride.

PROTEX INDUSTRIES INC.

Floyd Whitson

Floyd L. Whitson
Production Manager

NOTICE—All orders are subject to each of the following conditions: 1. Quotations are for immediate acceptance subject to change without notice. 2. Prices quoted are based on present freight rates, purchaser agrees to pay any increase therein. [illegible]

PROTEX INDUSTRIES INC.
1331 West Evans Avenue—Denver, Colorado 80223
Telephone: 303/935-3566 Cable: Protex

MANUFACTURER'S
CERTIFICATION

Re: Protex Concentrate Air Entraining Solution

Gentlemen:

We hereby certify that Protex Air Entraining Solution is manufactured to comply with the requirements of the U.S. Bureau of Reclamation, U.S. Corps of Engineers Specification CRD-C-13-66 as well as A.S.T.M. Specification C-260-73 and A.A.S.H.O. Specification M-154-70.

PROTEX INDUSTRIES, INC.

Floyd Whitson

Floyd Whitson
Production Manager

Subscribed and sworn to before me this 7th day of Aug. 1975.

Notary Public

My Commission Expires May 11,1977

NOTICE—All orders are subject to each of the following conditions: 1. Quotations are for immediate acceptance subject to change without notice. 2. Prices quoted are based on present freight rates, purchaser agrees to pay any

Appendix B

ASSUMPTIONS FOR CREDIBLE ABNORMAL CONDITION

MARTIN MARIETTA

Internal Correspondence

MARTIN MARIETTA ENERGY SYSTEMS, INC.

December 18, 1992

R.T. Primm, III

Assumptions for Criticality Calculations for Fissile Solids Storage at Building 3019

The following updated assumptions are appropriate for use in nuclear criticality safety evaluations to more reasonably describe conditions of the Cell 4 storage wells:

1. H:X ratio for all solids are a maximum of 3. This value came from:
   a. an assumed moisture content contributing H:X of 2.5, and

   b. plastic bagging of product cans — up to 31 g of PVC $(H_2CCHCl)_x$ per 700 g U (H;X up to 0.5).

2. The overall linear fissile loading density for U-233 is less than 1.42 Kg/ft. This is based on can-by-can evaluation of well loadings which found up to 1.42 Kg/ft..

3. Up to 2 adjacent wells containing fissile material may be open (and subject to fire suppression water ingress) at any time. This is based on procedural control of well access operations.

4. Any liquid water that flows into a storage well may mix intimately with the fissile material stored in cans within. This is due to container closures (except NFS) not being subjected to weld certifications. However, the moistened fuel would <u>not flow out</u> of its primary or secondary container since container structural integrity would be maintained and no mechanism for dissolution would exist.

Please call me if any additional information is needed on these assumptions.

Alan M Krichinsky

Alan M. Krichinsky, 3019, MS-6046 (4-6940) - No-RC

AMK:dsc

cc: E.C. Crume
C.M. Hopper
B.D. Patton
B.W. Starnes
R.M. Westfall

Appendix C

VALIDATION OF COMPUTER CODES AND CROSS SECTION LIBRARY FOR URANIUM-233 SYSTEMS

Appendix C

VALIDATION OF COMPUTER CODES AND CROSS SECTION LIBRARY FOR URANIUM-233 SYSTEMS

C.1 INTRODUCTION

The calculated parameters (KENO-Va, Hansen-Roach) for critical experiments performed with uranium-233 are reported in this appendix. The U-233 database is small relative to the plutonium and U-235 databases. The cases studied are contained in Refs. 1–4. Additional data initially believed to be applicable to 3019 analyses are available in Ref. 5. Due to inconsistencies noted subsequently, only a portion of these data were included in the validation study.

The reader is referred to Refs. 1–5 for detailed descriptions of the critical experiments. Brief descriptions of the experiments are provided in Tables C.1 and C.2. The Koponen Citation number refers to a compilation of critical experiments prepared under the direction of B. L. Koponen, Lawrence Livermore Laboratory.[6] Reference 1 is assigned the I.D. of 1727, Ref. 2 is 111, Ref. 3 is 1211, Ref. 4 is 114, and Ref. 5 is 1250.

The subcritical designation for five of the 111 entries means that these experiments could not be made critical in the experimental vessel. However, an extrapolation (usually small) was made to a critical height. This height exceeded the physical dimensions of the vessel and thus could not be verified to be critical. K-effectives for these experiments were calculated but were not used to derive subcritical limits.

C.2 EXPERIMENTAL AND CALCULATED NEUTRONICS PARAMETERS

While Tables C.1 and C.2 provide a summary of experimental data, those data must be translated into models for the SCALE analysis system. Each set of experiments is described and the assumptions made in translating the experimental data to a computer model are noted.

Table C.1. Uranium-233 benchmarks

Koponen citation I.D.	I.D. number source ref.	Description
1727-1	IV-1	bare, metal sphere
1727-2	IV-2	natural uranium reflected metal sphere
1727-3	IV-3	nat. U ref. metal sphere
1727-4	IV-4	nat. U ref. metal sphere
1727-5	IV-5	Tungsten ref. metal sphere
1727-6	IV-6	Tungsten ref. metal sphere
1727-7	IV-7	Be ref. metal sphere
1727-8	IV-8	Be ref. metal sphere
111-1 to 111-3	-	uranyl nitrate, diameter = 19.1 cm
111-4 to 111-10	-	uranyl nitrate, diameter = 20.5 cm
111-11 to 111-12	-	uranyl nitrate, diameter = 21.5 cm
111-13 to 111-14	-	uranyl nitrate, diameter = 22.9 cm
111-15 to 111-16	-	uranyl nitrate, diameter = 25.5 cm
111-17 to 111-19	-	uranyl nitrate, diameter = 30.5 cm

Table C.1. Uranium-233 benchmarks

Koponen citation I.D.	I.D. number source ref.	Description
111-20	-	uranyl nitrate, diameter = 26.4 cm
111-21	-	uranyl fluoride, diameter = 19.1
111-22	-	uranyl fluoride, diameter = 30.5
111-23 to 111-24	-	uranyl fluoride, diameter = 26.6
111-25 to 111-26	-	uranyl fluoride, diameter = 31.9
111-27	-	subcritical, fluoride, diam. = 20.5 cm
111-28	-	subcritical, fluoride, diam. = 21.5 cm
111-29	-	subcritical, fluoride, diam. = 22.9 cm
111-30 to 111-31	-	subcritical, fluoride, diam. = 25.5 cm
1211-1	-	nitrate, bare array, 8 elements
1211-2	-	nitrate, bare array, 27 elements
1211-3	-	nitrate, ref. array, 8 elements
1211-4	-	nitrate, ref. array, 27 elements
1211-5	-	nitrate, bare array, 8 elements
1211-6	-	nitrate, bare array, 27 elements
1211-7	-	nitrate, ref. array, 8 elements
1211-8	-	nitrate, ref. array, 27 elements
1211-9 to 1211-24	-	nitrate, bare single element
1211-25 to 1211-34	-	nitrate, ref. single element
114-5	5	dilute nitrate, 27.24 in sphere
114-6	6	dilute nitrate, 27.24 in sphere
114-7	7	dilute nitrate, 27.24 in sphere
114-8	8	dilute nitrate, 27.24 in sphere
114-9	9	dilute nitrate, 27.24 in sphere
114-11	11	dilute nitrate, 48.04 in sphere
114-17	17	dilute nitrate, 60.92 in cylinder
114-18	18	dilute nitrate, 60.92 in cylinder
114-19	19	dilute nitrate, 60.92 in cylinder
114-20	20	dilute nitrate, 60.92 in cylinder
1250-6	U-6	ref. array of cylinders
1250-7	U-7	ref. array of cylinders
1250-8	U-8	ref. array of cylinders
1250-9	U-9	ref. array of cylinders
1250-10	U-10	ref. array of cylinders
1250-11	U-11	ref. array of cylinders
1250-12	U-12	ref. array of cylinders

Table C.2. Characteristics of U-233 critical experiments

Koponen citation I.D.	H/U atom ratio	wt % ^{233}U	U density (g/cm^3)	Geometry	Reflector
1727-1	0	98.11	18.42	sphere	none
1727-2	0	98.11	18.42	sphere	Natural U
1727-3	0	98.2	18.64	sphere	Natural U
1727-4	0	98.2	18.62	sphere	Natural U
1727-5	0	98.2	18.64	sphere	W-alloy
1727-6	0	98.2	18.62	sphere	W-alloy
1727-7	0	98.2	18.64	sphere	Be
1727-8	0	98.2	18.62	sphere	Be
111-1	56.8	98.7	0.386	cylinder	paraffin
111-2	66.1	98.7	0.340	cylinder	paraffin
111-3	143.1	98.7	0.169	cylinder	paraffin
111-4	56.8	98.7	0.386	cylinder	paraffin
111-5	83.3	98.7	0.279	cylinder	paraffin
111-6	118.4	98.7	0.201	cylinder	paraffin
111-7	143.1	98.7	0.169	cylinder	paraffin
111-8	149.0	98.7	0.162	cylinder	paraffin
111-9	190.5	98.7	0.129	cylinder	paraffin
111-10	210.2	98.7	0.119	cylinder	paraffin
111-11	243.8	98.7	0.102	cylinder	paraffin
111-12	293.1	98.7	0.085	cylinder	paraffin
111-13	351.4	98.7	0.071	cylinder	paraffin
111-14	374.1	98.7	0.068	cylinder	paraffin
111-15	388.9	98.7	0.064	cylinder	paraffin
111-16	455.0	98.7	0.056	cylinder	paraffin
111-17	574.4	98.7	0.045	cylinder	paraffin
111-18	621.8	98.7	0.041	cylinder	paraffin
111-19	747.2	98.7	0.033	cylinder	paraffin
111-20	399.7	98.7	0.063	sphere	water
111-21	152.0	98.7	0.167	cylinder	paraffin
111-22	764.9	98.7	0.033	cylinder	paraffin
111-23	413.6	98.7	0.062	sphere	water
111-24	384.9	98.7	0.067	sphere	water
111-25	654.4	98.7	0.040	sphere	water
111-26	376.0	98.7	0.068	sphere	bare
111-27	246.8	98.7	0.103	cylinder	paraffin
111-28	324.7	98.7	0.079	cylinder	paraffin
111-29	390.9	98.7	0.066	cylinder	paraffin
111-30	515.2	98.7	0.050	cylinder	water

Table C.2. Characteristics of U-233 critical experiments

Koponen citation I.D.	H/U atom ratio	wt % ^{233}U	U density (g/cm^3)	Geometry	Reflector
111-31	152.0	98.7	0.167	cylinder	bare
1211-1	71.2	98.7	0.333	cylinder	bare
1211-2	71.2	98.7	0.333	cylinder	bare
1211-3	71.2	98.7	0.333	cylinder	polyethylene
1211-4	71.2	98.7	0.333	cylinder	polyethylene
1211-5	116.1	98.7	0.204	cylinder	bare
1211-6	116.1	98.7	0.204	cylinder	bare
1211-7	116.1	98.7	0.204	cylinder	polyethylene
1211-8	116.1	98.7	0.204	cylinder	polyethylene
1211-9	71.2	98.7	0.333	cylinder	bare
1211-10	119.0	98.7	0.204	cylinder	bare
1211-11	119.0	98.7	0.204	cylinder	bare
1211-12	119.0	98.7	0.204	cylinder	bare
1211-13	190.2	98.7	0.131	sphere	bare
1211-14	190.2	98.7	0.131	cylinder	bare
1211-15	190.2	98.7	0.131	cylinder	bare
1211-16	190.2	98.7	0.131	cylinder	bare
1211-17	246.8	98.7	0.102	sphere	bare
1211-18	246.8	98.7	0.102	cylinder	bare
1211-19	246.8	98.7	0.102	cylinder	bare
1211-20	340.4	98.7	0.075	sphere	bare
1211-21	340.4	98.7	0.075	cylinder	bare
1211-22	340.4	98.7	0.075	cylinder	bare
1211-23	566.7	98.7	0.045	sphere	bare
1211-24	566.7	98.7	0.045	cylinder	bare
1211-25	189.2	98.7	0.132	sphere	water
1211-26	189.2	98.7	0.132	cylinder	water
1211-27	189.2	98.7	0.132	cylinder	water
1211-28	189.2	98.7	0.132	cylinder	water
1211-29	266.3	98.7	0.095	sphere	water
1211-30	266.3	98.7	0.095	cylinder	water
1211-31	266.3	98.7	0.095	cylinder	water
1211-32	534.5	98.7	0.048	sphere	water
1211-33	534.5	98.7	0.048	cylinder	water
1211-34	534.5	98.7	0.048	cylinder	water
114-5	1533.0	97.7	0.017	sphere	bare
114-6	1470.0	97.7	0.018	sphere	bare
114-7	1417.0	97.7	0.019	sphere	bare

Table C.2. Characteristics of U-233 critical experiments

Koponen citation I.D.	H/U atom ratio	wt % ^{233}U	U density (g/cm^3)	Geometry	Reflector
114-8	1368.0	97.7	0.019	sphere	bare
114-9	1324.0	97.7	0.020	sphere	bare
114-11	1986.0	97.7	0.013	sphere	bare
114-17	1819.0	97.4	0.014	cylinder	bare
114-18	1900.0	97.4	0.014	cylinder	bare
114-19	1996.0	97.3	0.013	cylinder	bare
114-20	2106.0	97.2	0.013	cylinder	bare
1250-6	67.1	98.2	0.3262	array, cylinder	Lucite
1250-7 to 11	68.9	98.2	0.3181	array, cylinder	Lucite
1250-12	67.6	98.2	0.3232	array, cylinder	Lucite

C.2.1 Metal Spheres

Reference 1 (Koponen I.D. = 1727) contains data for eight, critical, ^{233}U spheres. While no details of the experimental setup or procedure are given, reference is made to other publicly available documents which provide considerable detail. The dimensions and masses reported in Ref. 1 have been corrected to account for room return effects and the impact of the experimental apparatus on the reactivity of the system. Thus, no compensations are required in the computational model and none were made.

The results are tabulated in Table C.3 along with the calculated average energy group causing fission. All of the results are for the CSAS25 module (KENO-Va program) of the NCSS version of the SCALE package and were generated using the Hansen-Roach cross-sections. All input datasets are stored on the floppy disk attached to the inside of the back cover of this report. The datasets are in the directory /crit_expts/u233/1727.cases. Because the datasets are so simple (a sphere and spherical reflector), no sketches are provided. The output from these cases are stored on microfiche and are available from the Nuclear Criticality Safety Group of the Facility Safety Section at Oak Ridge National Laboratory.

These experiments are not very applicable to the 3019 storage arrays. The neutron spectrum is very fast; much faster than would exist in any unpoisoned, concrete reflected configuration. Nevertheless, in a weak sense, these experiments provide an upper bound, in term of AGF, on the normal and credible abnormal cases under consideration.

Note that the range of k-effectives for natural uranium reflected experiments covers almost the full range of k-effectives for these eight experiments. Treating all eight calculated k-effectives as if they were from the same distribution, the mean value of k-effective is 1.0014.

Table C.3. Calculated parameters for 1727 ^{233}U metal experiments

Expt. I.D.	Critical Mass (kg ^{233}U)	Ref.	Ref. Thick (in)	k-effective	sigma	AGF[a]
1727-1	16.22	bare	none	1.00931	0.00411	3.077
1727-2	5.63	U(N)[b]	7.84	0.98943	0.00327	3.114
1727-3	7.47	U(N)	2.09	1.01044	0.00323	3.124
1727-4	9.84	U(N)	0.906	1.00165	0.00373	3.132
1727-5	7.47	W-alloy	2.28	0.99146	0.00365	3.334
1727-6	9.84	W-alloy	0.96	0.98712	0.00370	3.235
1727-7	7.47	Be (98%)	1.652	1.01410	0.00358	3.442
1727-8	9.84	Be (98%)	0.805	1.00771	0.00366	3.274

[a]AGF = Average energy group causing fission.
[b]U(N) = Natural uranium metal.

Regarding the k-effectives in Table C.3, the low tungsten-reflected values and the high Be-reflected values may be due to the relatively old cross-section data for these nuclides (late 1960s, early 1970s). However, the variation in k-effective for the three natural uranium reflected cases merits additional study in the future. Room return, frequently difficult to model, would not appear to be a problem due to the results for experiment 1727-3. As the critical mass increases in experiments 1727-3, 4, and 5, and reflector thickness decreases, the impact of room return should increase. However, no trend is seen.

Evaluations of the impact of experimental uncertainties on calculated k-effectives were performed using one-dimensional discrete ordinates theory (CSAS1X). The errors in the critical masses for cases 1727-1 and 1727-2 were reported to be 0.06 and 0.03 kg, respectively. The critical mass for 1727-1 was reduced to 16.16 kg and the critical mass for 1727-2 was increased to 5.66 kg. The uncertainties in the thicknesses of all of the reflectors were reported to be 1%. The thickness of the reflector for experiment 1727-3 was reduced to 2.07 in. Table C.4 shows the comparison of the perturbed calculations with the reference k-effectives from Table C.3. From these studies, the effect of reported experimental errors was determined to be noticeable, but on the order of the level of uncertainty in the Monte Carlo calculation. The accuracy of the corrections applied to the critical masses before those masses were reported in Ref. 1 was not assessed.

Table C.4. Impact of experimental uncertainties

Experiment No.	Perturbation		k-effective[a]	
	Parameter	Quantity	Reference	Perturbed
1727-1	Critical mass	-0.4%	1.0053	1.0029
1727-2	Critical mass	+0.5%	0.9994	1.0027
1727-3	Ref. thickness	-1.0%	1.0053	1.0045

[a]K-effective calculation converged to $1.0(10^{-4})$.

C.2.2 Single Units filled with Aqueous Solutions

Reference 2 contains data for isolated spheres and cylinders filled with either uranyl fluoride or uranyl nitrate. Three reflection conditions were examined - bare, water- and paraffin-reflected. Data for several

subcritical configurations were reported (Experiments 111-27 through 31) but these were not used in the derivation of subcritical limits. Table C.5 contains additional critical experiment data from Ref. 2 and allows for unambiguous correlation of Koponen I.D. to critical experiment (vessel dimensions needed to distinguish cases reported in Table C.2).

Table C.5. Single unit aqueous solution experiments

Koponen I.D.	$H/^{233}U$ ratio	Sol. density (g/cm^3)	^{233}U density (g/cm^3)	Ref.	Vessel diameter (cm)	Critical height (cm)
111-1	57.5	1.543	0.381	paraffin	19.1	16.3
111-2	67	1.480	0.336	paraffin	19.1	16.2
111-3	145	1.238	0.167	paraffin	19.1	18.6
111-4	57.5	1.543	0.381	paraffin	20.5	14.4
111-5	84.4	1.394	0.275	paraffin	20.5	14.7
111-6	120	1.287	0.198	paraffin	20.5	16.4
111-7	145	1.238	0.167	paraffin	20.5	16.7
111-8	151	1.232	0.160	paraffin	20.5	16.7
111-9	193	1.185	0.127	paraffin	20.5	18.8
111-10	213	1.165	0.117	paraffin	20.5	19.3
111-11	247	1.145	0.101	paraffin	21.5	19.4
111-12	297	1.121	0.084	paraffin	21.5	21.5
111-13	356	1.101	0.070	paraffin	22.9	21.3
111-14	379	1.093	0.067	paraffin	22.9	22.9
111-15	394	1.090	0.063	paraffin	25.5	19.3
111-16	461	1.077	0.055	paraffin	25.5	22.5
111-17	582	1.061	0.044	paraffin	30.5	21.1
111-18	630	1.056	0.040	paraffin	30.5	23.8
111-19	757	1.046	0.033	paraffin	30.5	30.4
111-20	405	1.087	0.062	water	26.6[b]	-
111-21	154	1.198	0.165	paraffin	19.1	18.4
111-22	775	1.035	0.033	paraffin	30.5	30.5
111-23	419	1.071	0.061	water	26.6[b]	-
111-24	390	1.076	0.066	water	26.6[b]	-
111-25	663	1.043	0.039	water	31.9	-
111-26	381	1.079	0.067	none	31.9	-
111-27	250	1.121	0.102	paraffin	20.5	20.2
111-28	329	1.090	0.078	paraffin	21.5	22.2
111-29	396	1.075	0.065	paraffin	22.9	23.1
111-30	522	1.059	0.049	water	25.5	25.9
111-31	154	1.198	0.165	none	25.5	24.0

[a]Experiments conducted in spherical vessels have no entry for height.
[b]Reference 2 specifies vessel diameter as 26.6 cm (10.4 in). 10.4 in = 26.4 cm.

The data presented in Table C.5 were used to derive atom densities for the KENO model. For the convenience of the reader, the derived nitrate and fluoride molarities are shown in Tables C.6 and C.7. For certain cases, the derived fluoride molarity is negative but only slightly so. In those cases, the HF molarity was assumed to be 0.0. The effect on the H and Fl atom densities of assuming zero versus the unrealistic negative value is less than 1%. An independent review of one of the experiments, 111-25, by C. M. Hopper confirmed the data inconsistency but also showed that the inconsistency was with the round-off error of the reported uranium concentration. It is, perhaps, proper to view these data inconsistencies as an indication of the uncertainty in the analytical chemistry measurements.

Table C.6. Nitrate molarity in some aqueous experiments

Koponen I.D.	Molarity
111-1	1.037
111-2	0.914
111-3	0.454
111-4	1.037
111-5	0.748
111-6	0.539
111-7	0.454
111-8	0.435
111-9	0.346
111-10	0.318
111-11	0.275
111-12	0.229
111-13	0.190
111-14	0.182
111-15	0.171
111-16	0.150
111-17	0.120
111-18	0.109
111-19	0.090
111-20	0.169

Table C.7. Fluoride molarity in some aqueous experiments

Koponen I.D.	Molarity
111-21	-0.157
111-22	0.256
111-23	0.231
111-24	-0.550
111-25	-0.727
111-26	0.352
111-27	0.073
111-28	-0.440
111-29	-0.521
111-30	0.511
111-31	-0.157

Another anomaly in the reported experimental data concerned the isotopic ratios of uranium. Reference 2 states that "the uranium...was first used as an aqueous solution of uranyl nitrate...and later as a solution of the more soluble uranyl fluoride". Yet the reported isotopic ratios for the nitrate solution were different than those for the fluoride solution. The reported values are shown in Table C.8. The averages of the two values for each isotope were computed and these values were used in calculating atom densities for the uranium isotopes.

Table C.8. Isotopic composition of uranium in solutions

Isotope	Wt % in $UO_2(NO_3)_2$ solution	Wt % in UO_2F_2 solution
^{233}U	98.7	98.7
^{234}U	0.50	0.54
^{235}U	0.01	0.04
^{238}U	0.79	0.72

The calculated k-effectives are tabulated in Table C.9 along with the calculated average energy group causing fission. All of the results are for the CSAS25 module of the NCSS version of the SCALE package and were generated using the Hansen-Roach cross-sections. All input datasets are stored on the floppy disk attached to the inside of the back cover of this report. The datasets are in the directory /crit_expts/u233/111.cases. Because the geometries are so simple (a sphere or cylinder and reflector), no sketches are provided. The output from these cases are stored on microfiche and are available from the Nuclear Criticality Safety Group of the Facility Safety Section at Oak Ridge National Laboratory.

Table C.9. Calculated parameters for single unit aqueous experiments

Koponen I.D.	AGF*	k-effective	sigma
111-1	13.99	0.97463	0.00455
111-2	14.16	0.97667	0.00397
111-3	14.87	0.98297	0.00421
111-4	13.98	0.96485	0.00424
111-5	14.38	0.96538	0.00411
111-6	14.71	0.98254	0.00422
111-7	14.86	0.97058	0.00468
111-8	14.90	0.97164	0.00405
111-9	15.06	0.98351	0.00405
111-10	15.12	0.98701	0.00416
111-11	15.20	0.98734	0.00390
111-12	15.29	0.98785	0.00433
111-13	15.37	0.97268	0.00399
111-14	15.39	0.99402	0.00403
111-15	15.41	0.96036	0.00384
111-16	15.47	0.98608	0.00345
111-17	15.53	0.97657	0.00377
111-18	15.54	0.98359	0.00327
111-19	15.61	0.99089	0.00343
111-20	15.41	0.96632	0.00381
111-21	14.92	1.00854	0.00488
111-22	15.61	1.00439	0.00309
111-23	15.43	0.99566	0.00371
111-24	15.40	1.01118	0.00355
111-25	15.57	0.99914	0.00359
111-26	15.27	0.97776	0.00461
111-27	15.21	0.99538	0.00387
111-28	15.34	0.99853	0.00386
111-29	15.42	0.99094	0.00363
111-30	15.51	0.99856	0.00537
111-31	14.58	0.97562	0.00390

*AFG = Average energy group for fissions.

Reference 2 reports that "results from critical experiments with uranyl fluoride...are good to $\pm 1\%$; data from the same vessels with uranyl nitrate have an uncertainty of no more than $\pm 3\%$. Experiment 111-15 was the one in which the deviation of k-effective from the expected value of 1.0 was the largest. Experiments 111-14 and 111-16 had similar solution compositions, geometries and the same reflector

material, yet had significantly higher k-effectives. The critical height for Experiment 111-15 was increased by 3% and k-effective was recalculated. The perturbed value of 0.96778 ± 0.00366 explains only a small portion of the variation of calculated k-effective from the expected value of 1.0.

Since reported experimental uncertainty appeared an unlikely explanation for the observed variation in calculated k-effectives (for this series of experiments, average k-effective was 0.9846 ± 0.0132), a statistical study was conducted to determine if a previously unidentified systematic error could be found. Attempts were made to correlate k-effective to various experimental parameters. The results are shown in Tables C.10 and C.11.

Table C.10 shows the results of a search for a linear relationship (one expects no relationship so the assumption of a linear trend is as good as any other) between a given variable and the calculated k-effectives. The value of the Pearson product moment correlation and its level of significance are shown. This coefficient is defined such that if a variable x can be expressed exactly as a linear function of another variable y, then the correlation is 1 or -1 depending on whether the two variables are directly related or inversely related (the lower the value of the significance level, the higher the degree of confidence that the computer correlation value represents a true phenomena).

Table C.10. Correlation of Koponen I.D. 111 experimental parameters to calculated k-effectives

Parameter	Correlation coefficient[a]	Significance level[b]
H/Total U	0.398	0.027
Solution density	-0.478	0.006
^{233}U density	-0.442	0.010
Critical diameter	0.159	0.392
Critical height	0.562	0.003
Acid molarity	-0.571	0.001
AGF[c]	0.470	0.008

[a]Pearson product-moment correlation ranges from 1 to -1.
[b]Generally, values less than 0.01 are significant, above 0.2, not significant.
[c]AGF = average energy group for fissions.

Table C.11 presents a sorting of the calculated k-effectives according to four classification variables. Systematic errors associated with a particular experimental vessel or analytical chemistry problems can be revealed by such classification schemes. The mean value for the nitrate experiments is significantly lower than that of the fluoride experiments. The mean value of k-effective from the subcritical-extrapolated-to-critical fluoride experiments (0.9918 ± 0.0043) is reasonably close to that derived from critical fluoride configurations. It is noteworthy that one of the five subcritical configurations differs significantly from the other four, having a k-effective of 0.9756. This experiment is reported as a bare configuration leaving the possibility that unreported room return could account for the variance. Note that Table C.11 indicates that reflected configurations may calculate higher than bare ones (the number of bare experiments is small). It will be seen that this trend is not supported by data presented in the next section.

Table C.11. Variation in k-effectives for Koponen I.D. 111 experiments due to experimental conditions

Parameter	Mean value of k-effective	Number of observations
Geometry		
All cylinders	0.9835	26
All spheres	0.9900	5
Reflectors		
Bare	0.9767	2
Paraffin	0.9832	24
Water	0.9942	5
Diameter of vessels[a] (cm)		
19.1	0.9857	4
20.5	0.9776	8
21.5	0.9912	3
22.9	0.9859	3
25.5	0.9802	4
26.6	0.9911	3
30.5	0.9889	4
31.9	0.9884	2
Fuel form		
Nitrate	0.9783	20
Fluoride[a] (all)	0.9960	11
Fluoride (critical)	0.9994	6

[a]Includes both critical and subcritical configurations.

The differences in k-effectives for different fuel types would lead one to question analytical chemistry procedures. Unfortunately, it is the fluoride measurements which do not appear to be stoichiometric yet these yield calculated k-effectives which are in excellent agreement (the bare case withstanding) with measured conditions. Furthermore, the results for other nitrate experiments reported subsequently support the current nitrate calculations and encompass the range of k-effectives exhibited by the fluoride experiments.

C.2.3 Uranyl Nitrate Experiments Conducted in Arrays and Simple Geometries

Reference 3 provides a description of three sets of experiments. One of these - ^{233}U nitrate solution in a tank filled with borosilicate Rasching rings - was not modeled as none of the storage arrays in building 3019 rely on this method of criticality control. The other two sets were modeled and k-effectives were calculated.

Reference 3 provides the following description of the array criticality experiments.

> Cylindrical containers, of 4.63 liters capacity and fabricated of 0.25-mm-thick stainless steel, had an outside diameter and a height of 18.28 and 17.67 cm, respectively. They were identically filled to within $\pm$ 0.5 g of solution. Critical assemblies of reflected and unreflected arrays at uranium concentrations of 333 and 204 g/liter were constructed. The reflector material was 15.2-cm-thick polyethylene (density = 0.93 g/cm^3) located from the peripheral cylinders of the array by a distance equal to one-half the surface separation between cylinders. The critical conditions for the arrays of cylinders at the two uranium concentrations are summarized in Table (C.12; these data remove the apparent ambiguity of assignment of Koponen I.D.s to experiments listed in Table C.2).

Table C.12. Critical parameters for cubic arrays of uranyl nitrate solution

Koponen I.D.	No. of Units	Ref. Thick (cm)	Center-to-Center Separation (cm)		U density (g/cm^3)	Solution type[a]
			Horizontal	Vertical		
1211-1	8	0	20.44	19.13	0.179	1
1211-2	27	0	25.72	24.57	0.088	1
1211-3	8	15.2	31.95	30.36	0.046	1
1211-4	27	15.2	41.03	38.57	0.022	1
1211-5	8	0	20.16	18.81	0.116	2
1211-6	27	0	25.01	23.89	0.059	2
1211-7	8	15.2	30.23	25.51	0.034	2
1211-8	27	15.2	38.05	36.74	0.017	2

[a] Solution type 1 contains 333 g of U per liter; $H/^{233}U$ = 73; specific gravity = 1.468.
Solution type 2 contains 204 g of U per liter; $H/^{233}U$ = 119; specific gravity = 1.280.

Calculated k-effectives for the array experiments are shown in Table C.13. There is an obvious difference between reflected and some of the bare experiments. No description is given in Ref. 3 of the experimental cell in which the critical experiments were performed. No mention is made of any correction for room return of neutrons to the experimental vessel. Curiously, one of the high leakage bare experiments, 1211-1 has essentially the same value of k-effective as the reflected experiments. Some documentation may be available in laboratory notebooks and further investigation of these experiments should be done in a future study. For these studies, since the description of the experiments is incomplete and since only concrete reflected conditions exist in Building 3019, experiments 1211-1, 2, 5, and 6 were not used in the determination of a safely subcritical margin. The calculated k-effectives for the reflected experiments are in agreement with other experimental data reported in Table C.9. The calculated k-effectives for the reflected arrays were included in the subsequent derivation of a subcritical limit for U-233 systems.

Table C.13. Calculated parameters for arrays of aqueous solutions

Koponen I.D.	AGF[a]	k-effective	sigma	Reflector
1211-1	13.56	0.96966	0.00456	bare
1211-2	13.54	0.94738	0.00446	bare
1211-5	14.23	0.92943	0.00447	bare
1211-6	14.22	0.92119	0.00409	bare
1211-3	14.19	0.97366	0.00430	poly[a]
1211-4	14.17	0.98301	0.00417	poly
1211-7	14.68	0.98204	0.00384	poly
1211-8	14.67	0.96246	0.00445	poly

[a] AGF = average energy group for fissions.
[b] poly = polyethylene.

Data and calculated parameters for the third set of experiments are contained in Table C.14. These data remove ambiguity in Koponen I.D. assignments introduced in Table C.2. All of these experiments were conducted in single unit geometries. The height entry for experiments 1211-26 through 34 are different

from that given in Ref. 3. Investigation by H. K. Clark, Savannah River Laboratory (reported in *Nuclear Science and Engineering*, Vol. 81, pp. 379-395, 1982) led to the correct values which are reported here.

Table C.14. Experimental and calculated parameters for uranyl nitrate solutions in simple geometries

Koponen I.D.	Solution specific gravity	Diameter (cm)	Height (cm)	k-effective	sigma	AGF*
1211-9	1.468	50.8	13.36	1.01878	0.00461	13.65
1211-10	1.280	50.8	13.51	0.99542	0.00457	14.34
1211-11	1.280	38.1	15.14	0.98179	0.00462	14.33
1211-12	1.280	25.3	24.69	0.96499	0.00409	14.32
1211-13	1.183	29.158	-	1.00381	0.00453	14.80
1211-14	1.183	50.8	14.07	0.97921	0.00449	14.81
1211-15	1.183	38.1	16.35	0.98266	0.00438	14.81
1211-16	1.183	25.3	28.52	0.97471	0.00466	14.80
1211-17	1.114	30.156	-	1.00870	0.00452	15.01
1211-18	1.114	38.1	17.60	0.98696	0.00439	15.02
1211-19	1.114	25.3	33.40	0.97949	0.00377	15.01
1211-20	1.106	31.642	-	1.00140	0.00411	15.23
1211-21	1.106	38.1	19.35	0.99088	0.00407	15.23
1211-22	1.106	25.3	43.69	0.97876	0.00406	15.22
1211-23	1.050	36.756	-	1.00143	0.00400	15.47
1211-24	1.050	38.1	26.37	0.99947	0.00394	15.47
1211-25	1.186	22.34	-	0.96497	0.00358	15.00
1211-26	1.186	38.1	11.80	0.97083	0.00422	14.98
1211-27	1.186	25.3	15.49	0.97272	0.00436	15.00
1211-28	1.186	20.3	21.16	0.98188	0.00443	15.02
1211-29	1.135	23.694	-	0.96788	0.00381	15.22
1211-30	1.135	25.3	17.92	0.98530	0.00397	15.21
1211-31	1.135	20.3	25.40	0.98765	0.00387	15.23
1211-32	1.068	29.158	-	0.98673	0.00369	15.50
1211-33	1.068	38.1	18.06	0.98184	0.00338	15.50
1211-34	1.068	25.3	25.90	0.95723	0.00343	15.51

* AGF = average energy group for fissions, one standard deviation less than 0.01.

Clark reports, "according to (J. T.) Thomas, the data reported in (Ref. 3) for the reflected cylinders are for the case where each cylinder was supported by 24.3-cm-high cylinder of Styrofoam of the same diameter, i.e., both the top and bottom of the cylinder were essentially unreflected, and some of these data are in error. The mass for the 38.1-cm-diam cylinder at 132 g/ℓ should be 2.02 instead of 1.77 kg, and the height for the 2.03-cm-diam cylinder at 95.0 g/ℓ should be 27.02 rather than 20.02 cm. Of more interest are unreported data for the case where the bottom and sides were reflected by water, i.e., the Styrofoam was replaced by water. These data are (supplied by Clark and are reported in Table C.14)". The seven, reflected styrofoam supported experiments were not calculated as the water-reflected criticals were judged to be "cleaner".

While not reported in Ref. 3, the unreflected cylinders were supported on blocks of Styrofoam of the same diameter as the cylinder (Ibid., p. 381). The models for the unreflected calculations reported in Table C.14 include the Styrofoam support blocks. According to the *Plastics Materials Handbook* by Alan B. Glanvill, Styrofoam is C_8H_8O and has a density of approximately 0.1603 g/cm^3. The derived atom densities for carbon and hydrogen were $6.42824*10^{-3}$ and the atom density for oxygen was $8.03530*10^{-4}$.

A horizontal view through the array as drawn by the KENO-Va program is shown in Fig. C.1. Material 1 is fissile solution, material 2 is the stainless steel tank, and material 3 is the polyethylene reflector. The atom densities of these materials are found in the datasets stored on the floppy disk is included with this report (directory = /critical.expts/u233/1211.expts).

A vertical view of the eight element array is shown in Fig. C.2. This plot is produced by the KENO-Va program and the zone identifiers are the same as for Fig. C.1 with the addition that the region identified by a "4" is air.

Horizontal and vertical views of one of the twenty-seven element arrays are shown in Fig. C.3 and C.4. These plots are produced by the KENO-Va program and the zone identifiers are the same as for Fig. C.1 with the addition that the region identified by a "4" is air.

With one exception, no experimental uncertainties were reported for these data. The solution loading in each bottle of the array experiment was identical to within $\pm$ 0.05 g, an uncertainty of less than 0.01%. Such a small error would not impact calculation of k-effective. The accuracy of the experimental parameters can be inferred from the number of significant figures reported in Table 2.16.3 of Ref. 3. If done, then the maximum experimental error for any measured parameter is less than 1%.

In an attempt to understand the variability in the calculated k-effectives, studies similar to those presented in the prior section were conducted. The mean calculated k-effective for the 26 single unit experiments was 0.9848 $\pm$ 0.0028, almost identical to that of the 111 series of experiments. Even if one considers the mean value of only those 111 experiments conducted with uranyl nitrate (0.9783), the agreement is good.

Pearson product-moment correlation coefficients were calculated for various parameters and are shown in Table C.15. While none of the variables appear to be correlated with k-effective, the calculations are not instructive due to the poor degree of confidence.

Table C.15. Correlation of 1211 experimental parameters to calculated k-effectives

Parameter	Correlation coefficient[a]	Significance level[b]
Solution density	0.18130	0.3754
H/U ratio	0.02323	0.9103
U density	0.21320	0.2957
Critical diameter	0.45894	0.0184
Critical height	-0.33025	0.1673
AGF[c]	-0.23933	0.2390

[a]Pearson product-moment correlation - ranges from 1 to -1.
[b]Generally, values less than 0.01 are significant, above 0.2 are not significant.
[c]Average energy group for fissions.

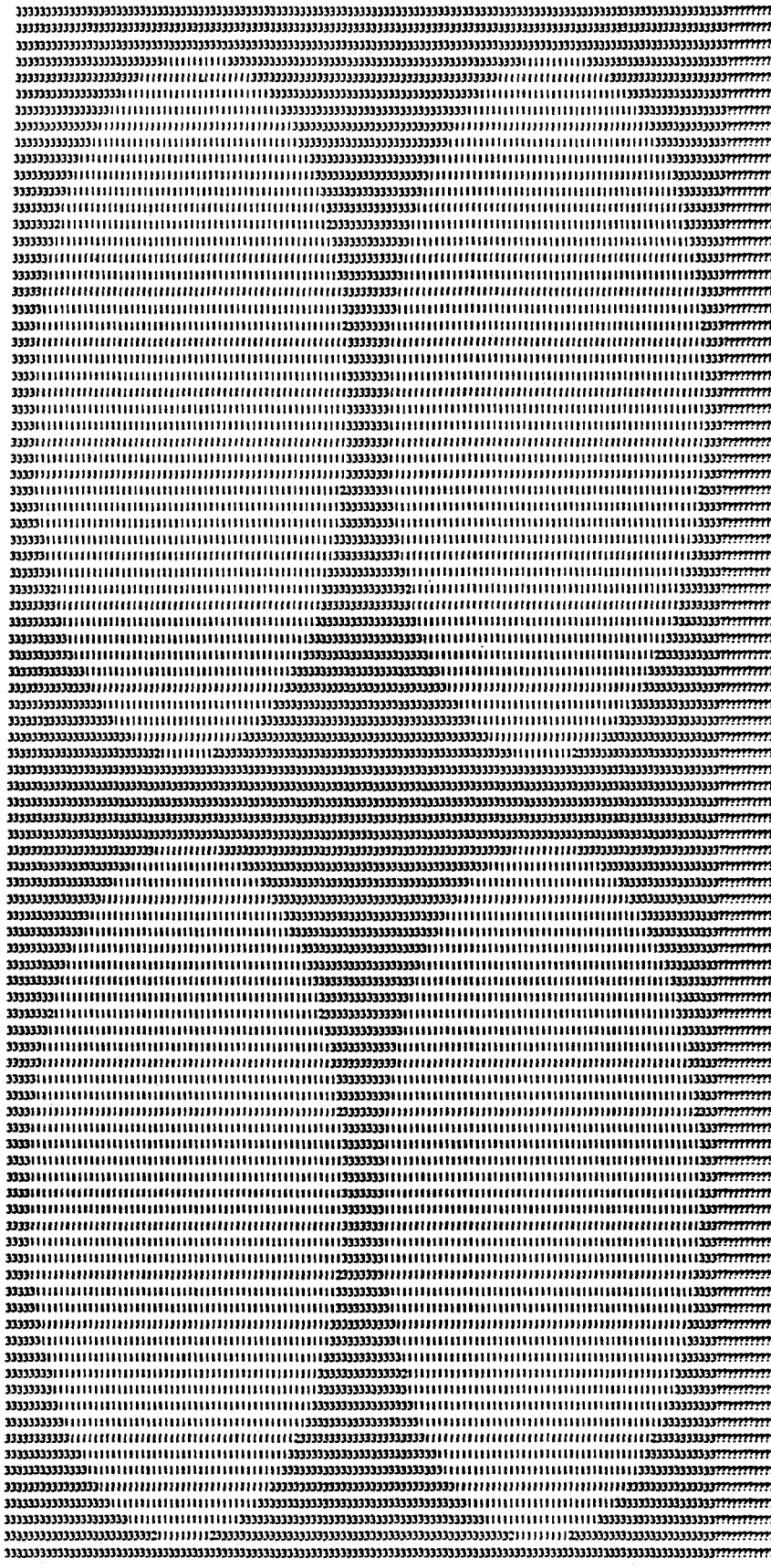

Fig. C.1. Horizontal view of experiment 1211-1 array produced by KENO-Va.

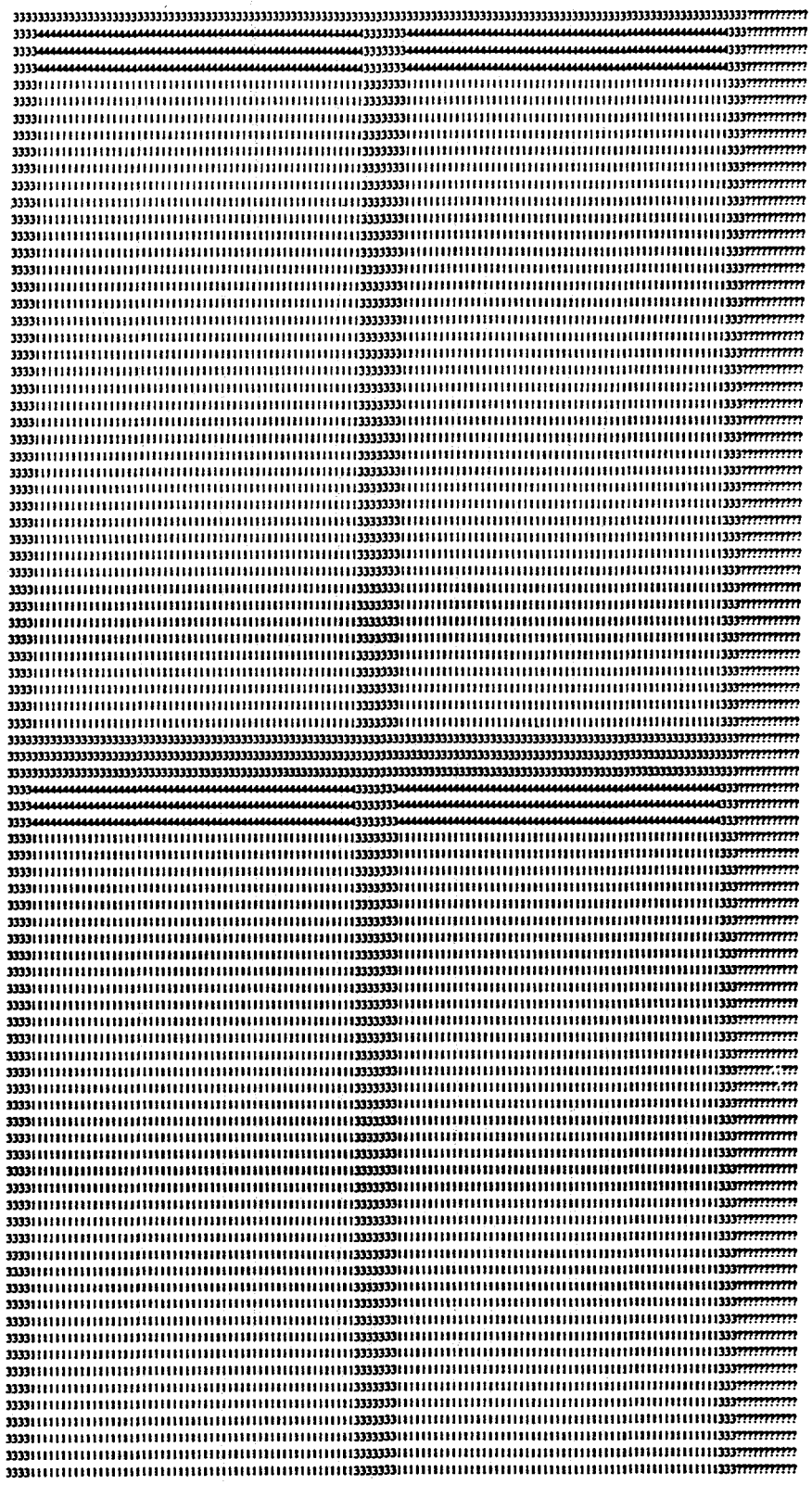

Fig. C.2 Vertical view of 1211-1 experiment as produced by the KENO-Va program.

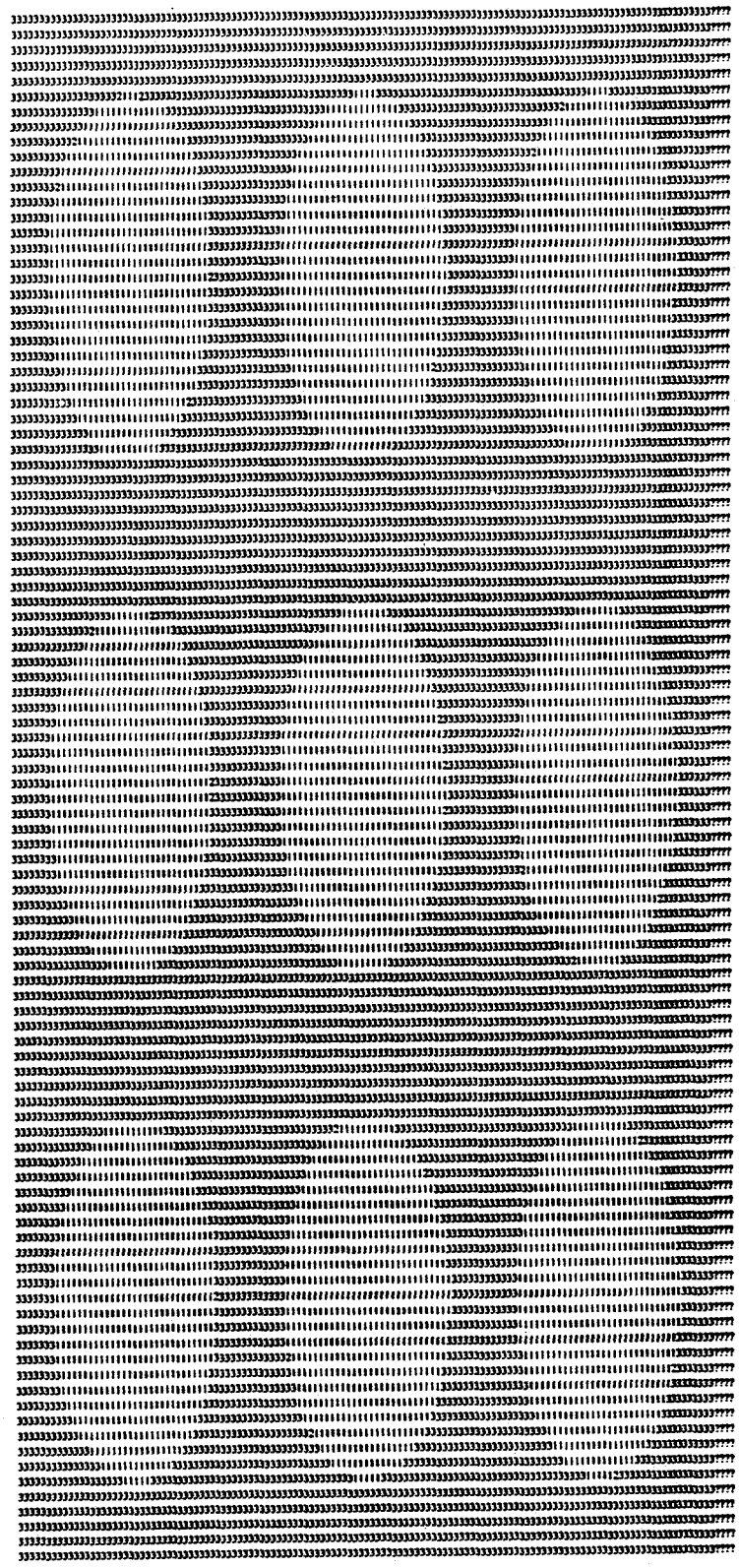

Fig. C.3 Horizontal view through array in experiment 1211-2.

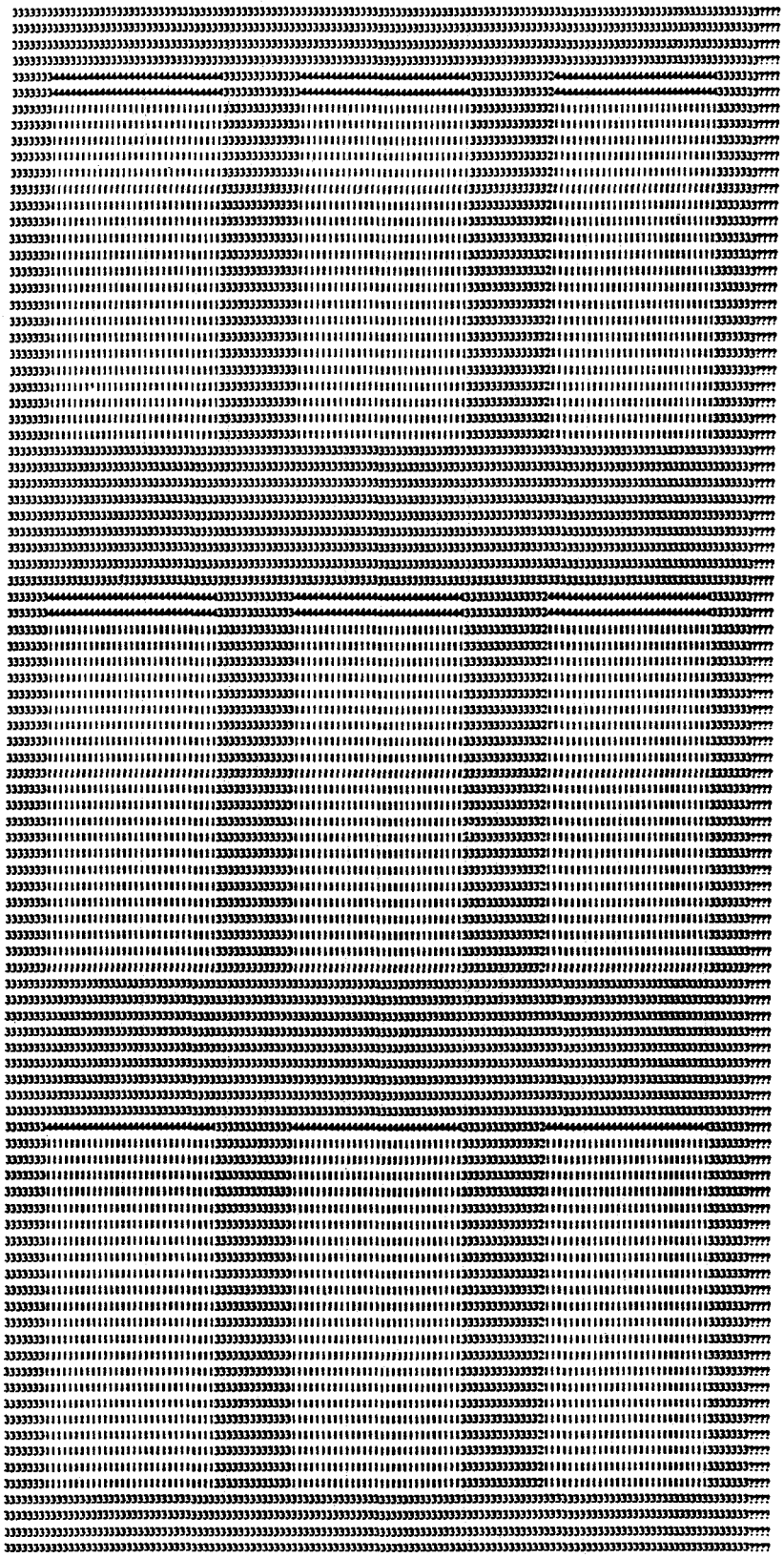

Fig. C.4 Axial view through array in experiment.

Again, as in the prior section, a classification scheme was employed to sort k-effectives. These results are reported in Table C.16. Contrary to the 111 experiments, the bare 1211 experiments calculate higher than the reflected experiments.

Table C.16. Variation in k-effectives for 1211 experiments due to experimental conditions

Parameter	Mean value of k-effective	Number of observations
Geometry		
All cylinders	0.9827	11
All spheres	0.9907	7
Reflectors		
Bare	0.9905	16
Water	0.9757	10
Solution density (g/cm^2)		
1.05	1.0004	2
1.068	0.9753	3
1.106	0.9903	3
1.114	0.9917	3
1.135	0.9803	3
1.183	0.9851	4
1.186	0.9726	4
1.28	0.9807	3
1.468	1.0188	1
Critical diameter (cm)		
20.3	0.9848	2
22.34	0.9650	1
23.694	0.9679	1
25.3	0.9733	7
29.158	0.9953	2
30.156	1.0087	1
31.642	1.0014	1
36.756	1.0014	1
38.1	0.9849	7
50.8	0.9978	3

Based on the results presented in Tables C.15 and C.16, the variability in the calculated k-effectives cannot be explained. Considering both the 111 and 1211 experiments, a bias in calculated k-effective of - 0.015 exists, but no trends are identified. The variability in the 1211 series of nitrate experiments obscures the nitrate/fluoride discrepancy observed in the 111 series of experiments.

C.2.4 Large, Unreflected Spheres Filled with Dilute Uranyl Nitrate

The experiments from Ref. 4 are the most thoroughly documented of all of the ^{233}U benchmarks. Approaches-to-critical were performed in 27- and 48-inch diameter spheres and in a 6-foot diameter cylinder. The goal of the measurements was to determine the value of eta, the number of fission neutrons produced per thermal neutron absorbed in the fissile isotope, for a highly thermalized system. Consequently large volumes of dilute solution were used to minimize leakage from the system.

Brief descriptions of the experiments are given in Tables C.1 and C.2. The datasets, stored on the floppy disk in directory /critical.expts/u233/114.cases, were contributed by W. C. Jordan and have been documented in Ref. 8. No changes were made to the datasets received from Jordan.

For these experiments, unlike those from Refs. 1-3, atom densities are provided by the experimenters. Thus, input preparation for CSAS25 (KENO-Va) is minimal. A more readily available, but slightly less complete description of these experiments is available in Ref. 9.

Calculated k-effectives and average energy group for fissions are shown in Table C.17. The mean value of calculated k-effective for these experiments is 1.00256.

These datasets were also executed on the ORNL CRAY-XMP (no longer operational) using the 27 group cross section library from ENDF/B-V. The calculated parameters are reported in Table C.18. The ENDF/B-V calculations should be interpreted as a machine-and-cross-section-library-independent verification of the models of experiments from Ref. 4. Within statistical uncertainty, the calculated k-effectives were the same.

Table C.17. Calculational results for large, dilute systems

Koponen I.D.	k-effective	Standard deviation for k-effective	Average energy group for fissions
114-5	1.00222	0.00226	15.73
114-6	1.00479	0.00223	15.71
114-7	1.00127	0.00250	15.70
114-8	0.99904	0.00276	15.69
114-9	1.00405	0.00274	15.68
114-11	1.00383	0.00173	15.77
114-17	0.99372	0.00170	15.75
114-18	1.00427	0.00198	15.76
114-19	1.00489	0.00159	15.77
114-20	1.00752	0.00165	15.77

Table C.18. Calculational results for 114 experiments using ENDF/B-V cross sections

Koponen I.D.	k-effective	Standard deviation for k-effective	Average energy group for fissions
114-5	1.00171	0.00255	24.62
114-6	1.00021	0.00207	24.60
114-7	1.00200	0.00240	24.57
114-8	1.00099	0.00214	24.54
114-9	1.00805	0.00222	24.52
114-11	0.99647	0.00180	24.73
114-17	0.99186	0.00195	24.70
114-18	0.99770	0.00189	24.71
114-19	0.99775	0.00159	24.73
114-20	0.99592	0.00142	24.75

The top and bottom energy boundaries for group 15 in the Hansen-Roach library are 0.4 and 0.1 eV, respectively. The top and bottom energy boundaries for group 24 in the 27 group ENDF/B-V library are 0.1 eV and 0.05 eV, respectively. The apparent discrepancy in calculated AGFs is likely due to the single thermal group present in the Hansen-Roach library. Since fission neutrons are born in groups 1-6, it is mathematically impossible that any fissioning system could have an AFG value of 16.0 regardless of the degree of thermalization present.

C.2.5 Arrays of Bottles of ^{233}U Nitrate Solution

Potentially useful data for interstitially moderated arrays of bottles of uranyl nitrate solution are contained in Ref. 5 (Koponen Citation I.D. is 1250). Multiplication measurements were performed with unreflected and Lucite-reflected arrays of bottles of ^{233}U solution. The effect on the critical number of bottles due to adding Lucite moderator between the bottles was also studied. Reference 5 provides the following description of the experimental parameters.

> The ^{233}U was in the form of uranyl nitrate hexahydrate, ... at a concentration of about 330 g ^{233}U/liter; the uranium solution (was about) 0.53M in excess nitrate acid concentration, (and) was contained in three-liter polyethylene bottles.... The bottles were 17.75-in. high and 4.7-in. o.d., with a wall thickness of 0.100 in. The average solution height was about 11.5 in., corresponding to 960 g uranium per bottle.... The bottles varied in (solution) content (which) amounted to less than $\pm$ 20 g ^{233}U/liter.... The bottles were placed in subcritical arrays on a remotely operated split-table device.... (T)he experiments required a series of multiplication measurements...for each spacing.... Criticality of the bottles of solution was determined for both bare and Lucite-reflected systems.... In the reflected arrays, the Lucite was placed touching the outside surface of the bottles, i.e., boxing in the array. The thickness of the top and bottom Lucite reflector was 4.5 in. and the side reflectors were 6 in. Experiments were performed with Lucite moderator positioned between the bottles of an array in both unreflected and reflected assemblies.

Experimental data for the reflected experiments are given in Table C.19. Unreflected experiments were modeled but the calculated k-effectives showed poor agreement with experiments, ranging from 0.90 to 1.06. Since all of the 3019 storage wells are concrete reflected and since Ref. 5 contains no information regarding location of the experiments relative to other structures within the experimental cell or the cell walls, the unreflected experiments were judged to be not applicable to 3019 analyses. Though hydrogen-bearing interstitial materials were present rather than concrete moderation, the reflected arrays were judged applicable to 3019 analyses as they represent the only ^{233}U, interacting array data with interstitial moderation.

Calculated neutronics parameters for the seven experiments are provided in Table C.20. The results for all experiments are generally good. There does not appear to be any correlation with the size of the array. There is an observable trend in k-effective as a function of the thickness of interstitial moderator between the bottles of solution. Relative to the analyses for Building 3019, the results are conservative as calculated k-effective increases as the amount of interstitial moderator increases. Since the pitch of the storage wells is approximately 30 cm (12 in.) extrapolation from these array data would yield a large positive bias for interstitial concrete moderation (momentarily ignoring the significant difference between experimental AGF and the AGF values expected to exist within the facility and concrete versus Lucite comparison). In the subsequent statistical derivation of the subcritical limit for ^{233}U systems, this positive bias will be ignored due to the paucity of experimental data.

Table C.19. Data for Koponen I.D. 1250 experiments

Expt. Number[a]	Solution Height (in.)	^{233}U Conc. (g/L)	Specific Gravity	Array Configuration	Critical surface-to-surface spacing (in.)	Thickness of interstitial Lucite (in.)
1250-6	11.72	326.2	1.450	1 x 3	0.6	—
1250-7	11.71	318.1	1.438	2 x 2	2.18	—
1250-8	11.71	318.1	1.438	2 x 2	2.48	0.5
1250-9	11.71	318.1	1.438	2 x 2	2.58	0.75
1250-10	11.71	318.1	1.438	2 x 2	2.66	1.0
1250-11	11.71	318.1	1.438	2 x 2	2.50	1.5
1250-12	11.64	323.2	1.444	3 x 3	3.98	—

[a]Suffix to 1250-is experiment I.D. in Ref. 5.

Table C.20. Calculated neutronics parameters for Koponen I.D. 1250 experiments

Experiment number	k-effective	One standard deviation for k-effective	Average Energy Group for fission
1250-6	0.9953	0.0042	14.29
1250-7	0.9911	0.0040	14.30
1250-8	1.0046	0.0042	14.39
1250-9	1.0084	0.0040	14.42
1250-10	1.0098	0.0042	14.46
1250-11	1.0168	0.0039	14.49
1250-12	0.9943	0.0040	14.29

C.3 SUBCRITICAL LIMIT FOR ^{233}U SYSTEMS

Calculated k-effectives for the uranium-233 critical experiments are shown in Fig. C.5. The low epithermal and thermal group values are repeated for clarity in Fig. C.6. The results are plotted as a function of average energy group for fission. All of the results are for the CSAS25 module of the NCSS version of the SCALE package and were generated using the Hansen-Roach cross-sections. Each k-effective had a standard deviation of $<= 0.005$.

The validation philosophy presented in Section 3.3.2 of this report was used (in conjunction with the statistical methodology in Ref. 7) to determine a safely subcritical limit for systems containing U-233. K-effective was assumed to be a function of six properties (identified by examination of the 3019 facility) and furthermore that the function which represents k-effective can be defined as the product of six independent functions (separation of variables technique), each of which is dependent on a different physical property.

C.3.1 Fissile Isotope Density Variation

Tables C.10 and C.15 and a comparison of the metal spheres with the dilute nitrate spheres and cylinders reveal that there is no apparent correlation between k-effective and fissile isotope density. No critical experiment data exist at concentrations corresponding to the fissile load limits identified in Table 20 (except for the unrestricted moderation case), however data do exist for some of the nominal loadings identified in Table 3. Interpolation to load limit values is possible and doing so reveals that k-effective has no dependence on fissile isotope density over the range of conditions which are expected to exist in Building 3019.

C.3.2 Physical Form of Fissile Material

The material stored in the 3019 arrays is mostly oxide with small quantities of metal and fluoride. No critical experiments have been conducted with uranium oxide. Some anomalies exist between experiments conducted with uranyl fluoride and uranyl nitrate (see Table C.11) but other nitrate experiments show such a broad variation in k-effective values (see Table C.14) that one cannot conclude that there is any bias due to fuel form. Since the oxygen absorption cross section is small and since there was no identifiable bias due to acid molarity (see Table C.10) - oxygen being present as NO_3 - k-effective is assumed to have no dependence on physical form of material, i.e., non-oxide bearing experiments can be used for validations of oxide material arrays.

C.3.3 Array of Storage Wells Instead of a Single Unit

Section C.2.3 provides data for both single units and arrays when each are filled with approximately the same fissile material. The mean calculated k-effective for the array (reflected) experiments is 0.9753 $\pm$ 0.0048. The mean calculated k-effective for the single unit experiments is 0.9848 $\pm$ 0.0029. The differences between these two means is statistically insignificant. However, to be conservative, k-effective will be assumed to be a step function of array size, i.e., for a single unit the function will be equal to 1.0 but for an array, the value will be 0.99.

C.3.4 Concrete Reflection

None of the ^{233}U critical experiments were conducted with concrete reflectors. However some of the ^{235}U and ^{239}Pu experiments were conducted with concrete. Appendix D provides documentation that k-effective for concrete reflected experiments is different from k-effective for hydrogeneously reflected experiments. The same bias (0.9927) was applied to ^{233}U data. No difference was found for plutonium experiments but to add conservation, the ^{235}U bias was included.

C.3.5 Interstitial Moderation

The 3019 storage arrays are interstitially moderated by concrete. In Section C.3.4, it was shown that the scattering characteristics of concrete can be modeled accurately. Neutron absorption in concrete is generally a function of the water content (ignoring those cases where the aggregate is a neutron absorber) and absorption data for water is well known. Section C.2.5 provides data for varying degrees of moderation between elements of an array. It is seen that increasing the quantity of moderator increases calculated k-effective even though the spectral shift in the configuration is small. A positive trend in k-effective as a function of moderator thickness is identified. This positive bias will not be used in this validation study as the results derived will be conservative and the proper extrapolation from 3.8 cm of Lucite to 30 cm of concrete is not well-defined.

C.3.6 Degree of Moderation in the Fissile Material

The parameter used as a surrogate for degree of moderation is AGF, the average energy group for fission. Figures C.5 and C.6 show all of the ^{233}U critical experiments as a function of AGF. No trends are obvious although the existence of a bias can be observed.

Figure C.7 shows a comparison of the relative number of fissions per energy group for the fastest credible configuration and the "closest" (in terms of AGF) critical experiment. The thermal group (16) ratios agree excellently. While not shown, validation for the fast energy groups is achieved by comparison with critical metal spheres. The low epithermal range (groups 13 and 15) is the major area of uncertainty.

Tables C.10 and C.15 provide information which show that there is no linear correlation between k-effective and AGF. Consequently, all the experiments, except for the array data, were treated as a group. The mean k-effective value was found to be 0.9888 and the confidence band (defined to be the difference between the mean k-effective and the lower bound at which there is a 95% confidence of including 99.9% of the data), calculated according to the procedure given in Ref. 7 was determined to be 0.0563.

C.3.7 Determination of the Safely Subcritical Limit for ^{233}U Systems

Following the separation of variables philosophy, critical k-effective for 3019 storage arrays for U-233 materials is 0.9888 * 0.99 * 0.9927 = 0.9718. Applying the confidence band derived in Section C.3.6, a calculated k-effective for a 3019 configuration plus two standard deviations being less than 0.9155 is considered to be safely subcritical.

C.3 REFERENCES

1. H. C. Paxton, Los Alamos Critical-Mass Data, LA-3067-MS, Rev. (December 1975).

2. J. K. Fox, L. W. Gilley and E. R. Rohrer, *Critical Mass Studies, Part VIII, Aqueous Solutions of ^{233}U,* ORNL-2143 (September 23, 1959).

3. J. T. Thomas, *Critical Experiments with Aqueous Solutions of Uranium-233 $O_2(NO_3)_2$,* ORNL-4280 (1968).

4. R. Gwin and D. W. Magnuson, *Critical Experiments for Reactor Physics Studies,* ORNL-CF-60-40-12 (September 16, 1960).

5. R. C. Lloyd, E. D. Clayton, and J. H. Chalmers, "Criticality of Arrays of ^{233}U Solution," *Nuclear Applications,* Vol. 4, No. 3, pp. 136—141 (March 1968).

6. B. L. Koponen, et. al., Nuclear Criticality Experiments from 1943 to 1978, An Annotated Bibliography, UCRL-52769 (April 1979).

7. H. R. Dyer, W. C. Jordan, V. R. Cain, "A Technique for Code Validation for Criticality Safety Calculations," *Trans. Am. Nucl. Soc.*, Vol. 63, pp. 238—239 (June 1991).

8. W. C. Jordan, N. F. Landers, and L. M. Petrie, "Validation of KENO V.a, Comparison with Critical Experiments," ORNL/CSD/TM-238 (December 1986).

9. R. Gwin and D. W. Magnuson, "The Measurement of Eta and Other Nuclear Properties of U^{233} and U^{235} in Critical Aqueous Solutions," *Nuclear Science and Engineering*, Vol. 12, pp. 364—380 (1962).

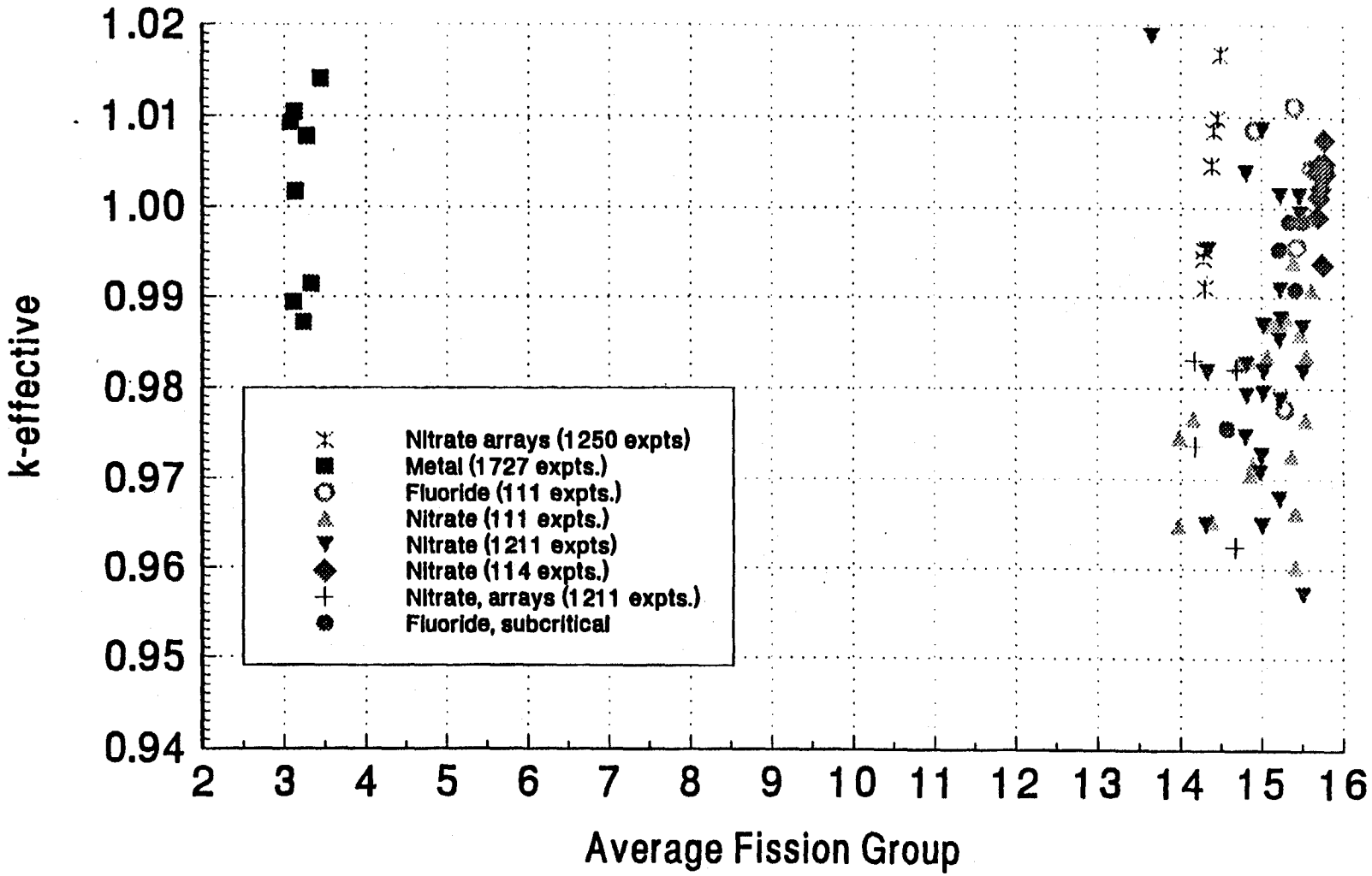

Fig. C.5. U-233 validation studies.

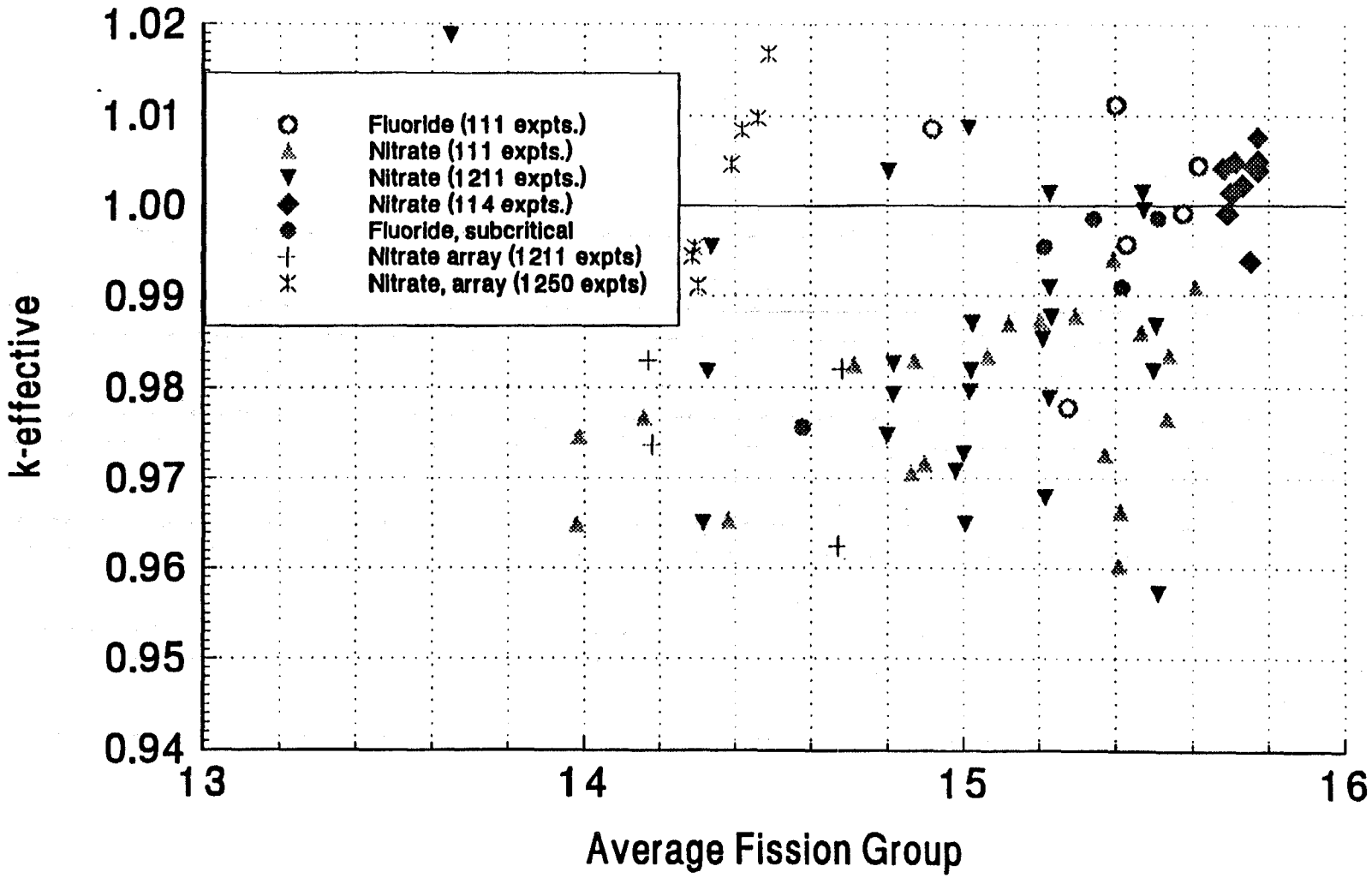

Fig. C.6. U-233 validation studies (thermal range).

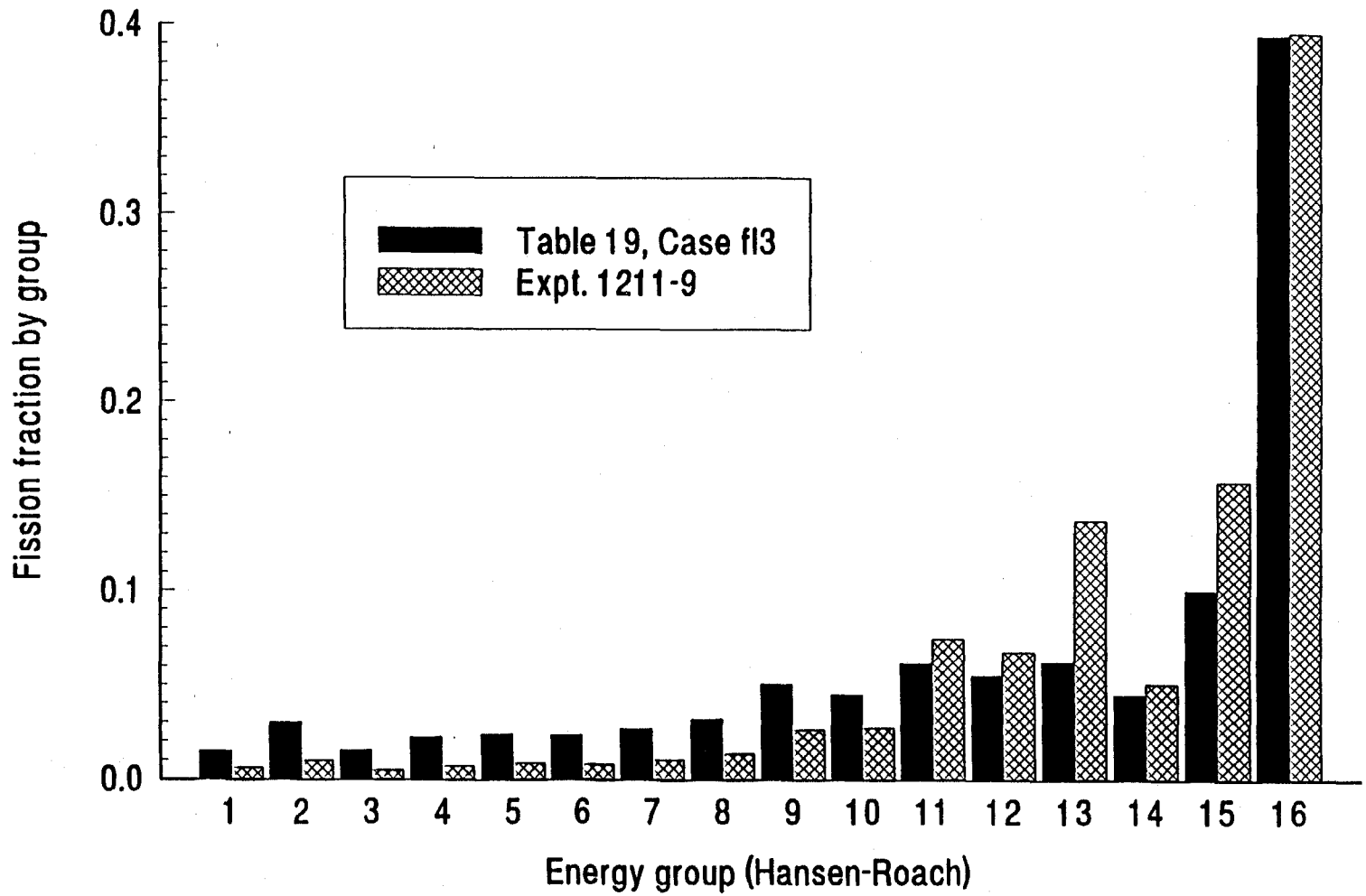

Fig. C.7. Comparison of groupwise fissions for ^{233}U systems.
(Maximum disparity between experiment and configuration)

Appendix D

VALIDATION OF COMPUTER CODES AND CROSS SECTION LIBRARY FOR URANIUM-235 SYSTEMS

Appendix D

VALIDATION OF COMPUTER CODES AND CROSS SECTION LIBRARY FOR URANIUM-235 SYSTEMS

D.1 INTRODUCTION

The calculated parameters for critical experiments performed with Uranium-235 are reported in this appendix. A recent (Ref. 1) validation study using 258 critical experiments serves as the basis for this work. A subset of the 258 experiments is identified which are applicable to conditions expected to exist in the 3019 wells. Only highly enriched fuels are considered. Very low concentration solution experiments are excluded as those concentrations (and associated well-thermalized neutron spectra) do not correspond to either normal or credible abnormal conditions in the facility.

The cases studied here are contained in 15 references[2-16]. The reader is referred to those references for detailed descriptions of the critical experiments. Brief descriptions of the experiments are provided in Table D.1. The Koponen citation number refers to a compilation of critical experiments prepared under the direction of B. L. Koponen, Lawrence Livermore Laboratory (Ref. 17).

Table D.1. Uranium-235 benchmarks

Ref. 1 I.D.	Ref. No.	Koponen citation I.D.	Description
CAA04	2	164-1	fluoride sphere, water ref., H/X=76.1
CAA05	2	164-2	fluoride sphere, water ref., H/X=126.5
CAA12	3	2095-1	bare, nitrate, cylinder, 142.92 g U/l
CAA13	3	2095-2	bare, nitrate, cylinder, 357.71 g U/l
CAA16	3	2095-3	bare, nitrate, cylinder, 357.71 g U/l
CAA18	3	2095-4	concrete ref., nitrate, cyl.
CAA20	3	2095-5	concrete ref., nitrate, cyl.
CAA22	3	2095-6	concrete ref., nitrate, cyl.
CAA24	3	2095-7	plexiglas ref., nitrate, cyl.
CAA26	3	2095-8	plexiglas ref., nitrate, cyl.
CAA28	3	2095-9	plexiglas ref., nitrate, cyl.
CAA30	3	2095-10	concrete ref., 4 x 4 array
CAA32	3	2095-11	concrete ref., 4 x 4 array
CAA34	3	2095-12	concrete ref., 2 x 2 array
CAA35	3	2095-13	concrete ref., 2 x 2 array
CAA36	3	2095-14	concrete ref., 2 x 4 array
CAA38	3	2095-15	plexiglas ref., 4 x 4 array
CAA40	3	2095-16	plexiglas ref., 4 x 4 array
CAA42	3	2095-17	plexiglas ref., 2 x 2 array
CAA43	3	2095-18	plexiglas ref., 3 x 2 array
CAS01	4	324-1	93.8% U metal sphere, unreflected (GODIVA)

Table D.1. Uranium-235 benchmarks

Ref. 1 I.D.	Ref. No.	Koponen citation I.D.	Description
CAS04	5	2004-1	93.2% U-Mo alloy cylinder annulus, unreflected
CAS07	6	1-1	93.5% U metal hemispherical shell, H_2O reflected
CAS08	7	838-1	93.2% U metal cylindrical annulus, graphite reflected
CAS09	6	1-2	94% U metal cuboid, natural U reflected
CAS10	8	653-1	93.1% U metal hemispherical shell, oil reflected
CAS11	8	653-2	93.1% U metal hemispherical shell, steel center and oil reflected
CAS02	9	2086-1	97.67% U metal sphere, H_2O reflected
CAS03	3	2095-18	93.172% $UO_2(NO_3)_2$ solution, 346.7 g U/1, in SS cylinder, unreflected
CAS12	10	801-1	93.2% U metal cylinder annulus, unreflected, smaller U cylinder in hole touching one wall
CAS22	10	801-2	93.2% U metal cylinder annulus, unreflected, smaller U block in hole touching one wall
CAS23	10	801-3	93.2% U metal, unreflected cylinders and cuboids in approximate circular arrangement, cylinder, cuboid, and hemisphere stack in center.
CAS24	11	110-1	93.2% U metal cylinders, 4 × 4 × 4 array, unreflected
CAS25	11	110-2	93.2% U metal cylinders, 2 × 2 × 2 array, each unit in the array is a smaller cylinder capped on each end by a larger cylinder, unreflected
CAS26	11	110-3	93.2% U metal cylinders, 2 × 2 × 2 array, paraffin reflected
CAS27	11	110-4	93.2% U metal cylinders, 2 × 2 × 2 array, each unit in the array is a smaller cylinder capped on each end by a larger cylinder, paraffin reflected
CAS28	11	110-5	93.2% U metal cylinders each in a Plexiglas box, 2 × 2 × 2 array of these units unreflected
CAS29	12	206-1	92.6% $UO_2(NO_3)_2$ solution, 415 g U/1, in Plexiglas cylinders, 3 × 3 × 3 array, unreflected
CAS14	13	1358-1	93.2% $UO_2(NO_3)_2$ solution, 505 g U/1, in SS cylinders, 4 × 4 array, standing in a solution slab, Plexiglas reflected.
CAS15	14	1413-1	93.2% U metal cylinders, 2 × 2 × 2 array, graphite moderated and polyethylene reflected
CAS16	12	206-3	92.6% $UO_2(NO_3)_2$ solution, 415 g U/1, in Plexiglas cylinders, 4 × 4 × 4 array, unreflected
CAS17	12	206-4	92.6% $UO_2(NO_3)_2$ solution, 415 g U/1, in Plexiglas cylinders, 3 × 3 × 3 array, paraffin reflected
CAS18	12	206-5	92.6% $UO_2(NO_3)_2$ solution, 415 g U/1, in Plexiglas cylinders, 3 × 3 × 3 array, paraffin reflected
CAS19	15,16	1744-1	93.1% $UO_2(NO_3)_2$ solution, 450.8 g U/1, in SS containers, square central column with 8 perpendicular cylindrical arms unreflected

Table D.1. Uranium-235 benchmarks

Ref. 1 I.D.	Ref. No.	Koponen citation I.D.	Description
CAS20	3	2095-18	93.17% $UO_2(NO_3)_2$ solution, 355.9 g U/1, in Al cylinders, 4 × 4 array, Plexiglas reflected
CAS21	3	2095-19	93.17% $UO_2(NO_3)_2$ solution, 364.1 g U/1, in Al cylinders, 4 × 4 array, concrete reflected
CAS60	12	206-7	92.6% $UO_2(NO_3)_2$ solution, 279 g U/1, in Plexiglas cylinders, 3 × 3 × 3 array, unreflected, walls, floor, and tank in experiment room included
CAS61	12	206-8	92.6% $UO_2(NO_3)_2$ solution, 279 g U/1, in Plexiglas cylinders, 2 × 2 × 2 array, unreflected, walls, floor, and tank in experiment room included
CAS62	12	206-9	92.6% $UO_2(NO_3)_2$ solution, 415 g U/1, in Plexiglas cylinders, 5 × 5 × 5 array, unreflected, walls, floor, and tank in experiment room included
CAS64	12	206-10	92.6% $UO_2(NO_3)_2$ solution, 415 g U/1, in Plexiglas cylinders, 4 × 4 × 4 array, unreflected, walls, floor, and tank in experiment room included
CAS63	12	206-11	92.6% $UO_2(NO_3)_2$ solution, 415 g U/1, in Plexiglas cylinders, 3 × 3 × 3 array, unreflected, walls, floor, and tank in experiment room included
CAS65	12	206-12	92.6% $UO_2(NO_3)_2$ solution, 415 g U/1, in Plexiglas cylinders, 2 × 2 × 2 array, unreflected, walls, floor, and tank in experiment room included
CAS90	12	206-13	92.6% $UO_2(NO_3)_2$ solution, 415 g U/1, in Plexiglas cylinders, 3 × 3 × 3 array, unreflected, 279 g U/1 in 5 central units, walls, floor, and tank in experiment room included
CAS66	12	206-14	92.6% $UO_2(NO_3)_2$ solution, 415 g U/1, in Plexiglas cylinders, 3 × 3 × 3 array, reflected, 15.24 cm paraffin on bottom, 1.27 cm Plexiglas on other faces
CAS67	12	206-15	92.6% $UO_2(NO_3)_2$ solution, 415 g U/1, in Plexiglas cylinders, 3 × 3 × 3 array, reflected, 15.24 cm paraffin on bottom, 2.54 cm Plexiglas on other faces
CAS68	12	206-17	92.6% $UO_2(NO_3)_2$ solution, 415 g U/1, in Plexiglas cylinders, 3 × 3 × 3 array, reflected, 15.24 cm paraffin on bottom, 1.27 cm Plexiglas on other faces
CAS69	12	206-18	92.6% $UO_2(NO_3)_2$ solution, 415 g U/1, in Plexiglas cylinders, 3 × 3 × 3 array, reflected, 15.24 cm paraffin on 5 faces, 15.24 cm Plexiglas on 1 face
CAS70	12	206-19	92.6% $UO_2(NO_3)_2$ solution, 415 g U/1, in Plexiglas cylinders, 3 × 3 × 3 array, reflected, 15.24 cm paraffin on bottom, 3.81 cm paraffin on other faces
CAS71	12	206-20	92.6% $UO_2(NO_3)_2$ solution, 415 g U/1, in Plexiglas cylinders, 3 × 3 × 3 array, reflected, 15.24 cm paraffin on bottom, 7.62 cm paraffin on other faces
CAS72	12	206-21	92.6% $UO_2(NO_3)_2$ solution, 415 g U/1, in Plexiglas cylinders, 3 × 3 × 3 array, reflected, 1.27 cm Plexiglas on other faces

Table D.1. Uranium-235 benchmarks

Ref. 1 I.D.	Ref. No.	Koponen citation I.D.	Description
CAS73	12	206-22	92.6% $UO_2(NO_3)_2$ solution, 415 g U/1, in Plexiglas cylinders, 3 × 3 × 3 array, reflected, 1.27 cm paraffin on all faces
CAS74	12	206-23	92.6% $UO_2(NO_3)_2$ solution, 415 g U/1, in Plexiglas cylinders, 3 × 3 × 3 array, reflected, 15.24 cm paraffin on all faces
CAS75	12	206-24	92.6% $UO_2(NO_3)_2$ solution, 415 g U/1, in Plexiglas cylinders, 3 × 3 × 3 array, reflected, 3.81 cm paraffin on all faces
CAS76	12	206-25	92.6% $UO_2(NO_3)_2$ solution, 415 g U/1, in Plexiglas cylinders, 2 × 2 × 2 array, reflected, 15.24 cm paraffin on bottom, 1.27 cm Plexiglas on other faces
CAS77	12	206-26	92.6% $UO_2(NO_3)_2$ solution, 415 g U/1, in Plexiglas cylinders, 2 × 2 × 2 array, reflected, 15.24 cm paraffin on bottom, 11.43 cm Plexiglas on other faces
CAS78	12	206-27	92.6% $UO_2(NO_3)_2$ solution, 415 g U/1, in Plexiglas cylinders, 2 × 2 × 2 array, reflected, 15.24 cm paraffin on bottom, 15.24 cm Plexiglas on other faces
CAS79	12	206-28	92.6% $UO_2(NO_3)_2$ solution, 415 g U/1, in Plexiglas cylinders, 2 × 2 × 2 array, reflected, 15.24 cm paraffin on bottom, 2.54 cm Plexiglas on other faces
CAS80	12	206-29	92.6% $UO_2(NO_3)_2$ solution, 415 g U/1, in Plexiglas cylinders, 2 × 2 × 2 array, reflected, 15.24 cm paraffin on bottom, 4.45 cm Plexiglas on other faces
CAS81	12	206-30	92.6% $UO_2(NO_3)_2$ solution, 415 g U/1, in Plexiglas cylinders, 2 × 2 × 2 array, reflected, 15.24 cm paraffin on bottom, 6.35 cm Plexiglas on other faces
CAS82	12	206-31	92.6% $UO_2(NO_3)_2$ solution, 415 g U/1, in Plexiglas cylinders, 2 × 2 × 2 array, reflected, 15.24 cm paraffin on bottom, 1.27 cm Plexiglas on other faces
CAS83	12	206-32	92.6% $UO_2(NO_3)_2$ solution, 415 g U/1, in Plexiglas cylinders, 2 × 2 × 2 array, reflected, 15.24 cm paraffin on bottom, 3.81 cm Plexiglas on other faces
CAS84	12	206-33	92.6% $UO_2(NO_3)_2$ solution, 415 g U/1, in Plexiglas cylinders, 2 × 2 × 2 array, reflected, 15.24 cm paraffin on bottom, 3.81 cm Plexiglas on other faces
CAS85	12	206-34	92.6% $UO_2(NO_3)_2$ solution, 415 g U/1, in Plexiglas cylinders, 2 × 2 × 2 array, reflected, 1.27 cm Plexiglas all faces
CAS86	12	206-35	92.6% $UO_2(NO_3)_2$ solution, 415 g U/1, in Plexiglas cylinders, 2 × 2 × 2 array, reflected, 1.27 cm paraffin all faces
CAS87	12	206-36	92.6% $UO_2(NO_3)_2$ solution, 415 g U/1, in Plexiglas cylinders, 2 × 2 × 2 array, reflected, 15.24 cm paraffin all faces
CAS88	12	206-37	92.6% $UO_2(NO_3)_2$ solution, 415 g U/1, in Plexiglas cylinders, 2 × 2 × 2 array, reflected, 3.81 cm paraffin all faces
CAS89	12	206-38	92.6% $UO_2(NO_3)_2$ solution, 415 g U/1, in Plexiglas cylinders, 2 × 2 × 2 array, reflected, 7.62 cm paraffin all faces

D.2 CALCULATED NEUTRONICS PARAMETERS

Calculated k-effectives as a function of average energy group causing fission for the ^{235}U-bearing critical experiments are shown in Fig. D.1. The results are given in Table D.2. All of the results are for the CSAS25 module of the NCSS version of the SCALE package and were generated using the Hansen-Roach cross-sections. The mean value of k-effective for all of the experiments was 0.9948 ± 0.0016.

Table D.2. Calculated results for ^{235}U experiments

Ref. 1 I.D.	Koponen citation I.D.	Average energy group for fission	k-effective	One standard deviation for k-effective
CAA04	164-1	14.79	0.99009	0.00394
CAA05	164-2	15.18	0.98264	0.00438
CAA12	2095-1	15.25	0.98307	0.00381
CAA13	2095-2	14.33	0.98335	0.00324
CAA16	2095-3	14.33	0.97797	0.00427
CAA18	2095-4	14.46	0.98572	0.00345
CAA20	2095-5	14.46	0.98923	0.00394
CAA22	2095-6	14.51	0.98082	0.00412
CAA30	2095-10	14.51	0.98829	0.00420
CAA32	2095-11	14.52	0.98308	0.00406
CAA34	2095-12	14.40	0.98156	0.00338
CAA35	2095-13	14.49	0.98183	0.00396
CAA36	2095-14	14.49	0.98848	0.00371
CAS01	324-1	3.34	0.99740	0.00329
CAS02	2086-1	5.84	0.99895	0.00311
CAS03	2095-18	14.39	0.98457	0.00462
CAS04	2004-1	3.38	0.99700	0.00300
CAS07	1-1	7.99	1.01388	0.00292
CAS08	838-1	4.53	1.01001	0.00323
CAS09	1-2	3.34	0.99991	0.00261
CAS10	653-1	7.16	1.01524	0.00356
CAS11	653-2	6.41	0.99810	0.00368
CAS12	801-1	3.33	0.99865	0.00304
CAS14	1358-1	14.14	1.03091	0.00394
CAS15	1413-1	5.60	1.01896	0.00302
CAS16	206-3	14.24	0.95988	0.00397
CAS17	206-4	14.60	1.00829	0.00356
CAS18	206-5	14.33	0.98510	0.00371
CAS19	1744-1	13.95	1.00939	0.00512
CAS20	2095-18	14.65	1.01862	0.00366
CAS21	2095-19	14.51	1.00981	0.00371
CAS22	801-2	3.34	1.00142	0.00319
CAS23	801-3	3.32	0.99417	0.00328
CAS24	110-1	3.32	0.98293	0.00312

Table D.2. Calculated results for ^{235}U experiments

Ref. 1 I.D.	Koponen citation I.D.	Average energy group for fission	k-effective	One standard deviation for k-effective
CAS25	110-2	3.32	0.99528	0.00294
CAS26	110-3	6.76	1.00397	0.00333
CAS27	110-4	6.89	1.00704	0.00328
CAS28	110-5	5.28	1.00278	0.00304
CAS29	206-1	14.26	0.97716	0.00429
CAS60	206-7	14.76	0.98238	0.00410
CAS61	206-8	14.78	0.98402	0.00439
CAS62	206-9	14.27	0.98169	0.00400
CAS63	206-11	14.26	0.98850	0.00370
CAS64	206-10	14.26	0.97966	0.00398
CAS65	206-12	14.28	0.98144	0.00356
CAS66	206-14	14.37	0.98964	0.00420
CAS67	206-15	14.45	0.99713	0.00426
CAS68	206-17	14.40	0.98719	0.00410
CAS69	206-18	14.59	1.00692	0.00359
CAS70	206-19	14.54	1.00237	0.00415
CAS71	206-20	14.60	1.01192	0.00420
CAS72	206-21	14.33	0.99009	0.00441
CAS73	206-22	14.35	0.98673	0.00379
CAS74	206-23	14.60	1.01704	0.00458
CAS75	206-24	14.54	1.00655	0.00425
CAS76	206-25	14.38	0.98616	0.00453
CAS77	206-26	14.61	1.01711	0.00388
CAS78	206-27	14.60	1.00887	0.00414
CAS79	206-28	14.44	0.98879	0.00435
CAS80	206-29	14.53	0.99556	0.00430
CAS81	206-30	14.58	1.00845	0.00371
CAS82	206-31	14.42	0.99273	0.00394
CAS83	206-32	14.55	1.00215	0.00398
CAS84	206-33	14.60	0.99691	0.00412
CAS85	206-34	14.34	0.98261	0.00385
CAS86	206-35	14.38	0.98698	0.00463
CAS87	206-36	14.60	0.99692	0.00439
CAS88	206-37	14.54	1.00468	0.00421
CAS89	206-38	14.60	1.00608	0.00366
CAS90	206-13	14.40	0.98043	0.00414

D.3 DERIVATION OF SUBCRITICAL LIMIT

The same limit derivation procedure was followed for U-235 systems as was followed for U-233 systems in Appendix C. That is, k-effective is assumed to be the product of six functions, each of which is dependent on a single physical property associated with the 3019 storage wells.

D.3.1 Density of Fissile Isotope

A test was performed to correlate uranium density with k-effective. The Pearson correlation coefficient for these two parameters was calculated to be 0.28319 with a confidence statistic of 0.0175. Thus, k-effective does not have a linear correlation with fissile density. No bias was attributed to density of U-235 in the critical experiment.

D.3.2 Physical Form of Fissile Material

Critical experiments were grouped according to the physical form of the fissile material and mean values of k-effectives were calculated. The results are shown in Table D.3.

Table D.3. Correlation of k-effective value to physical form of U-235 bearing material

Form	Mean k-effective	Std. error of mean
metal	1.0024	0.0023
nitrate	0.9933	0.0019
fluoride	0.9862	0.0037

There is a bias in calculated k-effective according to the physical form of the fissile material used in the critical experiment. Unfortunately, none of the experiments were conducted with uranium oxide which is the form of the material in the 3019 storage wells. Both uranyl nitrate and uranyl fluoride contain oxygen, but nitrogen and fluorine are better neutron absorbers. Based on the fact that there were 51 nitrate experiments and only 2 fluoride experiments and given the results of the studies in Appendix C, no bias was attributed to fuel form.

D.3.3 Array of Cylinders Versus Single Element

A considerable number of critical array experiments were calculated. The mean value of k-effective for array experiments was 0.9955 $\pm$ 0.0020. The mean value of k-effective for single element experiments was 0.9923 $\pm$ 0.0028. Thus no bias was found and array and single element experiment k-effectives were treated as if they were from a single distribution.

D.3.4 Concrete Reflection

Nine different conditions of reflection were present in the ^{235}U database. Mean values of k-effective for the conditions of reflection were calculated and reported in Table D.4. Note that the mean for the concrete reflected experiments was somewhat lower than the mean for all of the ^{235}U experiments. Consequently, a bias of 0.9876/0.9948 = 0.9927 was applied to the mean k-effective value for the set of ^{235}U experiments. This procedure is slightly conservative as the concrete reflected experiments were included in determining the mean of the set of ^{235}U experiments.

Table D.4. Correlation of k-effective and reflection condition

Reflector type	Mean k-effective	Std. error of mean	No. of observations
none	0.9869	0.0024	22
carbon	1.0100	-	1
concrete	0.9876	0.0030	9
water	0.9946	0.0067	4
oil	1.0065	0.0086	2
paraffin	1.0034	0.0024	13
plexiglas	0.9984	0.0033	17
polyethylene	1.0190	-	1
uranium-238	0.9999	-	1

D.3.5 Interstitial Array Moderation

Only one array experiment had interstitial moderation. Experiment 1413-1 (CAS15) was conducted with interstitial graphite moderation and had a polyethylene reflector. The calculated k-effective was 1.01896. This single data point supports the conclusion reached in Appendix C, that being that interstitial moderation increases the calculated value of k-effective relative to single element experiments and relative to arrays with no interstitial moderation. No credit was taken for this positive bias in establishing the subcritical limit for ^{235}U systems.

D.3.6 Variation in Degree of Moderation within Fissile Material

The AGF parameter is used as a surrogate for the variation in moderation due to varying the hydrogen content. The Pearson correlation coefficient for k-effective and AGF was calculated to be -0.23530 with a confidence statistic of 0.0499. Thus there is no linear correlation between k-effective and AGF. Inspection of Fig. D.1 does not reveal any other obvious functional correlation.

Figure D.2 shows a comparison of the relative number of fissions per energy group for the fastest credible configuration and the "closest" (in terms of AGF) critical experiments. The AGF values for these experiments "bracket" the value for the fastest credible configuration. These critical experiments, when treated as a pair, provide a good match to the fission distribution present in the 3019 configuration. Even though the ^{235}U critical experiment database does not contain entries with AGF values matching the 3019 configuration, the qualitative comparison in Fig. D.2 yields confidence that the database is adequate.

All of the critical experiments were treated as a group and a 95% confidence limit for 99.9% of the data was calculated. This confidence band was determined to be (0.9948 - 0.9458) = 0.0490.

D.3.7 Determination of Subcritical Limit

The mean value of k-effective for all of the critical experiments was adjusted using the concrete bias. The confidence band was then subtracted from this value to obtain a subcritical limit of 0.9948 * 0.9927 - 0.0490 = 0.9385. Calculated k-effective for any 3019 configuration plus two standard deviations should be less than this value.

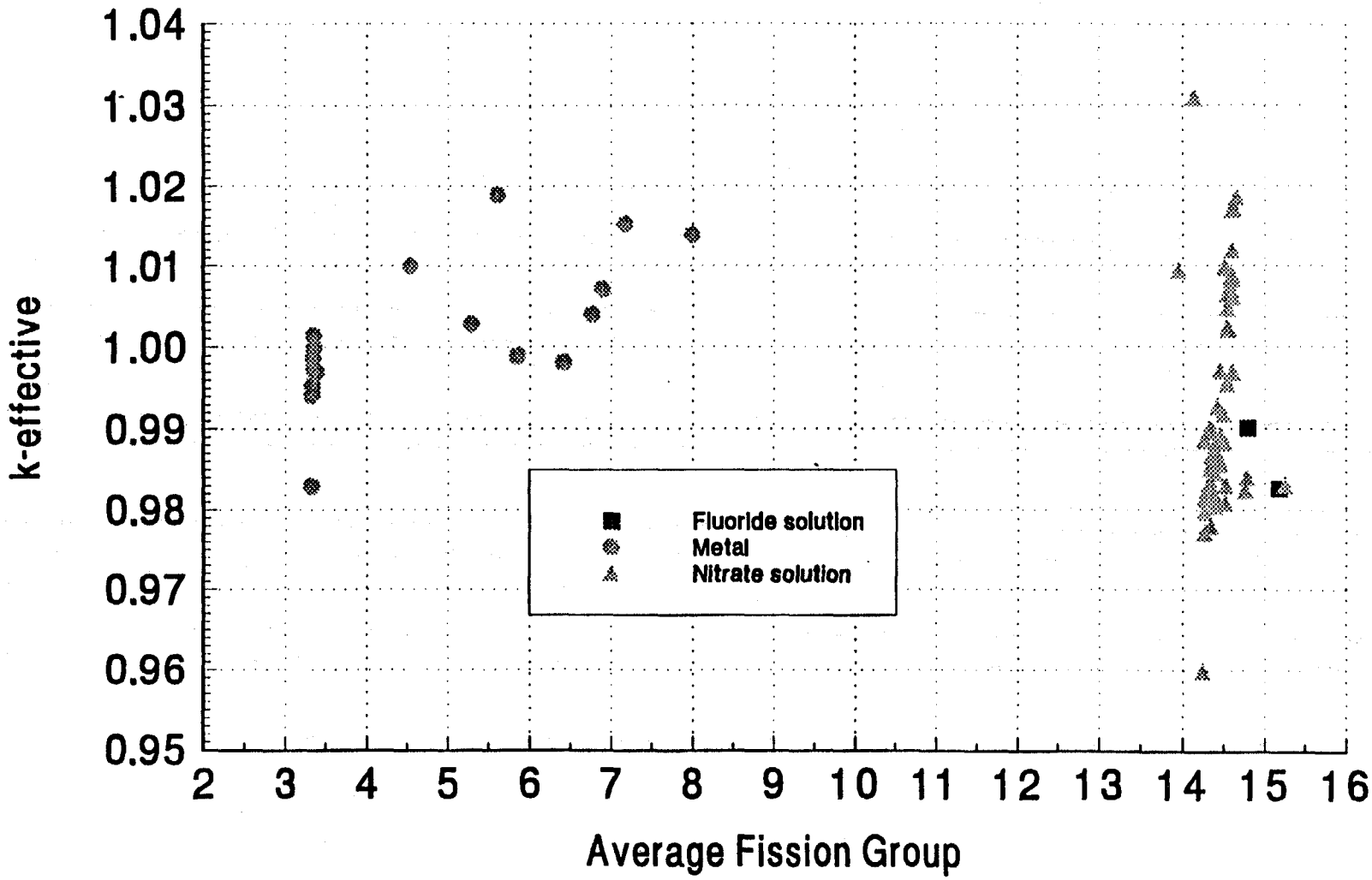

Fig. D.1. U-235 validation studies (KENO-Va, Hansen-Roach).

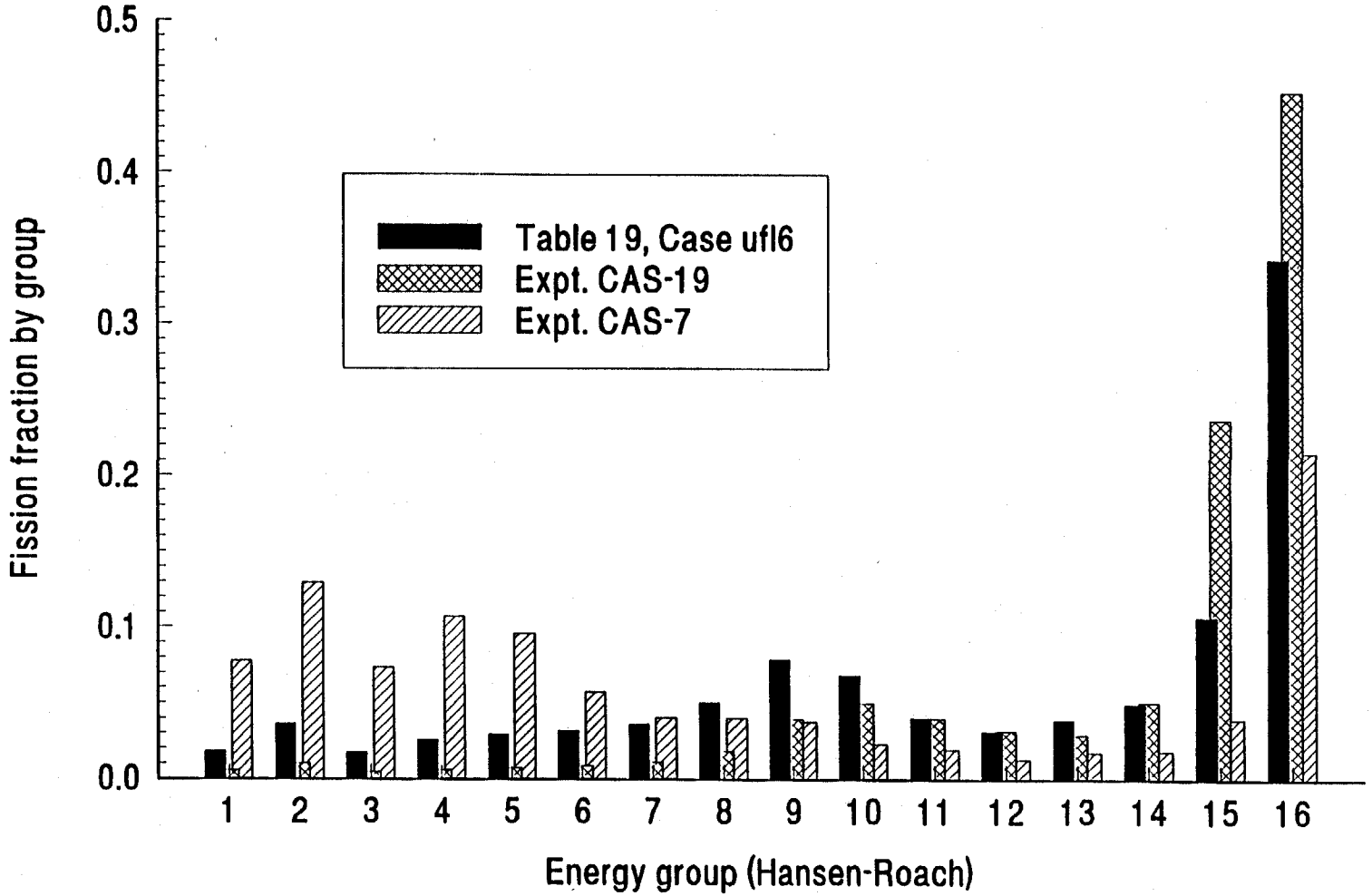

Fig. D.2. Comparison of groupwise fissions for ^{235}U systems.
(Maximum disparity between experiment and configurations)

D.4 REFERENCES

1. W. C. Jordan, N. F. Landers, L. M. Petrie, *Validation of KENO V.a, Comparison with Critical Experiments*, ORNL/CSD/TM-238 (December 1986).

2. J. K. Fox, "Critical Parameters of Uranium Solutions in Simple Geometry," p. 42 in *Neutron Physics Division Annual Progress Report for Period Ending September 1, 1958*, ORNL-2609, Union Carbide Corporation, Nuclear Division, Oak Ridge National Laboratory (1958).

3. R. E. Rothe, *Benchmark Critical Experiments on High Enriched Uranyl Nitrate Solution Systems*, NUREG/CR-0041, RFP-2710, U. S. Nuclear Regulatory Commission (1978).

4. G. E. Hanson, "Properties of Elementary Fast Neutron Critical Assemblies," p. 84 in *Proceedings of the Second United Nations International Conference on Peaceful Uses of Atomic Energy*, Vol. 12, Geneva (1958).

5. J. T. Mihalczo and W. E. Kinney, *Trans. Am. Nucl. Soc.*, Vol. 4, p. 302 (1961).

6. H. C. Paxton, *Los Alamos Critical Mass Data*, LAMS-3067, Los Alamos National Laboratory, Los Alamos, New Mexico (1964).

7. J. T. Mihalczo, *Trans. Am. Nucl. Soc.*, Vol. 8, p. 442 (1965).

8. G. Tuck, "Critical Masses of Spherical and Hemispherical Enriched Uranium Assemblies," *J. Nucl. Energy*, Vol. 23, p. 663 (1969).

9. C. C. Byers, J. J. Koelling, G. E. Hansen, D. R. Smith, and H. R. Dyer, "Critical Measurements of a Water-Reflected Enriched Uranium Sphere," *Trans. Am. Nucl. Soc.*, Vol. 27, p. 412 (1977).

10. D. C. Irving and J. T. Mihalczo, *Trans. Am. Nucl. Soc.*, Vol. 7, p. 287 (1964).

11. J. T. Thomas, *Critical Three-Dimensional Arrays of Neutron-Interacting Units, Part II - U(93.2) Metal*, ORNL-TM-868, Union Carbide Corporation, Nuclear Division, Oak Ridge National Laboratory (1964).

12. J. T. Thomas, *Critical Three-Dimensional Arrays of Neutron-Interacting Units*, ORNL-TM-719, Union Carbide Corporation, Nuclear Division, Oak Ridge National Laboratory (1963).

13. G. Tuck and H. E. Clark, "Critical Parameters of a Uranium Solution Slab-Cylinder System," *Nucl. Sci. Eng.*, Vol. 40, p. 407-413 (1970).

14. E. C. Crume and J. T. Thomas, *Critical and Near Critical Graphite Moderated Arrays of U(93.2) Cylinders*, Y-DD-32, Union Carbide Corporation, Nuclear Division, Oak Ridge Y-12 Plant (1969).

15. B. B. Ernst and C. L. Schuske, *Empirical Method for Calculating Pipe Intersections Containing Fissile Solution*, RFP-1197, Rockwell International, Rocky Flats, Golden, Colorado (1968).

16. D. Dickinson and C. L. Schuske, "An Empirical Model for Safe Pipe Interactions Containing Fissile Solution," *Nucl. Tech.*, Vol. 10, p. 179-187 (1971).

D.3 REFERENCES (cont'd)

17. B. L. Koponen, et. al., Nuclear Criticality Experiments from 1943 to 1978, An Annotated Bibliography, UCRL-52769 (April 1979).

18. H. R. Dyer, W. C. Jordan, V. R. Cain, "A Technique for Code Validation for Criticality Safety Calculations," *Trans. Am. Nucl. Soc.*, Vol. 63, pp. 238-239 (June 1991).

Appendix E

VALIDATION OF COMPUTER CODES AND CROSS SECTION LIBRARY FOR PLUTONIUM SYSTEMS

Appendix E

VALIDATION OF COMPUTER CODES AND CROSS SECTION LIBRARY FOR PLUTONIUM SYSTEMS

E.1 INTRODUCTION

The calculated parameters for critical experiments performed with plutonium fuels are reported in this appendix. The plutonium database is extensive and the cases studied here are those which were selected for publication in three reports.[1–3] Reference 1 notes the following criteria for experiment selection.

> The first criterion for the plutonium systems is to cover a wide range of H/Pu ratios. A wide range of H/Pu ratios implies a wide variation in the neutron spectrum which will emphasize the energy dependence of the neutron cross sections. The second criterion is to cover a range of ^{240}Pu contents.... A third criterion is to minimize leakage, because the leakage calculation introduces another uncertainty into the analysis.... Unreflected systems were chosen wherever possible because the reflector perturbs the neutron flux spectrum and adds an uncertainty to the calculation.... (W)here more than one experiment is available for a given H/Pu ratio and ^{240}Pu content, the most recent experiment was selected for benchmark purposes because we deemed the more recent experiments to be the most reliable data.

The reader is referred to Refs. 1—3 for detailed descriptions of the critical experiments. Brief descriptions of the experiments are provided in Tables E.1 and E.2. The Koponen citation number refers to a compilation of critical experiments prepared under the direction of B. L. Koponen, Lawrence Livermore Laboratory.[4] Reference 1 is assigned the I.D. of 2110, Ref. 2 is 2109 and Ref. 3 is 1727.

E.2 CALCULATED NEUTRONICS PARAMETERS

Calculated k-effectives, as a function of average energy group causing fission, for the plutonium critical experiments are shown in Fig. E.1. All of the results are for the CSAS25 module of the NCSS version of the SCALE package and were generated using the Hansen-Roach cross-sections. The values plotted in Fig. E.1 are tabulated in Table E.3. The mean value of all k-effectives for these experiments was 1.018826 ± 0.000897.

Table E.1. Plutonium benchmarks

Koponen citation IDs	ID number source reference	Description
2110-1	1	Infinite system of ^{239}Pu and water
2110-2	2	Solution with high Pu content
2110-3	3	Solution with low Pu content
2110-4	4	Solution with low Pu content
2110-5,6	5	Polystyrene compacts with low ^{240}Pu
2110-34	6	Metal with low ^{240}Pu, Jezebel expts.
2110-7	7	Solution with intermediate Pu content
2110-8 to 2110-13	9	Polystyrene compact with high ^{240}Pu
2110-14	10	Solution with low Pu content
2110-15 to 2110-22	11	Polystyrene compact with very little H
2110-23 to 2110-28	12	Polystyrene compact with high ^{240}Pu
2110-35	13	Metal with high ^{240}Pu
2110-29	14	Solution with very high ^{240}Pu
2110-30, 31	15a	Solution with stainless steel shell
2110-32, 33	15b	Solution with extra stainless steel shell
2109-20	20	Solution with 25.4 cm concrete ref.
2109-21	21	Solution with 10.16 cm concrete ref.
2109-22	22	Solution with 10.16 cm concrete ref.
2109-23	23	Solution with Cd shell and 10.16 cm concrete ref.
2109-24	24	Solution with Cd shell and 32 cm water ref.
2109-25	25	Metal with natural U ref.
1727-09	IIIA1-13	Metal with natural U ref.
1727-10	VA-1	Metal with no ref.

E.3 DETERMINATION OF SUBCRITICAL LIMIT

The procedure used to derive the subcritical limit for plutonium systems was the same as that used for ^{233}U and ^{235}U systems in Appendices C and D, respectively. The physical properties present in the 3019 storage arrays were used as a basis for testing for trends or biases in calculated k-effectives.

E.3.1 Plutonium-240 Content

Contrary to the ^{233}U and ^{235}U data, the plutonium isotopics varied significantly from experiment to experiment (^{240}Pu content ranged from essentially zero to 43%). The data were examined to determine if k-effective could be correlated with ^{240}Pu content. The Pearson correlation coefficient was computed and the value was 0.28712 with a confidence statistic of 0.0805. There appears to be no trend in calculated k-effective due to the varying ^{240}Pu content in the critical experiments.

E.3.2 Density of Fissile Isotope

Since the load limits derived in this report span a range of concentrations, the critical experiment data were examined for trends in calculated k-effective due to varying Pu density. The Pearson correlation coefficient for k-effective and plutonium density was -0.25922 with a confidence statistic of 0.1161. Though some scatter in the data apparently exist, there is no reason to expect a trend in calculated k-effective due to varying the plutonium density.

E.3.3 Physical Form of Fissile Material

Nineteen of the plutonium experiments were conducted with plutonium oxide. The mean k-effective value for the oxide experiments, 1.0284, was somewhat higher than the mean for all of the experiments, 1.0188. This bias was not applied leading to a conservative safety margin. The non-oxide experiments were not excluded from the database as they provided data for various moderation ratios not found in the oxide critical experiments.

E.3.4 Array Geometry versus Single Element

No array experiments were available in the plutonium database. Based on the results presented in Appendix C, no bias was applied due to the 3019 configurations being arrays rather than single elements.

E.3.5 Concrete Reflection

Concrete reflected experiments calculated slightly higher than water reflected experiments, 1.019 versus 1.003. This bias was not incorporated into the safety margin. Consequently the inclusion of non-concrete reflected experiments resulted in a conservative safety margin.

E.3.6 Interstitial Moderation

No array experiments were available in the plutonium database. Based on the results presented in Appendix C, no bias was applied due to the 3019 configurations being arrays with interstitial concrete moderation.

E.3.7 Variation in Degree of Moderation of Fissile Material

The average energy group for fission was used as a surrogate for examining changes in k-effective due to changes in moderation within the fissile material. The Pearson correlation coefficient for k-effective and AGF was computed to be -0.07830 with a confidence statistic of 0.6403. Examining Fig. E.1, the poor confidence statistic is understandable. It is possible that a second order polynomial could be fitted to the k-effective calculations. Nevertheless, considering the range of AGF values expected to exist in 3019 storage configurations, a simple average of the calculations would be more conservative than a second-order fit.

The statistical methodology discussed in Ref. 5 was used to determine a confidence band for the data. The value corresponding to a 95% confidence limit on 99.9% of the data was (1.0188 - 0.9623) = 0.0565.

E.3.8 Derivation of Subcritical Limit

No bias are determined for any of the physical properties associated with 3019 well storage. Consequently, a calculated k-effective plus two standard deviations being less than 0.962 is considered to be safely subcritical.

Table E.2. Characteristics of critical experiments

Koponen citation ID no.[a]	H/Pu atom ratio	% ^{240}Pu ratio	Pu density (g/cm**3)	Geometry	Reflector
2110-1	3695	0	0.007	Infinite	None
2110-2	125	5	0.172	Sphere	None
2110-3	980	1	0.026	Sphere	30 cm water
2110-4	758	5	0.034	Sphere	6.6 mm steel
2110-5	15	2	1.12	Parallelpiped	None
2110-6	15	2	1.12	Parallelpiped	Plexiglas
2110-34	0	5	15.6	Sphere	None
2110-7	422	5	0.058	Slab	None
2110-8	50	18	0.37	Parallelpiped	None
2110-9,13	50	18	0.37	Parallelpiped	Plexiglas
2110-14	210	8	0.116	Cylinder	20 cm water
2110-15,16	0	18	5.8	Parallelpiped	None
2110-17,22	0	18	5.8	Parallelpiped	Plexiglas
2110-23	5	11	2.3	Parallelpiped	None
2110-24,28	5	11	2.3	Parallelpiped	Plexiglas
2110-35	0	20	15.7	Sphere	None
2110-29	623	43	0.041	Cylinder	20 cm water
2110-30,31	1067	4.6	0.024	Sphere	20 cm water
2110-32,33	1031	4.6	0.025	Sphere	2 mm steel + 20 cm water
2109-20	684	4.6	0.036	sphere	25.4 cm concrete
2109-21	684	4.6	0.0355	sphere	10.16 cm concrete
2109-22	496	4.6	0.0452	sphere	10.16 cm concrete
2109-23	454	4.6	0.0509	sphere	0.762 mm Cd + 10.16 cm concrete
2109-24	540	4.6	0.0469	sphere	0.762 mm Cd + 32 cm water
2109-25	0	4.8	15.375	sphere	19.6 cm natural U
1727-09	0	5.5	19.74	cylinder	water
1727-10	0	4.9	15.62	sphere	none

[a] Comma denotes inclusive, i.e., 17,22 means experiments 17 through 22.

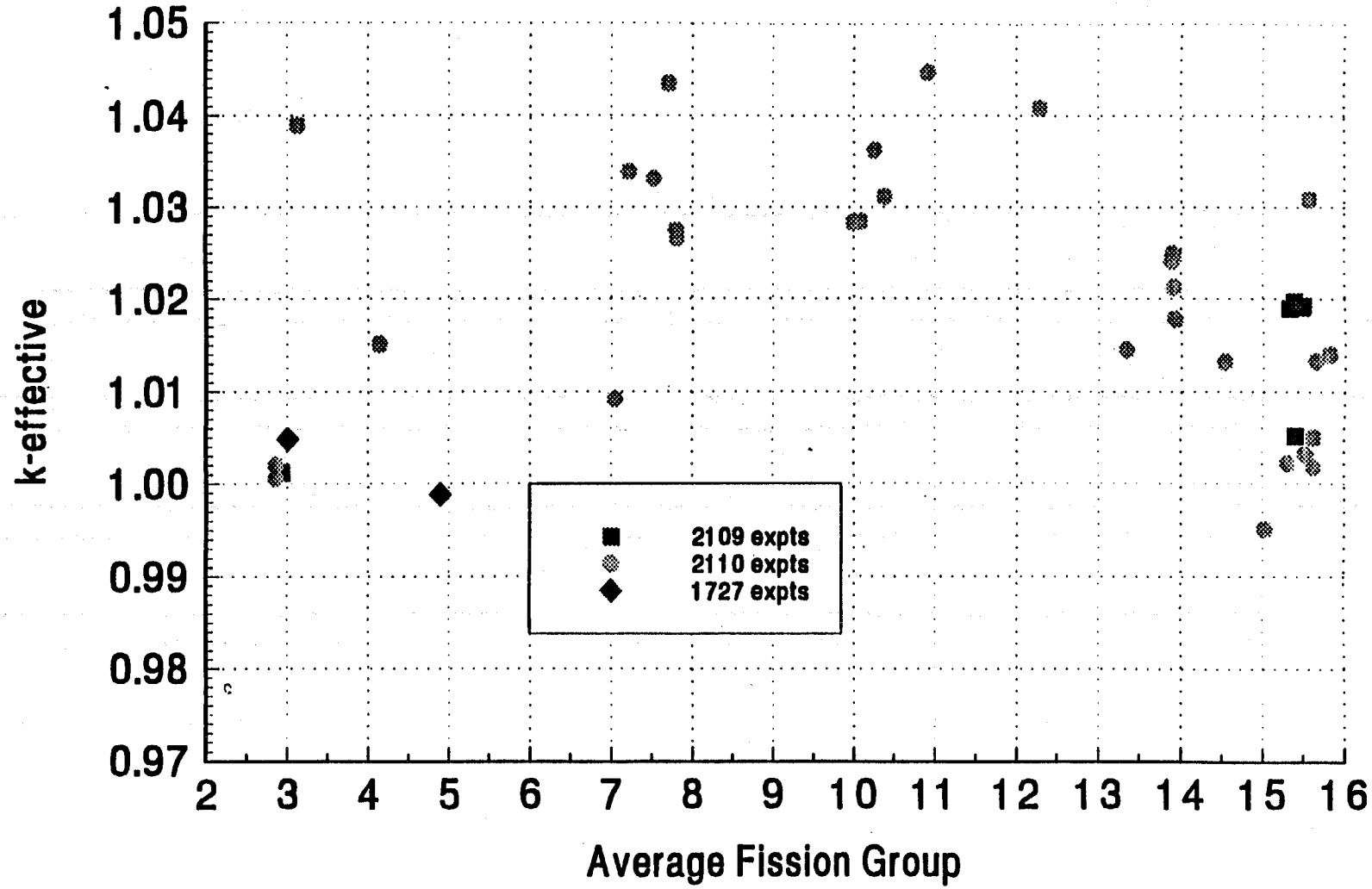

Fig. E.1. Pu validation studies (KENO-Va, Hansen-Roach).

Table E.3. Calculated results for Pu experiments

Koponen I.D.	Average energy group for fission	k-effective	One standard deviation for k-effective
2110_01	15.8141	1.01379	0.00121
2110_02	14.5266	1.01318	0.00413
2110_03	15.6204	1.00177	0.00335
2110_04	15.5240	1.00310	0.00568
2110_05	10.9156	1.04474	0.00567
2110_06	12.2897	1.04084	0.00522
2110_07	15.3083	1.00217	0.00350
2110_08	13.3357	1.01445	0.00449
2110_09	13.8822	1.02410	0.00423
2110_10	13.9067	1.02494	0.00495
2110_11	13.9159	1.02123	0.00435
2110_12	13.9278	1.01776	0.00540
2110_13	2.85431	1.00058	0.00407
2110_14	15.0225	0.99508	0.00493
2110_15	4.13615	1.01508	0.00577
2110_16	3.12138	1.03893	0.00472
2110_17	7.79590	1.02746	0.00330
2110_18	7.21474	1.03386	0.00362
2110_19	7.03649	1.00919	0.00341
2110_20	7.52232	1.03312	0.00521
2110_21	7.71081	1.04350	0.00348
2110_23	7.81691	1.02665	0.00460
2110_24	9.99949	1.02830	0.00326
2110_25	10.0796	1.02842	0.00357
2110_26	10.2562	1.03617	0.00339
2110_27	10.3766	1.03116	0.00327
2110_29	15.5700	1.03084	0.00323
2110_30	15.6421	1.01325	0.00483
2110_32	15.6269	1.00497	0.00489
2110_34	2.85706	1.00208	0.00396
2109_20	15.4829	1.01901	0.00340
2109_21	15.5007	1.01925	0.00322
2109_22	15.3919	1.01970	0.00325
2109_23	15.3304	1.01894	0.00343
2109_24	15.4068	1.00518	0.00381
2109_25	2.93253	1.00119	0.00346
1729_09	3.00875	1.00486	0.00356
1727_10	4.89416	0.99885	0.00393

E.4 REFERENCES

1. U. P. Jenquin and S. R. Bierman, *Benchmark Experiments to Test Plutonium and Stainless Steel Cross Sections*, NUREG/CR-0210, PNL-2273 R-C, (June 1978).

2. B. M. Durst, S. R. Bierman and E. D. Clayton, *Handbook of Critical Experiments Benchmarks*, PNL-2700 (March 1978).

3. H. C. Paxton, *Los Alamos Critical-Mass Data*, LA-3067-MS, Rev. (December 1975).

4. B. L. Koponen, et. al., *Nuclear Criticality Experiments from 1943 to 1978, An Annotated Bibliography*, UCRL-52769 (April 1979).

5. H. R. Dyer, W. C. Jordan, V. R. Cain, "A Technique for Code Validation for Criticality Safety Calculations", *Trans. Am. Nuc. Soc.*, Vol. 63, pp. 238-239 (June 1991).

Appendix F

VALIDATION OF COMPUTER CODES AND CROSS SECTION LIBRARY FOR MIXED U-233, U-235 SYSTEMS

Appendix F

VALIDATION OF COMPUTER CODES AND CROSS SECTION LIBRARY FOR MIXED U-233, U-235 SYSTEMS

F.1 INTRODUCTION

Approximately one-half of the wells in the Cell 4 storage array are filled with material from the Consolidated Edison Uranium Solidification Project (CEUSP). The uranium in this material is 9.7 wt % U-233 and 76.5 wt % U-235. Computational difficulties may exist in mixed systems which are not revealed by validating with critical experiments containing only one fissile nuclide. Overlapping resonances between two fissile nuclides may invalidate techniques used to derive cross section values for the resonance region. Consequently validating configurations of mixed fissile species requires critical experiments conducted with similar fuel mixtures.

Unfortunately, almost no critical configurations have been constructed with mixed U-233, U-235 fuels. Some experiments were performed with CEUSP-like fuel for reactor typical conditions. The water-to-fuel ratio of these experiments was far higher than any conditions expected to exist in the Cell 4 storage array. Two experiments, each with a U-233 metal core and an enriched U-235 reflector, are documented in Ref. 1. These experiments have a calculated spectra which is much faster than that expected to exist in any normal or credible abnormal configuration in Cell 4.

F.2 CALCULATED NEUTRONICS PARAMETERS

K-effectives for the two cases from Ref. 1 have been calculated and are reported in Table F.1. Some experimental parameters and calculated average energy group causing fission are also reported. All of the results are for the CSAS25 module of the NCSS version of the SCALE package and were generated using the Hansen-Roach cross-sections. The Koponen Citation number refers to a compilation of critical experiments prepared under the direction of B. L. Koponen, Lawrence Livermore Laboratory.[2]

Though not representative of the 3019 storage wells, these experiments indicate that there is no reason to expect that a mixed fissile system would induce an error in calculated multiplication factor not found in a single fissile isotope system. Clearly, additional experimental data is needed for the moderation range expected in Cell 4. In the absence of data, for mixtures of ^{235}U and ^{233}U, the lower of the two subcritical limits should be applied.

Table F.1. Spherical ^{233}U, ^{235}U reflected critical experiments

Koponen citation I.D.	wt % ^{233}U	U density (g/cm**3)	Diameter (in.)	Shell thickness (in.)	k-effective	sigma	Average fission group
1727-14	98.11	18.62	3.972	0.481	1.00574	0.00369	3.122
1727-15	98.11	18.64	3.622	0.783	1.00367	0.00349	3.149

F.3 REFERENCES

1. H. C. Paxton, Los Alamos Critical-Mass Data, LA-3067-MS, Rev. (December 1975).

2. B. L. Koponen, et. al., Nuclear Criticality Experiments from 1943 to 1978, An Annotated Bibliography, UCRL-52769 (April 1979).

Appendix G

AUTONOMOUS, IN-LINE ARRAY MODEL

Appendix G

AUTONOMOUS, IN-LINE ARRAY MODEL

A representative KENO-Va dataset is provided in Fig. G.1. The linear loading of ^{233}U for this case is 5.5 kg/ft. The $H/^{233}U$ ratio is 1.0. Material 1 is the fissile material. Material 2 is the steel well liner and material 3 is the cell wall concrete (atom densities provided in Section 2.0). Figure G.2 is a KENO plot showing a cross-section of the storage array.

```
csas25
Actual 3019-In-line intercell,  5.500 k/f u-233, h/x=  1.000, oxide
hansen-roach
multiregion
u-233  1 0.0 5.75262E-03 end
h  1 0.0 5.75262E-03 end
o  1 0.0 1.43815E-02 end
carbonsteel  2 1.0 end
c  3 0.0 3.82155E-04 end
s  3 0.0 2.52827E-05 end
na  3 0.0 9.58077E-05 end
mg  3 0.0 1.18155E-04 end
al  3 0.0 7.68645E-04 end
si 3 0.0 1.19239E-02 end
k  3 0.0 2.15730E-04 end
ca  3 0.0 1.71935E-03 end
fe  3 0.0 2.29130E-04 end
zn  3 0.0 9.36739E-06 end
o  3 0.0 2.62094E-02 end
end comp
buckledcyl vacuum reflected 0.0 373.38 end
1 5.08 oneextermod
2 5.68198 twoextermod
0 6.35 twoextermod
3 38.4525 oneextermod
end zone
Actual 3019-In-line intercell,  5.500 k/f u-233, h/x=  1.000, oxide
read para
gen=203 npg=300 tme=180 flx=yes fdn=yes pki=yes far=yes fmp=yes nub=yes
end para
read plot
ttl=/Axial View Through In-line Intercell Storage Array/
pic=mat
xul=76.2 yul=0.0 zul=400.0
xlr=76.2 ylr=400.0 zlr=-100.0
vax=1.0 wdn=-1.0
nax=132
run=yes plt=yes end
ttl=/Horizontal View Through In-line Intercell Storage Array/
pic=mat
xul=0.0 yul=0.0 zul=250.0
xlr=160.0 ylr=400.0 zlr=250.0
uax=1.0 vdn=1.0
nax=132
run=yes plt=yes end
end plot
read geom
box type  1
cylinder  1 1 5.08 373.38 0.0
cylinder  2 1 5.68198 373.38 0.0
cylinder  0 1 6.35 373.38 0.0
cuboid  3 1 76.2 -76.2 15.24 -15.24 373.38 0.0
corebdy  0 1 0.0 0.0 0.0
reflector  3 -1 0.0 0.0 764.54 121.92 121.92 820.82 1
end geom
read array
nux=1 nuy=9 nuz=1
loop
1 1 1 1 1 9 1 1 1 1
end loop
end array
end data
end
```

Fig. G.1. Representative KENO input for in-line calculations

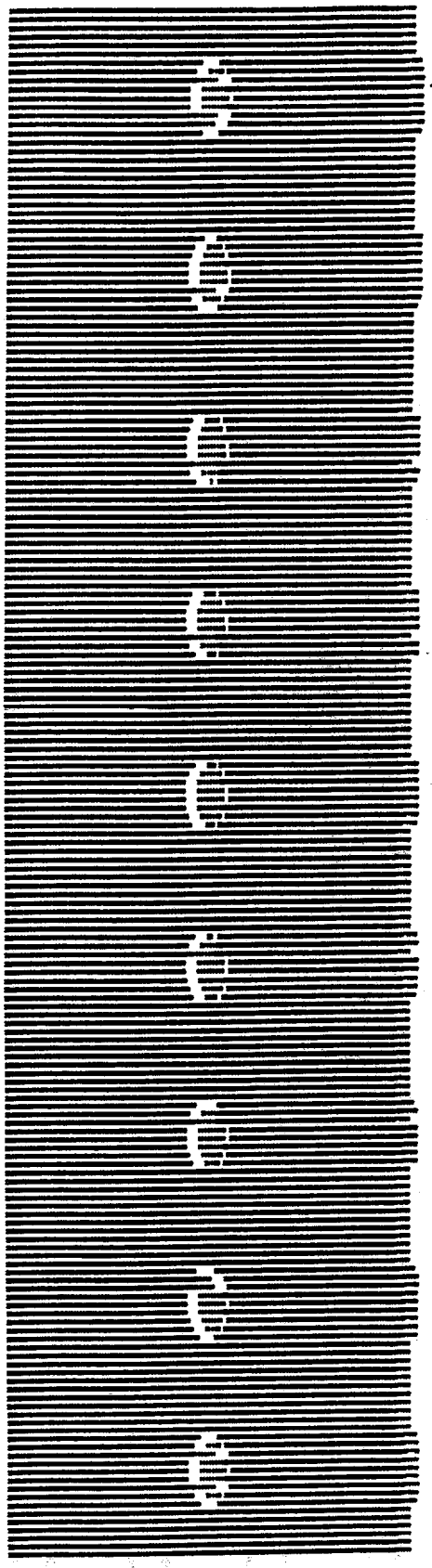

Fig. G.2 Cross-sectional KENO plot of in-line array.

Appendix H

AUTONOMOUS, CELL 4 MODELS

Appendix H

AUTONOMOUS, CELL 4 MODELS

H.1 MODEL FOR COMPARISON TO REF. 1 STUDIES

As noted in Section 4.2.1, the first Cell 4 model was intended to be a close reconstruction of the model used in the calculations reported in Ref.1. The KENO-Va input for case cell4_1 from Table 12 is provided as Fig. H.1. This dataset is also stored on the floppy disk accompanying this report. The definition of the materials in the KENO input is given in Table H.1. The definition of the KENO geometry input is given in Table H.2. Figure H.2 is a KENO plot from the dataset in Fig. H.1. The numerical symbols which constitute Fig. H.2 correspond to the values in Table H.1. Note that Fig. H.2 is the inverted, mirror-image of Fig. 8.

```
#csas25
3019-Cell 4, H/U=1, Bound H2O, Nominal
hansen-roach
latticecell
u-235  1 0.0 3.33319e-3 end
h  1 0.0 3.33319e-3 end
o  1 0.0 8.33298e-3 end
carbonsteel  2 1.0 end
h  3 0.0 7.25655e-3 end
c  3 0.0 1.05173e-2 end
o  3 0.0 4.49751e-2 end
na  3 0.0 1.28310e-5 end
mg  3 0.0 5.09498e-3 end
al  3 0.0 4.16956e-4 end
si  3 0.0 2.67500e-3 end
s  3 0.0 9.61505e-5 end
k  3 0.0 1.27795-5 end
ca  3 0.0 8.76440e-3 end
fe  3 0.0 1.39779e-4 end
zn  3 0.0 1.11783e-5 end
n  4 0.0 1.98881e-5 end
o  4 0.0 5.33497e-6 end
orconcrete  5 1.0 end
end comp
triangpitch 32.385 3.1 1 3 end
3019-Cell 4, H/U=1, Bound H2O, Nominal
read para
gen=303 tme=60 flx=yes fdn=yes pki=yes nub=yes
end para
read plot
ttl=/Axial View Through Top of Cell 4 Storage Array/
pic=mat
xul=18.6975 yul=0.0 zul=800.0
xlr=18.6975 ylr=300.0 zlr=960.0
vax=1.0 wdn=1.0
nax=132
run=yes plt=yes end
ttl=/Horizontal View Through Cell 4 Storage Array/
pic=mat
xul=0.0 yul=0.0 zul=400.0
xlr=300.0 ylr=300.0 zlr=400.0
uax=1.0 vdn=1.0
nax=132
run=no plt=yes end
end plot
read geom
box type  1
cylinder  1 1 5.715 914.4 0.0
cylinder  2 1 6.35 914.4 0.0
cylinder  3 1 16.0031 914.4 0.0
global
box type  2
cuboid  4 1 609.6 0.0 584.64 0.0 914.4 0.0
hole  1  1.86975E+01 1.61925E+01 0.0
hole  1  1.86975E+01 4.85775E+01 0.0
hole  1  1.86975E+01 8.09625E+01 0.0
hole  1  1.86975E+01 1.13348E+02 0.0
hole  1  1.86975E+01 1.45732E+02 0.0
hole  1  1.86975E+01 1.78117E+02 0.0
hole  1  1.86975E+01 2.10502E+02 0.0
hole  1  1.86975E+01 2.42887E+02 0.0
hole  1  4.67437E+01 3.23850E+01 0.0
hole  1  4.67437E+01 6.47700E+01 0.0
hole  1  4.67437E+01 9.71550E+01 0.0
hole  1  4.67437E+01 1.29540E+02 0.0
hole  1  4.67437E+01 1.61925E+02 0.0
hole  1  4.67437E+01 1.94310E+02 0.0
```

```
hole 1 4.67437E+01 2.26695E+02 0.0
hole 1 7.47899E+01 1.61925E+01 0.0
hole 1 7.47899E+01 4.85775E+01 0.0
hole 1 7.47899E+01 8.09625E+01 0.0
hole 1 7.47899E+01 1.13348E+02 0.0
hole 1 7.47899E+01 1.45732E+02 0.0
hole 1 7.47899E+01 1.78117E+02 0.0
hole 1 7.47899E+01 2.10502E+02 0.0
hole 1 7.47899E+01 2.42887E+02 0.0
hole 1 1.02836E+02 3.23850E+01 0.0
hole 1 1.02836E+02 6.47700E+01 0.0
hole 1 1.02836E+02 9.71550E+01 0.0
hole 1 1.02836E+02 1.29540E+02 0.0
hole 1 1.02836E+02 1.61925E+02 0.0
hole 1 1.02836E+02 1.94310E+02 0.0
hole 1 1.02836E+02 2.26695E+02 0.0
hole 1 1.30882E+02 1.61925E+01 0.0
hole 1 1.30882E+02 4.85775E+01 0.0
hole 1 1.30882E+02 8.09625E+01 0.0
hole 1 1.30882E+02 1.13348E+02 0.0
hole 1 1.30882E+02 1.45732E+02 0.0
hole 1 1.30882E+02 1.78117E+02 0.0
hole 1 1.30882E+02 2.10502E+02 0.0
hole 1 1.30882E+02 2.42887E+02 0.0
hole 1 1.58928E+02 3.23850E+01 0.0
hole 1 1.58928E+02 6.47700E+01 0.0
hole 1 1.58928E+02 9.71550E+01 0.0
hole 1 1.58928E+02 1.29540E+02 0.0
hole 1 1.58928E+02 1.61925E+02 0.0
hole 1 1.58928E+02 1.94310E+02 0.0
hole 1 1.58928E+02 2.26695E+02 0.0
hole 1 1.86975E+02 1.61925E+01 0.0
hole 1 1.86975E+02 4.85775E+01 0.0
hole 1 1.86975E+02 8.09625E+01 0.0
hole 1 1.86975E+02 1.13348E+02 0.0
hole 1 1.86975E+02 1.45732E+02 0.0
hole 1 1.86975E+02 1.78117E+02 0.0
hole 1 1.86975E+02 2.10502E+02 0.0
hole 1 1.86975E+02 2.42887E+02 0.0
hole 1 2.15021E+02 3.23850E+01 0.0
hole 1 2.15021E+02 6.47700E+01 0.0
hole 1 2.15021E+02 9.71550E+01 0.0
hole 1 2.15021E+02 1.29540E+02 0.0
hole 1 2.15021E+02 1.61925E+02 0.0
hole 1 2.15021E+02 1.94310E+02 0.0
hole 1 2.15021E+02 2.26695E+02 0.0
hole 1 2.43067E+02 1.61925E+01 0.0
hole 1 2.43067E+02 4.85775E+01 0.0
hole 1 2.43067E+02 8.09625E+01 0.0
hole 1 2.43067E+02 1.13348E+02 0.0
hole 1 2.43067E+02 1.45732E+02 0.0
hole 1 2.43067E+02 1.78117E+02 0.0
hole 1 2.43067E+02 2.10502E+02 0.0
hole 1 2.43067E+02 2.42887E+02 0.0
cuboid 5 1 670.56 -60.96 645.60 -60.96 1005.84 -60.96
end geom
read bias
id=400 2 2 end bias
end data
end
```

Fig. H.1. Representative KENO input for initial Cell 4 model.

Table H.1. Definition of KENO materials input

Mixture I.D. number	Description
1	Fissile material stored throughout array
2	Steel liner for wells
3	Cell 4 array concrete
4	Air
5	Cell wall concrete

Table H.2. Definition of KENO geometry input

KENO geometry region	Description
box type 1	Unit cell for array
cylinder 1	Fissile material
cylinder 2	Steel liner
cylinder 3	Cell 4 array concrete surrounding well
global	
box type 2	Representation of Cell 4
cuboid 4	Air in which array is to be placed
hole 1	Placement of unit cell
cuboid 5	Concrete block representing cell walls

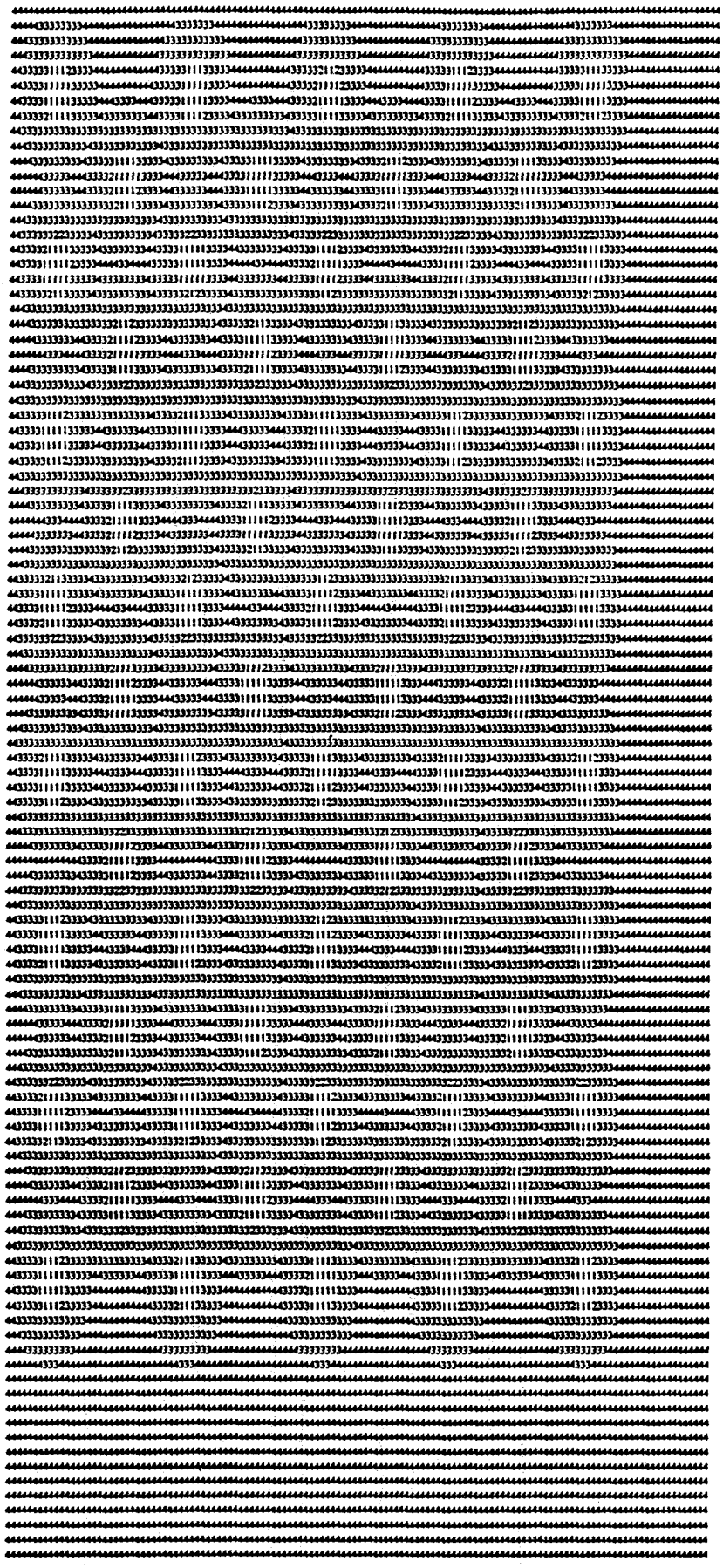

Fig. H.2. KENO plot from Fig. H.1 input.

H.2 MODEL OF CELL 4 WITH EXPLICIT CEUSP AND U4 REPRESENTATION

As noted in Section 4.2.3, this model, designated C4WC, was developed in order to increase the allowable fissile load limits above those values derived in Ref. 1. Consequently the CEUSP and U4 materials were explicitly included in the model in order to provide a more realistic estimate of the k-effective of the array under various loading conditions.

The KENO-Va input for case c4_u330 from Table 13 is provided as Fig. H.3. It is representative of all the cases in this series of calculations. This dataset is also stored on the floppy disk accompanying this report. The definition of the materials in the KENO input is given in Table H.3. The definition of the KENO geometry input is given in Table H.4. Figure H.4 is a KENO plot from the dataset in Fig. H.3. The numerical symbols which constitute Fig. H.4 correspond to the values in Table H.3 with the exception that the symbol A is substituted for material 10 and the symbol B is substituted for material 11. Note that Fig. H.4 is the inverted, mirror-image of Fig. 8.

```
#csas25
Actual 3019-Cell 4,  2.000 k/f u-233, h/x=  3.000, oxide
hansen-roach
latticecell
u-233  1 0.0 2.09186E-03 end
h  1 0.0 6.27558E-03 end
o  1 0.0 7.32151E-03 end
u-233  6 0.0 3.30566E-03 end
h  6 0.0 4.95848E-03 end
o  6 0.0 9.09055E-03 end
u-233  8 0.0 1.65283E-03 end
h  8 0.0 4.95848E-03 end
o  8 0.0 5.78490E-03 end
u-233  9 0.0 1.57256e-4 end
u-234  9 0.0 2.25997e-5 end
u-235  9 0.0 1.22966e-3 end
u-236  9 0.0 8.96327e-5 end
u-238  9 0.0 1.07925e-4 end
h  9 0.0 1.60707e-4 end
o  9 0.0 8.03537e-5 end
u-233  10 0.0 1.24251e-4 end
u-234  10 0.0 1.78565e-5 end
u-235  10 0.0 9.71581e-4 end
u-236  10 0.0 7.08209e-5 end
u-238  10 0.0 8.52741e-5 end
h  10 0.0 1.26979e-4 end
o  10 0.0 6.34893e-5 end
u-233  11 0.0 1.02475e-3 end
h  11 0.0 1.02475e-4 end
o  11 0.0 5.12375e-5 end
carbonsteel  2 1.0 end
h  3 0.0 7.25655e-3 end
c  3 0.0 1.05173e-2 end
o  3 0.0 4.49751e-2 end
na  3 0.0 1.28310e-5 end
mg  3 0.0 5.09498e-3 end
al  3 0.0 4.16956e-4 end
si  3 0.0 2.67500e-3 end
s  3 0.0 9.61505e-5 end
k  3 0.0 1.27795-5 end
ca  3 0.0 8.76440e-3 end
fe  3 0.0 1.39779e-4 end
zn  3 0.0 1.11783e-5 end
n  4 0.0 1.98881e-5 end
o  4 0.0 5.33497e-6 end
c  5 0.0 3.82155E-04 end
s  5 0.0 2.52827E-05 end
na  5 0.0 9.58077E-05 end
mg  5 0.0 1.18155E-04 end
al  5 0.0 7.68645E-04 end
si 5 0.0 1.19239E-02 end
k  5 0.0 2.15730E-04 end
ca  5 0.0 1.71935E-03 end
fe  5 0.0 2.29130E-04 end
zn  5 0.0 9.36739E-06 end
o  5 0.0 2.62094E-02 end
```

```
h2o-x(e)-hr  7 1.0 end
end comp
triangpitch 32.385 5.08 1 3 end
Actual 3019-Cell 4,  2.000 k/f u-233, h/x=  3.000, oxide
read para
gen=203 npg=301 tme=180 flx=yes fdn=yes pki=yes far=yes fmp=yes
nub=yes
end para
read plot
ttl=/Axial View Through Top of Cell 4 Storage Array/
pic=mat
xul=18.6975 yul=0.0 zul=800.0
xlr=18.6975 ylr=300.0 zlr=960.0
vax=1.0 wdn=1.0
nax=132
run=yes plt=yes end
ttl=/Horizontal View Through Cell 4 Storage Array/
pic=mat
xul=0.0 yul=0.0 zul=400.0
xlr=300.0 ylr=300.0 zlr=400.0
uax=1.0 vdn=1.0
nax=132
run=yes plt=yes end
end plot
read geom
box type  1
cylinder  1 1 5.08 914.4 0.0
cylinder  2 1 5.68198 914.4 0.0
cylinder  3 1 16.0031 914.4 0.0
box type  4
cylinder  9 1 5.08 914.4 0.0
cylinder  2 1 5.68198 914.4 0.0
cylinder  3 1 16.0031 914.4 0.0
box type  2
cylinder  6 1 5.715 30.0 0.0
cylinder  7 1 5.715 60.0 0.0
cylinder  6 1 5.715 90.0 0.0
cylinder  7 1 5.715 120.0 0.0
cylinder  6 1 5.715 150.0 0.0
cylinder  7 1 5.715 180.0 0.0
cylinder  6 1 5.715 210.0 0.0
cylinder  7 1 5.715 240.0 0.0
cylinder  6 1 5.715 270.0 0.0
cylinder  7 1 5.715 300.0 0.0
cylinder  6 1 5.715 330.0 0.0
cylinder  7 1 5.715 360.0 0.0
cylinder  6 1 5.715 390.0 0.0
cylinder  7 1 5.715 420.0 0.0
cylinder  6 1 5.715 450.0 0.0
cylinder  7 1 5.715 480.0 0.0
cylinder  6 1 5.715 510.0 0.0
cylinder  7 1 5.715 540.0 0.0
cylinder  6 1 5.715 570.0 0.0
cylinder  7 1 5.715 600.0 0.0
cylinder  6 1 5.715 630.0 0.0
cylinder  7 1 5.715 660.0 0.0
```

```
cylinder  6 1 5.715 690.0 0.0
cylinder  7 1 5.715 720.0 0.0
cylinder  6 1 5.715 750.0 0.0
cylinder  7 1 5.715 780.0 0.0
cylinder  6 1 5.715 810.0 0.0
cylinder  7 1 5.715 840.0 0.0
cylinder  6 1 5.715 870.0 0.0
cylinder  7 1 5.715 914.0 0.0
cylinder  2 1 6.35 914.4 0.0
cylinder  3 1 16.0031 914.4 0.0
box type  3
cylinder  8 1 5.715 914.4 0.0
cylinder  2 1 6.35 914.4 0.0
cylinder  3 1 16.0031 914.4 0.0
box type  5
cylinder  10 1 5.715 914.4 0.0
cylinder  2 1 6.35 914.4 0.0
cylinder  3 1 16.0031 914.4 0.0
box type  6
cylinder  11 1 5.715 914.4 0.0
cylinder  2 1 6.35 914.4 0.0
cylinder  3 1 16.0031 914.4 0.0
global
box type  7
cuboid  3 1 260.0 0.0 260.0 0.0 914.4 0.0
hole  1  1.86975E+01 1.61925E+01 0.0
      ⋮
array positions the same as in Fig. H.1
      ⋮
hole  3  2.43067E+02 1.45732E+02 0.0
hole  3  2.43067E+02 1.78117E+02 0.0
hole  3  2.43067E+02 2.10502E+02 0.0
hole  3  2.43067E+02 2.42887E+02 0.0
cuboid  4 1 609.6 0.0 584.64 0.0 914.4 0.0
cuboid  5 1 670.56 -60.96 645.60 -60.96 1005.84 -60.96
end geom
read bias
id=400 2 2 end bias
end data
end
```

Fig. H.3. Representative KENO-Va input for Cell 4 model with explicitly modeled CEUSP and U4 material.

Table H.3. Definition of materials in Fig. H.3

Mixture I.D. number (from Fig. H.3)	Description
1	available 4 inch wells (variable composition)
2	steel well liner
3	Cell 4 array concrete
4	air
5	Cell wall concrete
6	material in flooded 4.5 inch wells
7	water
8	available 4.5 inch wells (variable composition)
9	CEUSP in 4 inch wells
10	CEUSP in 4.5 inch wells
11	U4 material in 4.5 inch wells

Table H.4. Definition of geometric zones in Fig. H.3

KENO Box type	Description
1	available 4 inch wells
2	flooded 4.5 inch wells
3	available 4.5 inch wells
4	CEUSP in 4 inch wells
5	CEUSP in 4.5 inch wells
6	U4 material in 4.5 inch wells
7	Concrete block representing Cell 4 array

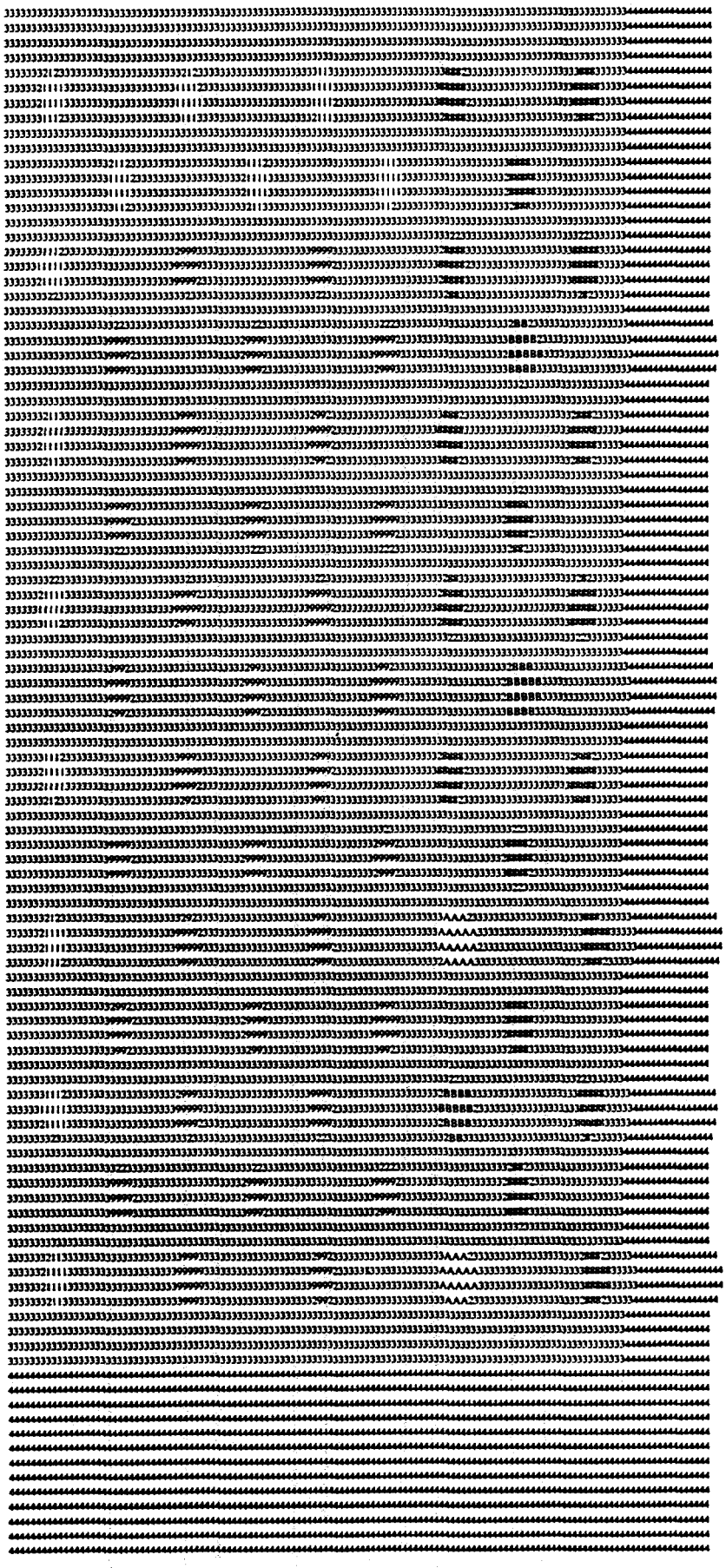

Fig. H.4 KENO plot produced from input in Fig. H.3.

The C4WC model presents cross section processing problems not present in earlier models. The C4WC model contains six different types of "unit cells", i. e. six types of fissile material. Table H.4 shows that there are variations in physical dimensions as well as considerable variation in fissile materials composition among the Cell 4 wells. Even though no cross-section collapsing is being performed, in order for the correct resonance treatments to be performed, each of these unit cells should be treated separately. Currently the SCALE system does not have an automated procedure for performing this function.

Fortunately, the geometry of the arrays being studied allowed for problem simplification. Both the in-line and Cell 4 arrays have wide, 30.5 cm (12 in) pitches. Neutrons leaving the fissile material region almost always have their next collision in the concrete. Consequently the Dancoff factor, the average transmission probability for the moderator (which here is the concrete), should be very close to zero no matter which material is stored in a given well.

Dancoff factors for the two possible Cell 4 lattice cell models were computed and are reported in Table H.5. Any given dataset from Section 4.2.3 can be used. The parameter "parm=chk", encoded starting in column 12 of the first line of the dataset (#CSAS25), enables output of Dancoff factors from the SCALE system. Factors are reported in the SCALE output for all materials but the values reported in Table H.5 for the "fuel" are the values of interest and certify the hypothesis that the Dancoff factor should be very near zero.

Table H.5. Computed Dancoff Factors for Cell 4 materials

Lattice Cell Model	Dancoff Factor
4 inch well	$4.38*10^{-7}$
4.5 inch well	$6.24*10^{-7}$

L. M. Petrie, ORNL, states that in the SCALE LATTICECELL option, such as that shown in Fig. H.3, the Dancoff factors for all regions outside the fuel and clad region are set to zero. That is, the regions are assumed to be infinitely homogeneous. Since Table H.5 shows that the values for all Cell 4 positions are effectively zero, it is appropriate to model all of the fissile materials which could be contained in the Cell 4 array (or the in-line arrays) in a single CSAS25 model. The resulting cross section preparation is vastly simplified while retaining accuracy.

It is noted in the footnotes to Tables 13-15 that many calculations were performed with the cross section processing portion of the CSAS25 having the well radius set to 3.1 cm. (The KENO portion of the CSAS25 input had the correct dimensions.) The value had been inadvertently carried forward from previous calculations. All final calculations (Table 16) were performed with the more accurate value of 5.08. Note that the assumption of 3.1 cm would only reduce the Dancoff factors from the Table H.5 values. Consequently, one would not expect this error to have any impact on k-effective and indeed that conclusion was verified.

Appendix I

COMBINED CELL 4 AND IN-LINE STORAGE ARRAY MODELS

Appendix I

COMBINED CELL 4 AND IN-LINE STORAGE ARRAY MODELS

Two models were created for examining possible interactions between the Cell 4 array and adjacent in-line storage arrays. As shown in Fig. 2 of the report, in-line wells 4 & 5 are immediately adjacent to the Cell 4 array. However, the in-line wells extend only 12 feet down from the level of the equipment hatch for Cell 4 whereas the Cell 4 wells extend approximately 31 feet below the level of the Cell 4 hatch.

In all of the calculations performed with the combined model, the Cell 4 and in-line wells were completely filled. This treatment is conservative as A. M. Krichinsky, Chemical Technology Division, has reported that the maximum height of material in *any* of the storage wells is 24 feet.

The materials and atom densities for the in-line portion of the combined model are the same as has been presented in Appendix G. Likewise the materials and atom densities for the Cell 4 portion of the model are the same as presented in Appendix H. The combined model was created by forming a 2 unit array. For the Cell 4 and in-line 3 & 4 model the in-line unit was placed to the right of the Cell 4 unit. For the Cell 4 and in-line 4 & 5 model the in-line unit was placed to the left of the Cell 4 unit. The definitions of box types for the combined model is given in Table I.1.

Table I.1. Box type definition for combined model

Box Type	Description
8	Concrete block representing Cell 4 array
9	Concrete wall representing inline array

The portion of the KENO input describing placement of the units for the Cell 4, 3 & 4 model is given in Fig. I.1. A printer plot at altitude (z-direction) of 800 cm for this model is shown in Fig. I.2. The in-line wells are shown by the symbol "A" along the right side of the plot. Material "4" is air, "3" is the concrete of the Cell 4 array, "5" is the cell wall concrete. The Cell 4 wells, located on a triangular pitch, are visible in the lower left portion of Fig. I.2 as non "3" or "5" symbols.

```
box type  8
cuboid  3 1 260.0 0.0 260.0 0.0 914.4 0.0
hole  1  1.86975E+01 1.61925E+01 0.0
hole  1  1.86975E+01 4.85775E+01 0.0
hole  1  1.86975E+01 8.09625E+01 0.0

. . . . Cell 4 well locations not shown . . . .

hole  3  2.43067E+02 2.10502E+02 0.0
hole  3  2.43067E+02 2.42887E+02 0.0
cuboid  4 1 609.6 0.0 584.64 0.0 914.4 0.0
cuboid  5 1 609.6 -152.4 645.60 -152.4 1005.84 -152.4
box type  9
cuboid  5 1 76.2 -76.2 645.60 -152.4 1005.84 -152.4
hole 7  0.0 30.48 533.4
hole 7  0.0 60.96 533.4
hole 7  0.0 91.44 533.4
hole 7  0.0 121.92 533.4
hole 7  0.0 152.4 533.4
hole 7  0.0 182.88 533.4
hole 7  0.0 213.36 533.4
hole 7  0.0 243.84 533.4
hole 7  0.0 274.32 533.4
end geom
read array
nux=2 nuy=1 nuz=1
loop
8 1 1 1 1 1 1 1 1
9 2 2 1 1 1 1 1 1
end loop
end array
```

Fig. I.1. Portion of KENO Va input describing geometry of Cell 4, in-line 3 & 4 model.

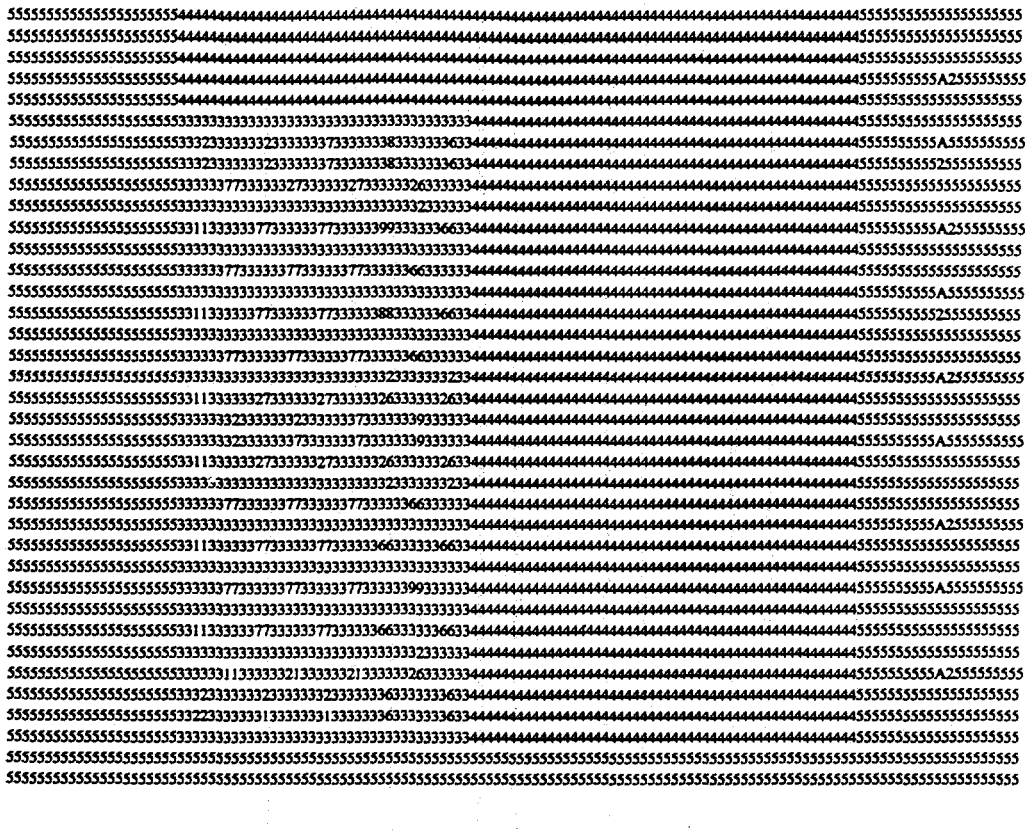

Fig. I.2. KENO plot produced from data in Fig. I.1.

The corresponding input and plot for the Cell 4, 4 & 5 model is shown in Figs. I.3 and I.4. Note that Fig. I.4 encompasses a much smaller view than Fig. I.2. Only the Cell 4 array and immediately adjacent 4 & 5 in-line storage are shown.

```
box type  8
cuboid  3 1 260.0 0.0 260.0 0.0 914.4 0.0
hole  1  1.86975E+01 1.61925E+01 0.0
hole  1  1.86975E+01 4.85775E+01 0.0
hole  1  1.86975E+01 8.09625E+01 0.0

. . . . Cell 4 well locations not shown . . . .

hole  3  2.43067E+02 1.78117E+02 0.0
hole  3  2.43067E+02 2.10502E+02 0.0
hole  3  2.43067E+02 2.42887E+02 0.0
cuboid  4 1 609.6 0.0 584.64 0.0 914.4 0.0
cuboid  5 1 670.56 0.0 645.60 -152.4 1005.84 -152.4
box type  9
cuboid  5 1 76.2 -76.2 645.60 -152.4 1005.84 -152.4
hole 7  0.0 30.48 533.4
hole 7  0.0 60.96 533.4
hole 7  0.0 91.44 533.4
hole 7  0.0 121.92 533.4
hole 7  0.0 152.4 533.4
hole 7  0.0 182.88 533.4
hole 7  0.0 213.36 533.4
hole 7  0.0 243.84 533.4
hole 7  0.0 274.32 533.4
end geom
read array
nux=2 nuy=1 nuz=1
loop
8 2 2 1 1 1 1 1 1 1
9 1 1 1 1 1 1 1 1 1
end loop
end array
```

Fig. I.3. Portion to KENO Va input describing geometry of Cell 4, in-line 4 & 5 model.

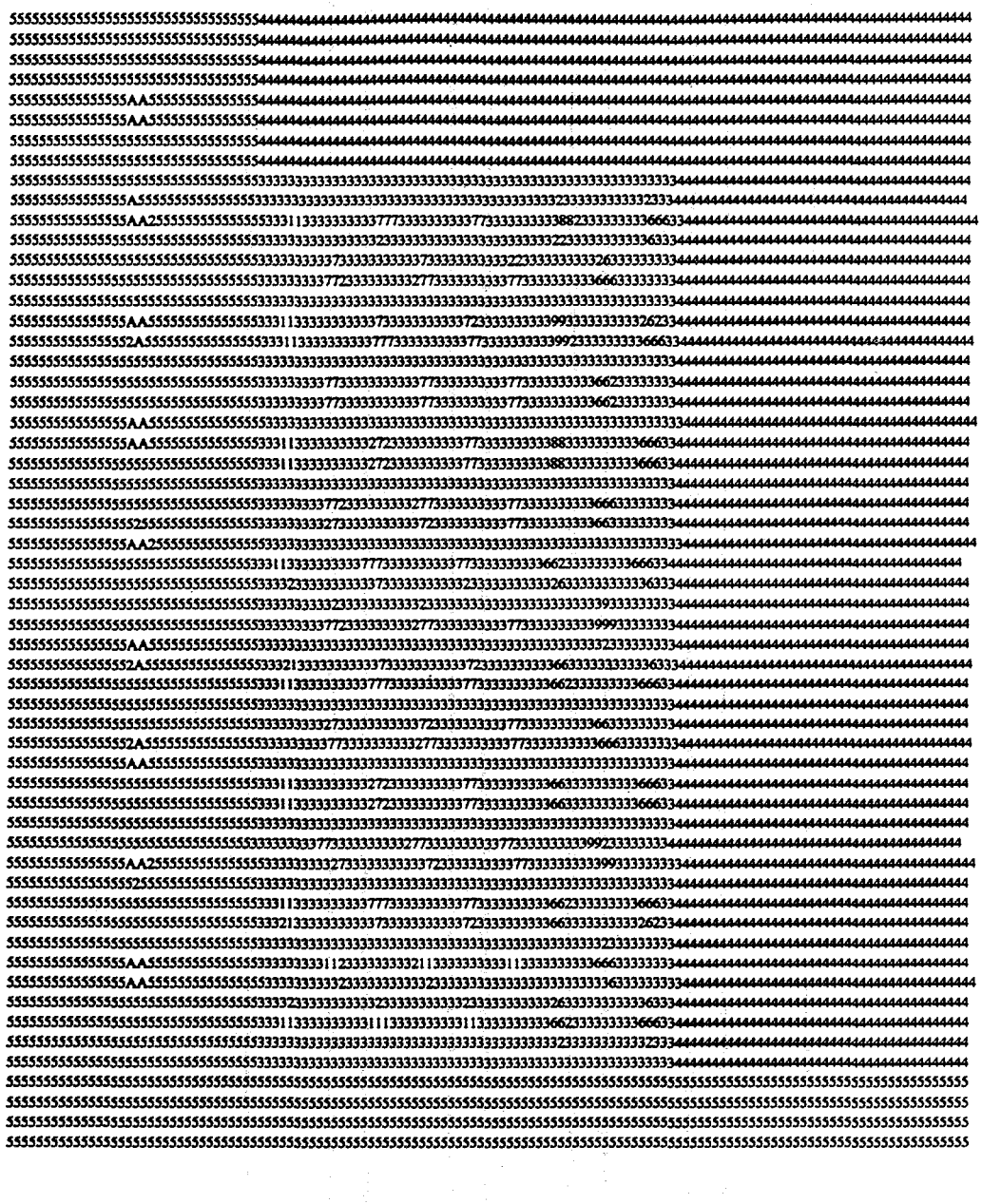

Fig. I.4. KENO plot produced from data in Fig. I.3.

I.1. INCLUSION OF HEMISPHERES INTO REFERENCE MODEL

Subsequent to the investigation of interactions between storage arrays and after initial assessment of fissile load limits (which were very nearly the same as the final values in the report), it was discovered that the loading in well M of In-line array 4 & 5 contained three hemispheres of ^{233}U metal which had a linear loading greater than the newly-derived limits. To account for this violation of the limit, a new model was created whereby the hemispheres were modeled explicitly. The exact location of the hemispheres in well M was readily available so they were assumed to be located symmetrically about the axial centerpoint of the well.

A printer plot of one of the hemispheres is presented in Fig. I.5. The view is projected "upside-down". Symbol "5" is concrete, "7" is ^{233}U metal, "0" is air, and "1" represents other ^{233}U fuel subject to the currently-calculated load limits. The hemispheres were known to have a center-to-center separation of 43.18 cm (17 inches) inside the column. The positions of the other two hemispheres in the KENO model were verified.

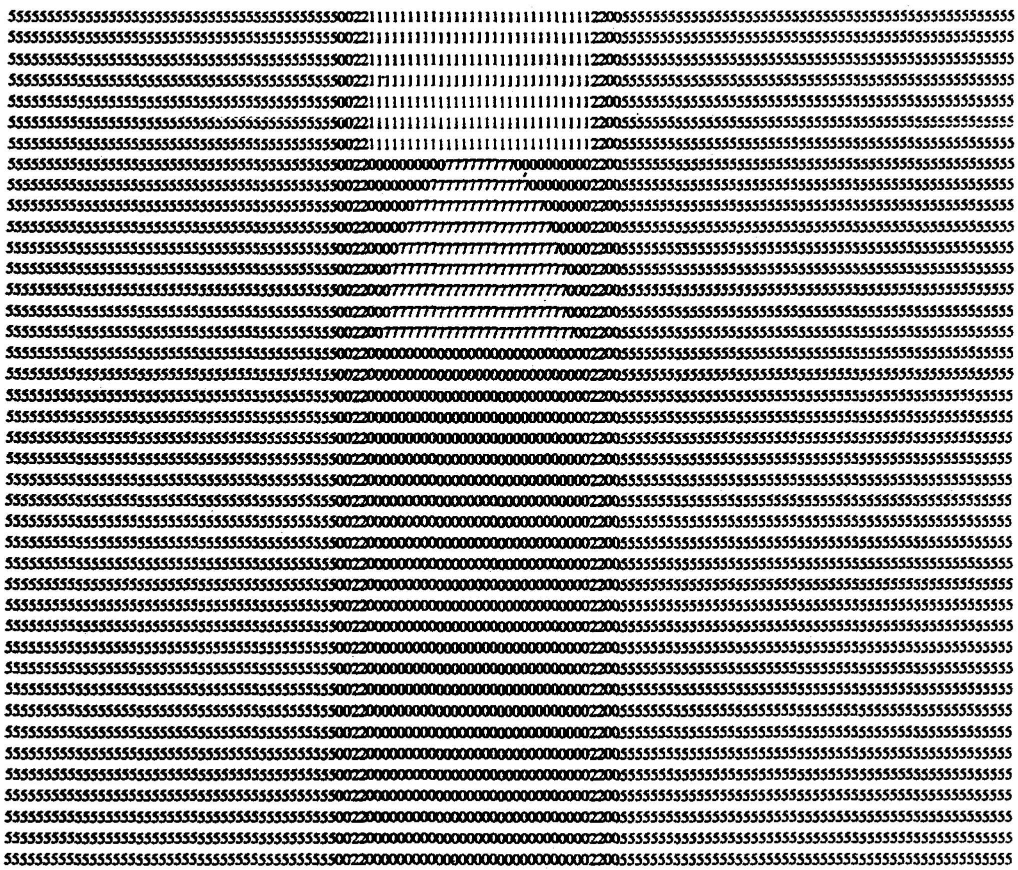

Fig. I.5. Explicitly modeled hemisphere in well M.

Once the hemispheres were added to the model, additional changes were required. Because the hemispheres were so small relative to the remainder of the in-line and Cell 4 arrays, no neutrons were being started (under the default KENO starting algorithm) in the hemispheres. The solution was to input a starting distribution. The necessary input was created so that, out of an initial start batch of 500

neutrons, 20% would be allocated to the hemispheres, another 20% would be allocated to the in-line wells and the remainder would be distributed within the Cell 4 fissile positions. The distribution was flat over the in-line and Cell 4 arrays. Investigation of the fission densities revealed that some neutrons were "seeing" the hemispheres but that the Cell 4 array positions were still the "driver" of the whole system. This starting distribution was used in all of the calculations for determining the fissile load limit.

Datasets for all combined models are stored on the floppy disk attached to the back cover of this report. The datasets are in the directory named /appendix.i. The dataset which contains both the hemispheres and the revised starting distribution is named final_w_hemi.

I.2. FINAL, COMBINED MODEL CONTAINING TWO WATER-FLOODED COLUMNS

As noted in Section 4.3.2, the reactivity effect of flooding two, non-adjacent columns was investigated. BOX TYPE 2 in the Appendix H KENO model for Cell 4 had been intended for use as a flooded column unit cell. In the early Cell 4 models, BOX TYPE 2 was composed of alternating regions, each 30 cm tall, of fissile material and water. The large water regions in this configuration effectively isolated the fissile material and no or negative change was seen in multiplication factor. Consequently, water flooding had been ignored in all previous cases.

Following the discussion in Section 4.3.2, in the final combined model, BOX TYPE 2 was modified to include a smaller radius for the fissile material and homogeneous mixing of fissile material and water subject to the minimum density constraint of 1.5 g oxide/cm^3. The height of the fissile material in each 30.48 cm (1 foot) segment of the flooded well was determined by the linear load limit under investigation and the oxide density. If with the minimum oxide density, the oxide/water mixture did not fill the canister, then water was assumed to exist above the oxide. Within the range of available oxide densities (a maximum density of 3.5 kg oxide/cm^3 had been identified by E. C. Crume, Jr, ORNL), the value was chosen which led to the canister being filled with the oxide/water mixture. There were no cases in which the linear loading being investigated and the maximum oxide density yielded an unrealistic volume for a flooded canister. The space between the fissile material and the well liner in the flooded columns was filled with water.

Datasets for all combined models are stored on the floppy disk attached to the back cover of this report. The datasets are in the directory named /appendix.i. The dataset which contains the hemispheres, the revised starting distribution, and the revised flooded column model is named final_w_hemi.